# Terminal Web and Associated Proteins Mediate Signaling to Promote Nematode Single-Cell Tubulogenesis

By
Zhe Yang

Submitted to the graduate degree program in Department of Molecular Bioscience and the Graduate Faculty of the University of Kansas in partial fulfillment of the requirements for the degree of Doctor of Philosophy.

_____

Chair: Matthew Buechner

_____

Liang Xu

_____

Lisa Timmons

_____

Robert Ward

_____

William Dentler

_____

Jennifer Gleason

Date Defended: 6th May 2020

The dissertation committee for Zhe Yang certifies that this is the approved version of the following dissertation:

# Terminal Web and Associated Proteins Mediate Signaling to Promote Nematode Single-Cell Tubulogenesis

_____

Chair: Matthew Buechner

Date Approved: May. 15th, 2020

## Abstract

Single-celled tubules represent one of the most difficult structures to form during development, requiring extension of a narrow cytoplasm surrounding a lumen exerting osmotic pressure that can burst the luminal membrane. Genetic studies on the excretory canal cell of *C. elegans* have revealed many proteins that regulate the cytoskeleton, vesicular transport, and physiology of the narrow canals. Here, we show that $\beta_H$-spectrin SMA-1 regulates the placement of intermediate filament proteins IFA-4 and EXC-2/IFC-2 to form a terminal web around the lumen, and that the terminal web EXC-2 in turn retains a highly conserved protein (EXC-9/CRIP1) that regulates apical endosomal trafficking. EXC-1/IRG, the binding partner of EXC-9, is also localized to the apical membrane and affects apical actin placement and RAB-8-mediated vesicular transport. The results suggest that an intermediate filament protein acts in a novel signal transduction pathway to direct the traffic of vesicular cargo to locations of lengthening apical surface during single-celled tubule development.

**Acknowledgments**

The research in this dissertation was conducted at Matthew Buechner's laboratory in the University of Kansas, Lawrence, KS.

Over the course of my graduate school, my mentor Dr. Matthew Buechner was always there to help and guide me. We talked about small or big events from my research to the whole globe. I am tremendously grateful to Dr. Matthew Buechner for his unreserved and continued support. No matter whatever question I may encounter, I can always talk to Dr. Matthew Buechner immediately. His consideration and insights in science always trigger new thoughts on my understanding of the organism.

Besides Dr. Matthew Buechner, Dr. Hikmat Al-Hashimi also kindly helped me throughout the years from teaching techniques to sharing life experiences, especially during the years that Dr. Matthew Buechner headed to NSF. Also I would like to express the appreciation to my committee members Dr. Liang Xu, Dr. Lisa Timmons, Dr. Robert Ward, Dr. William Dentler, and Dr. Jennifer Gleason, who kindly shared their valuable ideas, experience, and guidance for years. Especially I want to thank Dr. Liang Xu for the collaboration and abundant help from members of his laboratory, including Dr. Lan Lan and Dr. Xiaoqing Wu.

Last but not least, I would like to thank my parents for their perseverance and support. Whenever I feel discouraged, you are always their pointing at the right direction. Also my fiancé Ziqiong shared many joyful and depressed moments. I have deeply engraved your understanding and encouragement within me. You are the best I have!

## Table of Contents

## List of Figures

## List of Tables

## List of Genes

| | |
|---|---|
| CRH-1 | cAMP Responsive Element Binding Protein |
| EXC-1 | Immunity-related GTPase |
| EXC-2 | Intermediate Filament |
| EXC-4 | Chloride Intracellular Channel |
| EXC-5 | Guanine Exchange Factor |
| EXC-7 | RNA-Binding Protein |
| EXC-9 | Cysteine Rich Protein |
| GOA-1 | G Protein Subunit Alpha o1 |
| HuR | Human Antigen R/RNA Binding Protein |
| IFA-4 | Intermediate Filament |
| MSI-1 | Musashi RNA Binding Protein |
| RAB-8 | RAB Family GTPase |
| RME-1 | EH Domain Containing Protein |
| SMA-1 | Beta Heavy Spectrin |
| TPH-1 | Tryptophan Hydroxylase |

# Chapter 1. Introduction

*Caenorhabditis elegans*, as a great genetic model, is a transparent nematode about 1 mm in length (Brenner, 1974). It has two genders including hermaphrodite, which is the vast majority, and male, which is less than 1% of the wild-type population (Brenner, 1974). The normal environment of *C. elegans* is soil, with temperatures ranging between 15 and 25°C. *C. elegans* has several developmental stages, including embryonic stage, four larval stages (L1-L4) (Fig. 1.1), and adulthood. Alternatively, *C. elegans* can also enter a different developmental path in the case of food depletion (Wood, 1988). By the end of L1 stage, if food is not available, the worm will enter dauer stage instead of normal L3 growth. Meanwhile, the mouth and anus are sealed and the worm can survive for months until food is available. *C. elegans* provides a great combination of advantages for genetics study, such as transparency, large brood size, easy maintenance, long-term storage, and fast life cycle (Brenner, 1974; Wood, 1988).

## 1.1 The Excretory Canal Cell.

*C. elegans* excretory system has five cells, including a pore cell, a duct cell, an excretory canal cell, and a fused pair of gland cells (Fig. 1.2). The function of the excretory cell, similar to the renal system of other animals, is osmotic/ionic regulation and waste elimination (F. K. Nelson, Albert, & Riddle, 1983) (F.K. Nelson & Riddle, 1984). The excretory canal cell is the largest cell in *C. elegans*. It is composed of a cell body posteriorly next to the pharynx, and two branches extended from the head to the tail of the animal, which overall resemble an “H-shape” (Buechner, Hall, Bhatt, & Hedgecock, 1999; F. K. Nelson et al., 1983) (Fig. 1.3). Excretory tubes exhibit many typical epithelial characteristics, especially the polarity of the cell. Typical apical markers CRB-1/Crumbs, PAR-3, PAR-6, and PKC-3 all label the apical surface of each tube (Armenti,

Chan, & Nance, 2014; Knust & Bossinger, 2002; Mancuso et al., 2012).

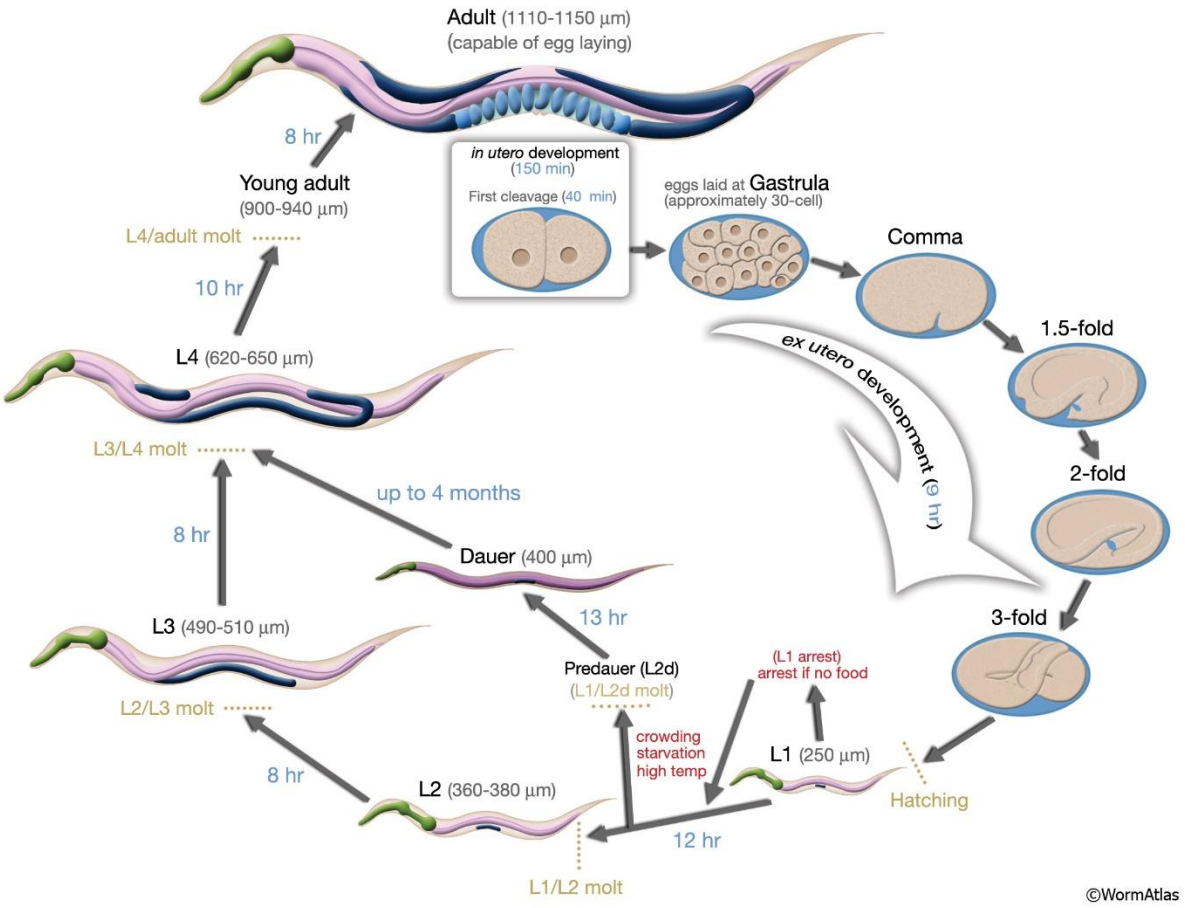


**Figure 1.1 *C. elegans* life cycle.**

Picture adapted from Wormatlas. (From http://www.wormatlas.org.)

"From webpage https://www.wormatlas.org/copyrightanduse.htm":

"Images or text created by Wormatlas may be used by individuals or organizations for non-profit educational and scientific purposes with proper acknowledgement of Wormatlas http://www.wormatlas.org."

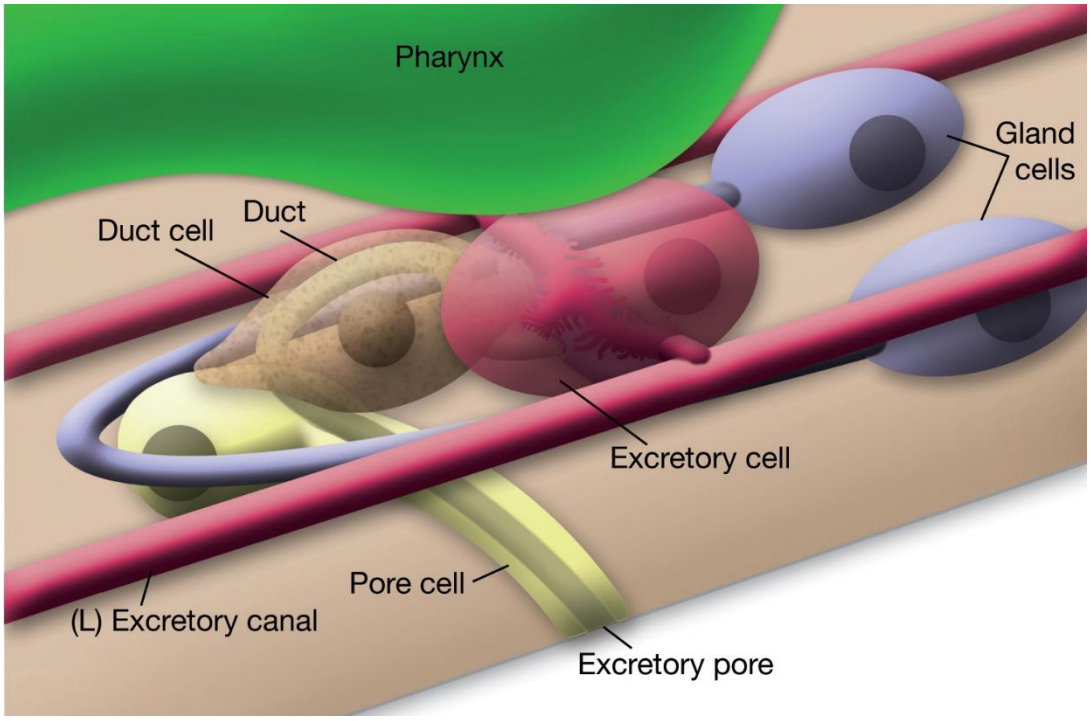


**Figure 1.2. Canal Excretory system.**

Four cell types constitute the excretory system. They are connected to form a passage for liquid.

Picture adapted from Wormatlas. (From http://www.wormatlas.org.)

"From webpage https://www.wormatlas.org/copyrightanduse.htm":

"Images or text created by Wormatlas may be used by individuals or organizations for non-profit educational and scientific purposes with proper acknowledgement of Wormatlas http://www.wormatlas.org."

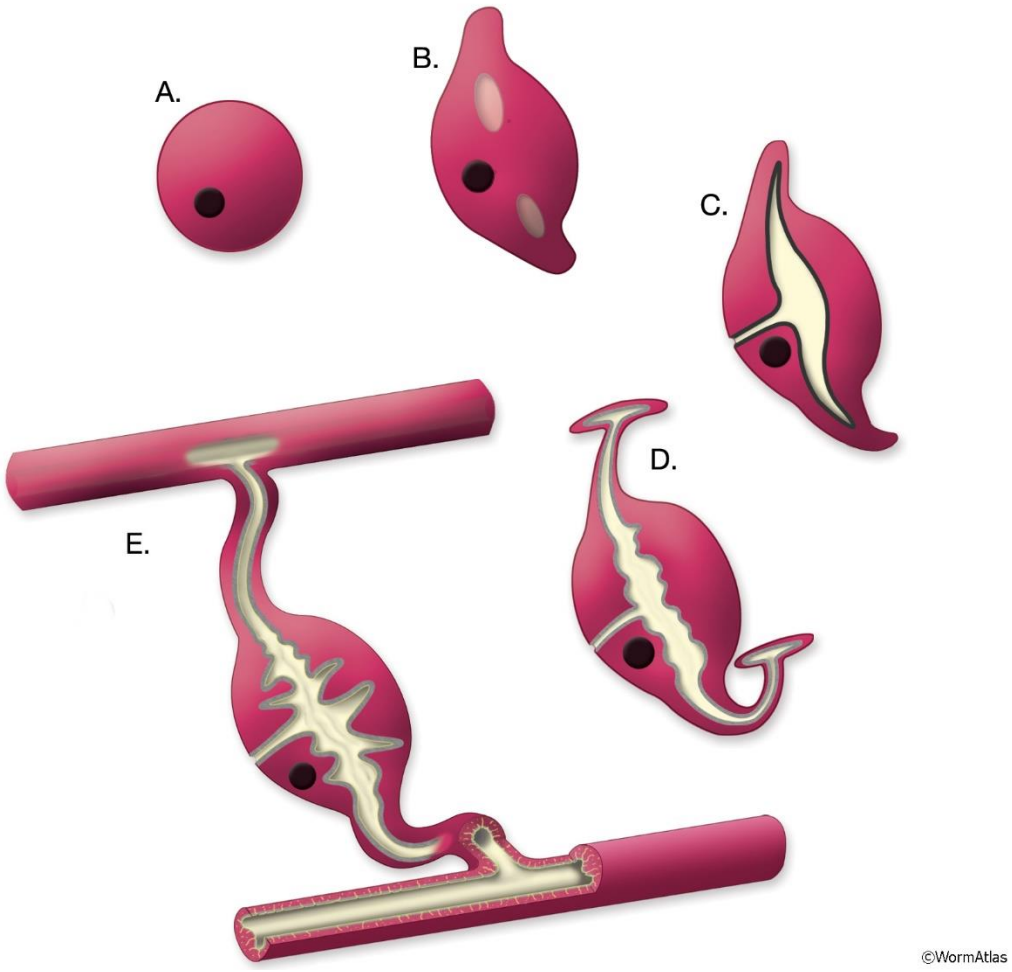


**Figure 1.3. Excretory Canal cell Development.**

**A**. The excretory cell is born ~270 minutes after first cell division

**B.** At ~300-330 minutes, one or two vacuoles with apical surfaces (light gray) appear.

**C.** At 400-430 minutes of development, the apical surface expands and the tubular arms extend from the vacuoles into the canals.

**D.** Past the two-fold stage. On reaching the lateral hypodermis, the canals bifurcate and extend anteriorly and posteriorly.

**E.** Post-hatching and adult stages.

Picture adapted from Wormatlas. (From http://www.wormatlas.org.)

"From webpage https://www.wormatlas.org/copyrightanduse.htm":

"Images or text created by Wormatlas may be used by individuals or organizations for non-profit

educational and scientific purposes with proper acknowledgement of Wormatlas http://www.wormatlas.org."

## 1.2 Genes affecting excretory canal cell structure.

Many types of proteins are found to be vital for development and maintenance of the excretory canals (Sundaram & Buechner, 2016). For example, transcription factors are key for differentiation of the canal cell. LIN-26 is a nematode-specific C2H2 zinc finger protein and is likely to play an important early step in epithelial determination (Labouesse, Hartwieg, & Horvitz, 1996). PROS-1 is a prospero homeobox transcription factor (Kolotuev, Hyenne, Schwab, Rodriguez, & Labouesse, 2013). Many genes regulated by PROS-1 are directly or indirectly related to the canal (Kolotuev et al., 2013). CEH-6 is a POU-family homeobox transcription factor and regulates aqp-8 and nac-2 (Mah et al., 2007) (Armstrong & Chamberlin, 2010). NHR-31 is a nuclear hormone receptor and NHR-31 is required for expression of a vacuolar ATPase subunit (Hahn-Windgassen & Van Gilst, 2009); Cytoskeletal organizers are also involved in canal maintenance, including integrins PAT-3, PAT-2, and INA-1 (Baum & Garriga, 1997; Gettner, Kenyon, & Reichardt, 1995; Hedgecock, Culotti, Hall, & Stern, 1987), kinesins UNC-116 and KLC-2 (Patel, Thierry-Mieg, & Mancillas, 1993; Shaye & Greenwald, 2015), actin anchor ERM protein ERM-1 (Khan et al., 2013), small GTPase RAL-1 that is associated with exocytosis (Armenti et al., 2014), ACT-5 (actin) (MacQueen et al., 2005), beta H-spectrin SMA-1 (Bennett & Healy, 2008), EXC-6, a formin with both actin polymerization and MT-binding activities (Shaye & Greenwald, 2015), beta-tubulin TBB-2 (Shaye & Greenwald, 2015), intermediate filaments IFB-1, IFA-4 and EXC-2/IFC-2 (Al-Hashimi, Hall, Ackley, Lundquist, & Buechner, 2018; Kolotuev et al., 2013; Woo, Goncharov, Jin, & Chisholm, 2004), Rho-family GTPase CDC-42 (Mattingly & Buechner, 2011); and other proteins, including immunity-related GTPase EXC-1 (Grussendorf et al., 2016), chloride intracellular channel EXC-4 (Berry, Bulow, Hall, & Hobert, 2003), guanine exchange factor EXC-5 (Mattingly & Buechner, 2011), RNA-binding protein EXC-7 (Fujita et al., 2003), cysteine-rich intestinal protein EXC-9

(Tong & Buechner, 2008), and STRIPAK complex scaffold protein CCM-3 (Lant et al., 2015).

EXC-1 is homologous to the mammalian immunity-related GTPase (IRG) family. EXC-5 is homologous to the mammalian FGD family of guanine nucleotide exchange factors (GEFs). EXC-9 is homologous to mammalian cysteine-rich intestinal protein (CRIP). A previous screen found several excretory canal cell (*exc*) genes that were named based on their cystic canal phenotype (Buechner et al., 1999). *exc-1*, *exc-5*, or *exc-9* mutants have similar phenotypes in that canal length is shorter and the canal lumen becomes dilated or cystic. The cystic regions are enriched for the early endosome marker EEA-1, but depleted of the recycling endosome marker RME-1 (Mattingly & Buechner, 2011). Overexpression of *exc-1*, *exc-5*, or *exc-9* all result in a convoluted-lumen phenotype (Grussendorf et al., 2016; Mattingly & Buechner, 2011; Tong & Buechner, 2008). Overexpression phenotypes revealed that, genetically, EXC-9 acts upstream of EXC-1, and both act upstream of EXC-5, while EXC-9 binds to wild-type EXC-1 N' terminus shown by means of yeast-2-hybrid assay. (Grussendorf et al., 2016; Mattingly & Buechner, 2011; Tong & Buechner, 2008).

SMA-1 is homologous to the beta H-spectrin (Bennett & Healy, 2008). SMA-1 is located at the apical membrane of the canal cell (Praitis, Ciccone, & Austin, 2005). When *sma-1* is mutated, the canal is severely dilated (Buechner et al., 1999) .

EXC-2/IFC-2 encodes intermediate filament C2. Previous results found that EXC-2, together with the other two intermediate filament proteins IFB-1 and IFA-4, is required for canal integrity (Al-Hashimi et al., 2018; Buechner et al., 1999). EXC-2 is localized to the apical surface of the canals and binds to IFA-4 while the apical localization of EXC-2 does not require the presence of IFA-4 (Al-Hashimi et al., 2018). However, the function of EXC proteins and potential interaction between proteins are largely unknown. In the work presented in this thesis, I

hypothesize that EXC-2 mediate the vesicle trafficking in formation of the excretory canals through EXC-9, EXC-1 and EXC-5.

# Chapter 2. Terminal Web and Associated Proteins Mediate Signaling to Promote Nematode Single-Cell Tubulogenesis

*This manuscript has been submitted and revised for publication*

## 2.1 Introductions

The interactions of cell cytoskeleton with vesicle trafficking are crucial to provide cells with the shape needed to perform specialized functions. For example, microtubule and actin filament structure mediates transport of cargo to form and maintain the nerve terminal at the end of an axon (Hakanen, Ruiz-Reig, & Tissir, 2019; Kiral, Kohrs, Jin, & Hiesinger, 2018); rab proteins regulate the apical specialized functions of multiple cell types in intestinal villi(Zhang & Gao, 2016); and defects affecting endosomal trafficking (in either neurons and glia) underlie several neural diseases such as Charcot-Marie-Tooth syndrome and Niemann-Pick disease(Neefjes & van der Kant, 2014). Advances in understanding these interactions have arisen from studies in a wide range of tissues and organisms, from yeast (Chiou, Balasubramanian, & Lew, 2017; Pires & Boxem, 2018) to *C. elegans*(Sato, Norris, Sato, & Grant, 2014), *Drosophila* (Mack & Georgiou, 2014; Nemetschke & Knust, 2016), and mammalian cells such as MDCK cells in culture(Román-Fernández et al., 2018). An interesting specialized case is the formation and extension of narrow tubular structures, which require both the cytoskeletal extension to reach out to target tissues as well as curvature of the apical surface to create a patent tubule (Barry et al., 2015; Sigurbjörnsdóttir, Mathew, & Leptin, 2014; Sundaram & Cohen, 2017).

The excretory canal cell of *C. elegans* offers a tractable genetic model for studying single-celled tubular morphogenesis in a "seamless cell" without intracellular junctions to hold the tube together along its length (Sundaram & Buechner, 2016; Sundaram & Cohen, 2017). This cell sends out long hollow projections that reach the length of the animal to collect and eliminate excess liquid (Falin, Morrison, Ham, & Strange, 2009) (Igual Gil, Jarius, von Kries, & Rohlfing, 2017; F. K. Nelson et al., 1983; Sundaram & Buechner, 2016). While the excretory system as a whole is required for organismal survival, a large number of viable mutants have been found that impair the

ability of the excretory canals to form narrow tubular extensions (Al-Hashimi, Chiarelli, Lundquist, & Buechner, 2019; Buechner et al., 1999; Igual Gil et al., 2017); cloning of the underlying genes has revealed a wide variety of cytoskeletal proteins involved, including ERM (ezrin-radixin-moesin) and $\beta_H$-spectrin anchors of the actin cytoskeleton (Khan et al., 2013; Praitis et al., 2005), a *Diaphanous* formin that links actin to the microtubule cytoskeleton (Shaye & Greenwald, 2015), and three intermediate filament proteins that wrap around the apical (luminal) surface to form a terminal web similar to that surrounding intestinal tubes (Al-Hashimi et al., 2018; Geisler et al., 2019; Khan et al., 2019; Kolotuev et al., 2013).

In addition, vesicle trafficking is important for canal morphogenesis. Mutants impairing function of the exocyst (Armenti et al., 2014) show profound defects in canal formation, as do mutations affecting the CCM-3/STRIPAK machinery needed for mammalian brain capillary formation (Lant et al., 2015). Finally, three proteins affecting vesicle transport act in a genetic pathway to regulate canal formation: EXC-9/CRIP1, EXC-1/IRG, and EXC-5/FGD (Grussendorf et al., 2016; Mattingly & Buechner, 2011; Tong & Buechner, 2008). All of the three encoded proteins have close human homologues: CRIP1 increases metastatic transformation and invasiveness in cell culture (Cousins & Lanningham-Foster, 2000); IRGM is involved with autophagy and pathogenic responses (Howard, Hunn, & Steinfeldt, 2011; Kumar et al., 2018; Pilla-Moffett, Barber, Taylor, & Coers, 2016); and FGD genes are loci of developmental diseases Aarskog-Scott Syndrome and Charcot-Marie-Tooth Syndrome Type 4H (Delague et al., 2007; Gao, Estrada, Cho, Ellis, & Gorski, 2001; Stendel et al., 2007). Mutants in these nematode genes show similar defects in vesicle transport: Buildup of RAB-5-labelled vesicles and loss of RME-1-labelled vesicles in areas of cystic dilation (Grussendorf et al., 2016; Mattingly & Buechner, 2011).

In this work, we show an unexpected linkage between the intermediate filament

cytoskeleton and proteins that regulate vesicle transport. The results show that the EXC-1/IRG and EXC-9/CRIP protein, which regulate endosomal trafficking, are closely retained to the apical surface of the canals. Retention of EXC-9 is mediated by the C-terminal domain of EXC-2/IFC-2. Finally, overexpression of RAB-8 partially suppresses the effects of mutations in *exc-9* and *exc-1* (but not *exc-5*) on the development of narrow canal tubules. These results delineate a novel signal transduction pathway from intermediate filament matrix to vesicle trafficking proteins that regulate the formation of the luminal diameter in this highly regulated polarized tubule cell.

## 2.2 Material and Method

### *C. elegans* strains

*C. elegans* strains were grown on BK16 bacteria (a streptomycin-resistant derivative of OP50) (Brenner, 1974) at 20°C. All strains used are listed in Table 1.

### DNA constructs and plasmids

EXC-2 NTD (amino acids 1-767), EXC-2 CTD (amino acids 1112-1339), RAB-8, and GFP::RAB-11.1 constructs were built by means of Gibson assembly (NEBuilder® HiFi DNA Assembly Master Mix, Cat. #E2621S). pCV01 was used as the backbone vector(Oka & Futai, 2000). Detailed primers are listed in Table 2. CRISPR/Cas9 modifications were carried out according to the protocols of the Goldstein laboratory(Dickinson, Pani, Heppert, Higgins, & Goldstein, 2015). Modification introduced through CRISPR/Cas9 system is listed in Table 3.

### Microscopy

Animals were examined via a Zeiss microscope equipped for both epifluorescence and DIC microscopy (Carl Zeiss, Thornwood, NY) with 40x (NA 1.3) and 63x (NA 1.4) objectives, and photographs captured by use of an Optronics MagnaFire Camera. Animals were placed on 2% agarose pads in M9 solution + 35mM NaN3. Contrast on DIC images was uniformly enhanced over the entire image to increase clarity. The subcellular location of fluorescent proteins at high resolution was examined through a FluoView FV1000 laser-scanning confocal microscope (Olympus, Tokyo, Japan) with 60x objective (NA 1.42). Lasers were set to 488 nm excitation and 520 nm emission (for GFP and CFP), or 543 nm excitation and 572 nm emission (mKate2 and mCherry). All confocal images were captured via FluoView software (Olympus) and collocation was analyzed by use of ImageJ software. Electron microscopy on thin sections of immersion-fixed animals was performed on a Philips CM10 electron microscope, following standard methods(Hall,

1995).

**Table 1. Strain list used in this study.**

| Strain | Genotype | Reference |
|---|---|---|
| **N2** | Wild-type | CGC |
| **NJ51** | *exc-1(rh26)* | Buechner lab |
| **BK601** | *exc-1(rh26); glt-3p::CFP + glt-3p::LifeAct::TagRFP(arIs198)* | This study |
| **BK597** | *exc-1::gfp::3xflag(qp127)* | This study |
| **BK598** | *exc-1::gfp::3xflag(qp127); exc-2(qp110)* | This study |
| **BK599** | *exc-1::gfp::3xflag(qp127); exc-9(qp130)* | This study |
| **NJ678** | *exc-2(rh247)* | Buechner lab |
| **BK530** | *exc-2(qp110)* | Buechner lab |
| **BK531** | *gfp::3xflag::exc-2 (qp111)* | This study |
| **BK592** | *gfp::3xflag::exc-2 (qp111); sma-1(ru18)* | This study |
| **BK593** | *gfp::3xflag::exc-2 (qp111); exc-4(rh133)* | This study |
| **NJ731** | *exc-5(rh232)* | Buechner lab |
| **BK602** | *exc-5(rh232); glt-3p::CFP + glt-3p::LifeAct::TagRFP(arIs198)* | This study |
| **GS7637** | *cyk-1(or596); glt-3p::CFP + glt-3p::LifeAct::TagRFP(arIs198)* | CGC |
| **MT6984** | *exc-9(n2669)* | Buechner lab |
| **BK603** | *exc-9(n2669); glt-3p::CFP + glt-3p::LifeAct::TagRFP(arIs198)* | This study |
| **BK596** | *exc-9(qp130)* | This study |
| **BK583** | *gfp::3xflag::exc-9(qp124)* | This study |
| **BK584** | *gfp::3xflag::exc-9(qp124); exc-1(rh26)* | This study |
| **BK585** | *gfp::3xflag::exc-9(qp124); exc-2(rh247)* | This study |

| | | |
|---|---|---|
| **BK586** | *gfp::3xflag::exc-9(qp124); sma-1(ru18)* | This study |
| **BK587** | *gfp::3xflag::exc-9(qp124); ifa-4(ok1717)* | This study |
| **BK588** | *gfp::3xflag::exc-9(qp124); mKate2::3xmyc::ifa-4(qp112)* | This study |
| **AZ30** | *sma-1(ru18)* | Buechner lab |
| **BK604** | *sma-1(ru18); glt-3p::CFP + glt-3p::LifeAct::TagRFP(arIs198)* | This study |
| **VC1221** | *ifa-4(ok1717)* | Buechner lab |
| **BK532** | *mKate2::3xmyc::ifa-4(qp112)* | Buechner lab |
| **BK589** | *exc-9::gfp::3xflag(qp125)* | This study |
| **BK590** | *mKate2::3xmyc::exc-9(qp126)* | This study |
| **BK591** | *mKate2::3xmyc::exc-9(qp126); gfp::3xflag::exc-2(qp111)* | This study |
| **BK600** | *gfp::3xflag::exc-9 3LIM mutation(qp128)* | This study |
| **BK594** | *mKate2::3xmyc::ifa-4(qp112); sma-1(ru18)* | This study |
| **BK595** | *mKate2::3xmyc::ifa-4(qp112); exc-4 (rh133)* | This study |
| **BK605** | *vha-1p::gfp::rab-11(qpIs131)* | This study |
| **BK211** | *exc-9p::mCherry::rme-1(qpIs101)* | Buechner lab |
| **BK606** | *gfp::rab-11(qpIs131); mCherry::rme-1(qpIs101)* | This study |

**Table 2. Primers for overexpression constructs.**

| Description | Primer sequence |
|---|---|
| **EXC-2(1-767)::GFP *Forward*** | **attaattttcactcagatgtttcaggtatg atgTCGTTAACATCCACACCATTTAGTACC** |
| **EXC-2(1-767)::GFP *Reverse*** | **tttttctaccggtaccttacgcttctt ACGTTCACGCGCGTCAC** |
| **EXC-2(1112-1339)::GFP *Forward*** | **attaattttcactcagatgtttcaggtatgatg ACAACGTACACCTCCAATACG** |
| **EXC-2(1112-1339)::GFP *Reverse*** | **tttttctaccggtaccttacgcttctt GTCAAGGTAGACAAACCAGGC** |
| **GFP::RAB-11 *Forward*** | **ggagcatcgggagcctcaggagcatcg ATGGGCTCTCGTGACGATGAATAC** |
| **GFP::RAB-11 *Reverse*** | **ctcagttggaattctacgaatg TTATGGGATGCAACACTGCTTCTTTG** |
| **RAB-8 *Forward*** | **gaaattaattttcactcagatgtttcaggt ATGGCAAAAACTTACGACTACTTG** |
| **RAB-8 *Reverse*** | **ctattatttttgacaccagacaagttgg TTAAAGCAAATTGCAGCTCCAG** |

**Table 3. Modifications introduced through CRISPR/Cas9 system.**

| Description | Sequence |
|---|---|
| ***exc-1::gfp::3xflag (qp127)*** | **X:15470796 X:15470795** |
| **CRISPR/Cas9 insertion** | **…CAGCCGGAGTTCATTGA ttcattgtctgtggagac….** |
| ***exc-9::3xflag::gfp(qp125)*** | **IV:7940020 IV:7940019** |
| **CRISPR/Cas9 insertion** | **…tttcagGTTTAA gccatcaactgcttc…** |
| ***gfp::3xflag::exc-9(qp124)*** | **IV:7940808 IV:7940807** |
| **CRISPR/Cas9 insertion** | **…ccatttcagagagccaaca ATGCCAAATTGCCCGCGTT…** |
| ***mKate2::3xmyc::exc-9(qp126)*** | **IV:7940808 IV:7940807** |
| **CRISPR/Cas9 insertion** | **…ccatttcagagagccaaca ATGCCAAATTGCCCGCGTT…** |
| ***exc-9(qp128)*** | **Substitution: IV:7940678 to IV:7940652** |
| **CRISPR/Cas9-induced LIM mutation** | **GCCCTTCGTGCCGAGAATGAAGCAGCC** |
| ***exc-9 (qp130)*** | **Deletion: IV:7940808 to 7940800** |
| **CRISPR/Cas9-induced deletion** | **…ccatttcagagagccaac/a ATGCCAAA/TTGCCCGCGTT…** |

## Statistical Analysis

Canal length was measured as percentage of full-length posterior canals (reaching past the anus; full-length was rated 100%; canals reaching to the vulva in the center of the animal length 50%; and complete lack of extension 0%; lengths between these landmarks were interpolated. Comparisons of canal length were calculated via one-way ANOVA.

# Chapter 3.

## 3.1 EXC-9 is localized to the apical surface of excretory canals by expression of EXC-2

EXC-9 (Human CRIP1 orthologue) is a small protein required for development and maintenance of the excretory canals; mutants develop shortened canals with large fluid-filled cysts (Tong & Buechner, 2008). The 85 amino acids of EXC-9 encode a single conserved LIM domain of the CRP class (Davis, Blanchard, Lanningham-Foster, & Cousins, 1998; M. A. Smith et al., 2010) at the N-terminus (60 amino acids) followed by a short tail of unknown function conserved from nematodes to humans. In the *exc-9* (*n2669*) mutant, cystic canals always form a medium-size (¼–to-½ the diameter of the animal) cyst at the distal ends of the lumen though cyst size and canal length varies depending on allele used (Fig. 3.1.1). Allele *n2669* is a strong allele that was previously studied (Tong & Buechner, 2008). Allele *qp130*, a putative null CRISPR/Cas9-induced deletion of the first 8 nucleotides of the coding region (the next ATG is not in-frame), produces significantly shorter canals than seen in *n2669* homozygotes, while insertion of GFP at the C-terminus of the protein (see below) creates a milder mutant phenotype, with smaller cysts and longer canals.

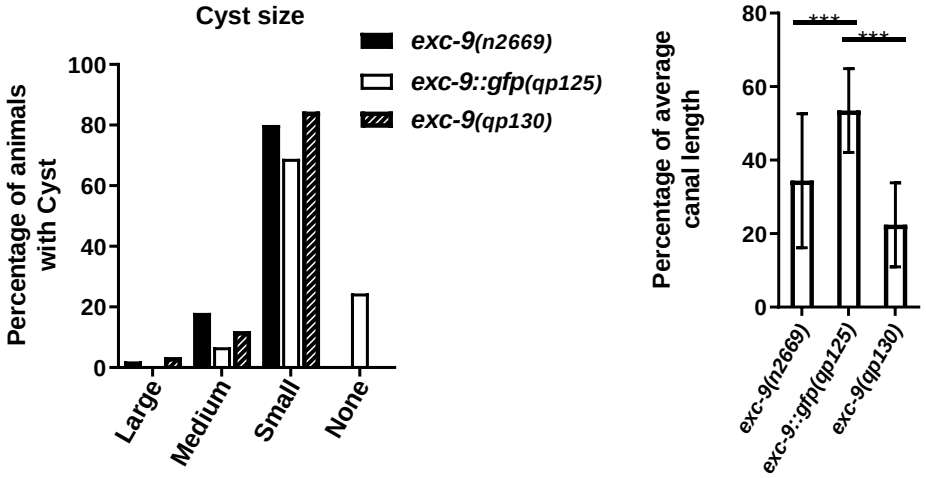


**Figure 3.1.1 *exc-9* mutant exhibits canal defects.**

In order to determine the subcellular location of EXC-9, the CRISPR/Cas9 system was utilized to insert the *gfp* coding region at either the 5'- or 3'-terminus of *exc-9* (Dickinson et al., 2015). Expression of N-terminal GFP::EXC-9 (BK583) allowed the protein to remain fully functional and form long thin, hollow canals, with the protein located predominantly at the apical surface (Fig. 3.1.2a). Expression was also seen at lower levels within the uterine seam cell, both distal tip cells, and lumbar ganglion. Within the canals, expression was largely coincident with the intermediate protein marker mKate2::IFA-4, which labels the terminal web surrounding the canal lumen (Al-Hashimi et al., 2018), though some EXC-9 was also found within the cell cytoplasm. As noted above, when GFP was inserted at the C-terminus (BK589), the function of EXC-9 was compromised (Fig. 3.1.2b). However, EXC-9::GFP was still enriched at the apical surface. Blockage of the C-terminal tail by GFP impaired EXC-9 function without affecting apical localization.

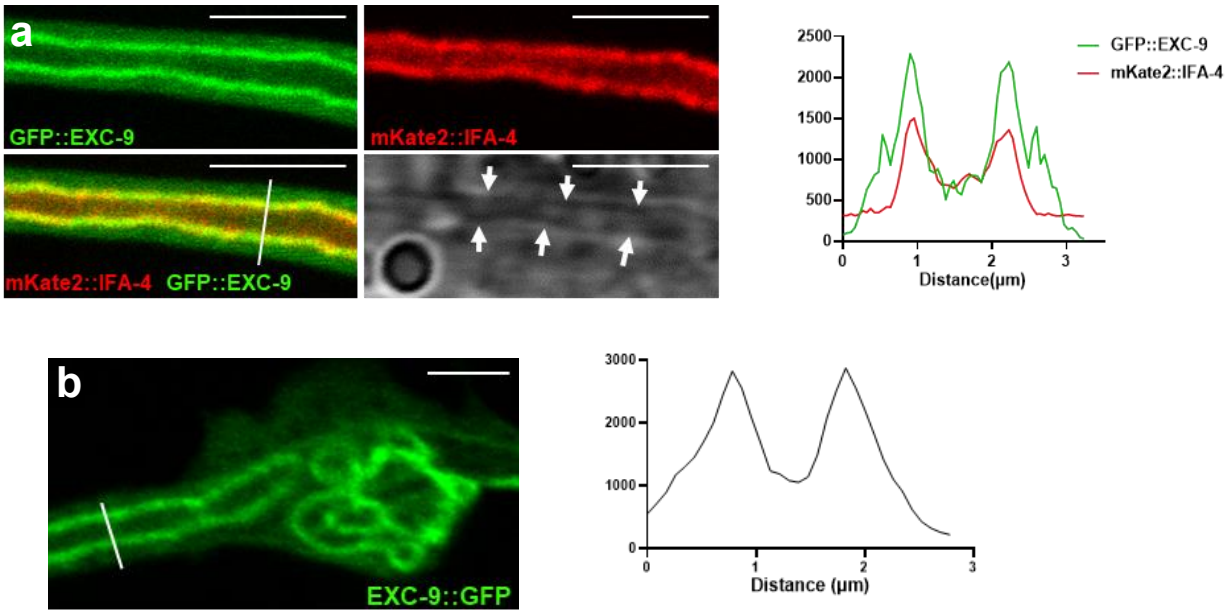


**Figure 3.1.2 Both GFP::EXC-9 and EXC-9::GFP localizes at apical surface.**

However, EXC-9::GFP is not functional. All scale bars, 5 μm.

As EXC-9 has no transmembrane domain but is enriched at the apical membrane, we examined how EXC-9 is retained at the membrane by crossing our fully functional GFP::EXC-9 strain to mutants defective in known canal apical lumen cytoskeletal proteins (Fig. 3.1.3-3.1.4). In the absence of the large intermediate filament protein EXC-2(Al-Hashimi et al., 2018), GFP::EXC-9 lost apical localization and became evenly distributed throughout the canal cytoplasm (Fig. 3.1.3). In contrast, loss of another canal-specific intermediate filament, IFA-4, which likely forms heterodimers with EXC-2, didn't affect EXC-9's ability to be retained at the apical surface (Fig. 3.1.4a). Similarly, loss of β-heavy SMA-1 causes formation of large irregular cysts throughout the length of the canals (Buechner et al., 1999), but retains strong expression of EXC-9 predominantly at the apical surface (Fig. 3.1.4b). Finally, loss of the IRG GTPase protein EXC-1, a known EXC-9 binding partner (Grussendorf et al., 2016), also had no effect on the apical retention of EXC-9 (Fig. 3.1.4c). The results indicate that EXC-2 retains the majority of EXC-9 protein at the apical surface; this was confirmed by co-expression of functional labeled EXC-2 and EXC-9, which were completely collocated at the canal apical surface (Fig. 3.1.4d).

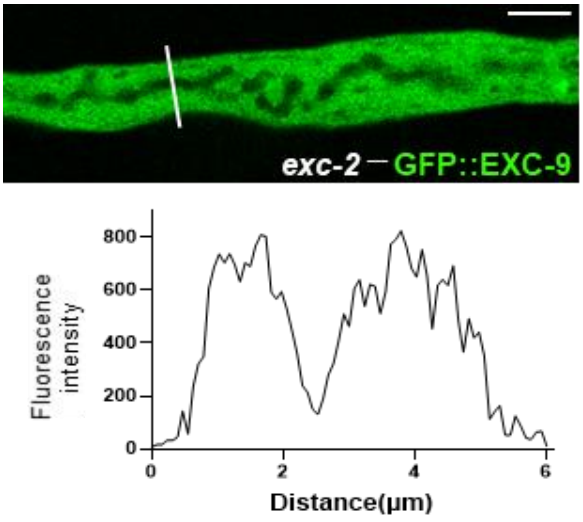


**Figure 3.1.3 GFP::EXC-9 lost apical localization in *exc-2* mutant.**

All scale bars, 5 μm.

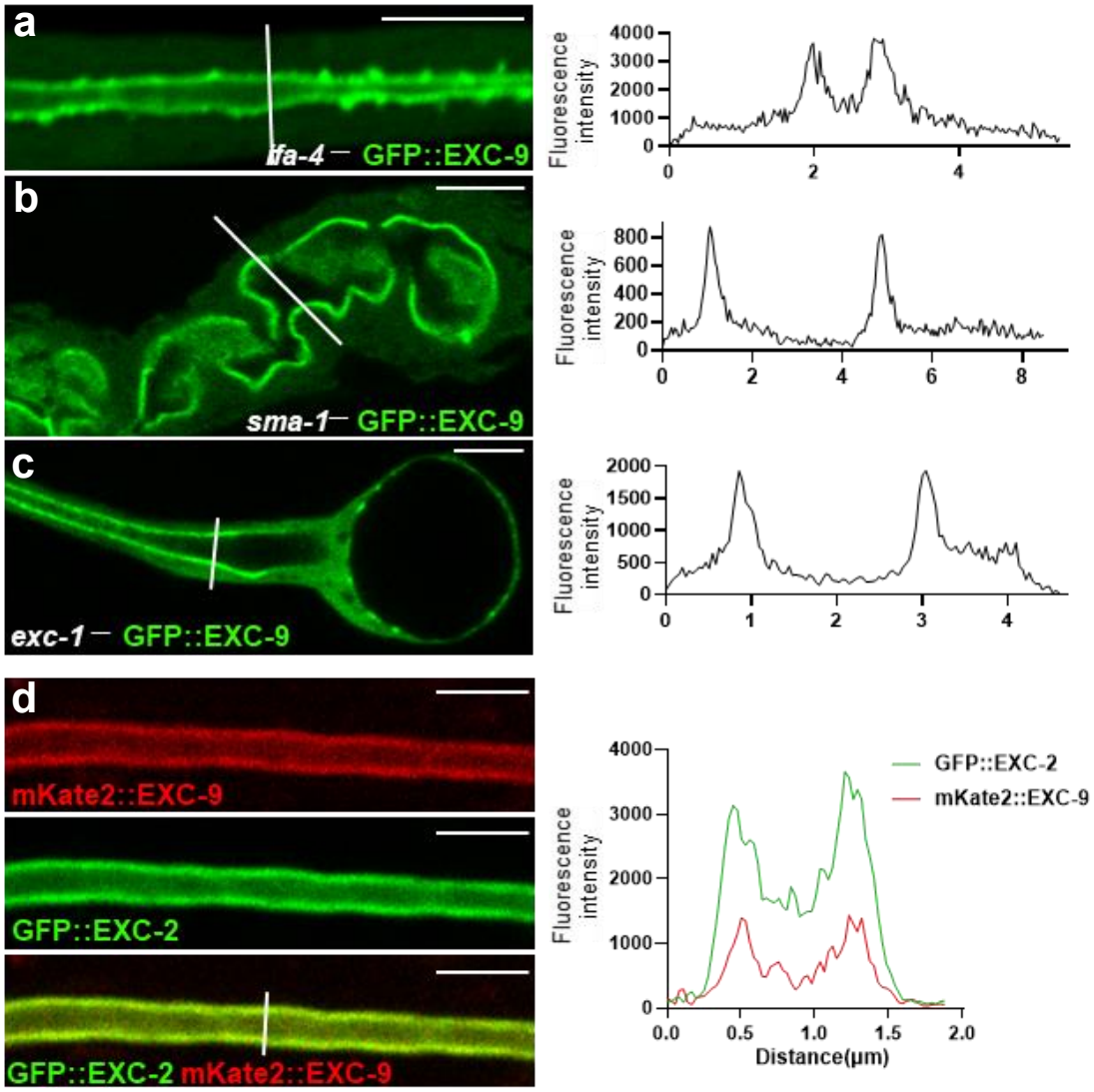


**Figure 3.1.4 GFP::EXC-9 is apical localized in various mutants**

***a.*** *ifa-4*$^{-/-}$

***b.*** *sma-1*$^{-/-}$

***c.*** *exc-1*$^{-/-}$

**d**. GFP::EXC-2 and mKate2::EXC-9 colocalize at apical surface. All scale bars, 5 μm.

### 3.2 EXC-2 C-terminal domain localizes EXC-9 to the apical surface

Intermediate filaments usually consist of a short N-terminal domain (NTD) and longer C-terminal domain (CTD) flanking a conserved filament domain used for dimerization(Herrmann & Aebi, 2016). While IFA-4 and IFB-1 follow this plan (including a conserved lamin tail domain within the CTD (Carberry, Wiesenfahrt, Windoffer, Bossinger, & Leube, 2009; Zuela & Gruenbaum, 2016), EXC-2 has a much longer NTD, and no lamin-tail homology in its CTD (Fig. 3.2a). In order to determine which section of EXC-2 is required for binding EXC-9 to the luminal surface, the long NTD (amino acids 1-767) and short CTD (amino acids 1112-1339) were each cloned into a fluorescence translational construct for overexpression in wild-type and in the *exc-2*(*qp110*) null mutant background. Overexpression of each of these constructs caused shortened canals with small-to-medium-sized cysts (Fig. 3.2b, c) resembling an *exc-9* mutant phenotype (Tong & Buechner, 2008). In the wild-type background, overexpressed EXC-2NTD::GFP remained apically localized (Fig. 3.2b), but labeled EXC-9 was not. EXC-9 appears not to have bound to the N-terminal domain, and was therefore excluded from the luminal surface.

Overexpression of EXC-2CTD::GFP exhibited a unique polarized fluorescence phenotype (Fig. 3.2c): Canals were generally wild-type in diameter along their length, but did not grow to full-length, and terminated in medium-sized cysts at the distal ends. In addition, fluorescently labeled EXC-2CTD and labeled EXC-9 were fully collocated, but strongly enriched towards the distal end, with very bright fluorescence at the distal tip of the canal lumen. The canals lack large cysts for most of their length (unlike the canals in *exc-2*, *ifa-4*, or *ifb-1* mutants, which are cystic along their entire length), so all three wild-type intermediate filaments must be located along the majority of the length of the canals (Al-Hashimi et al., 2018). We infer that the CTD of EXC-2 recruits EXC-9, and that they were able to remain at high concentration at the canal apical surface

only at the luminal tip of the canals.

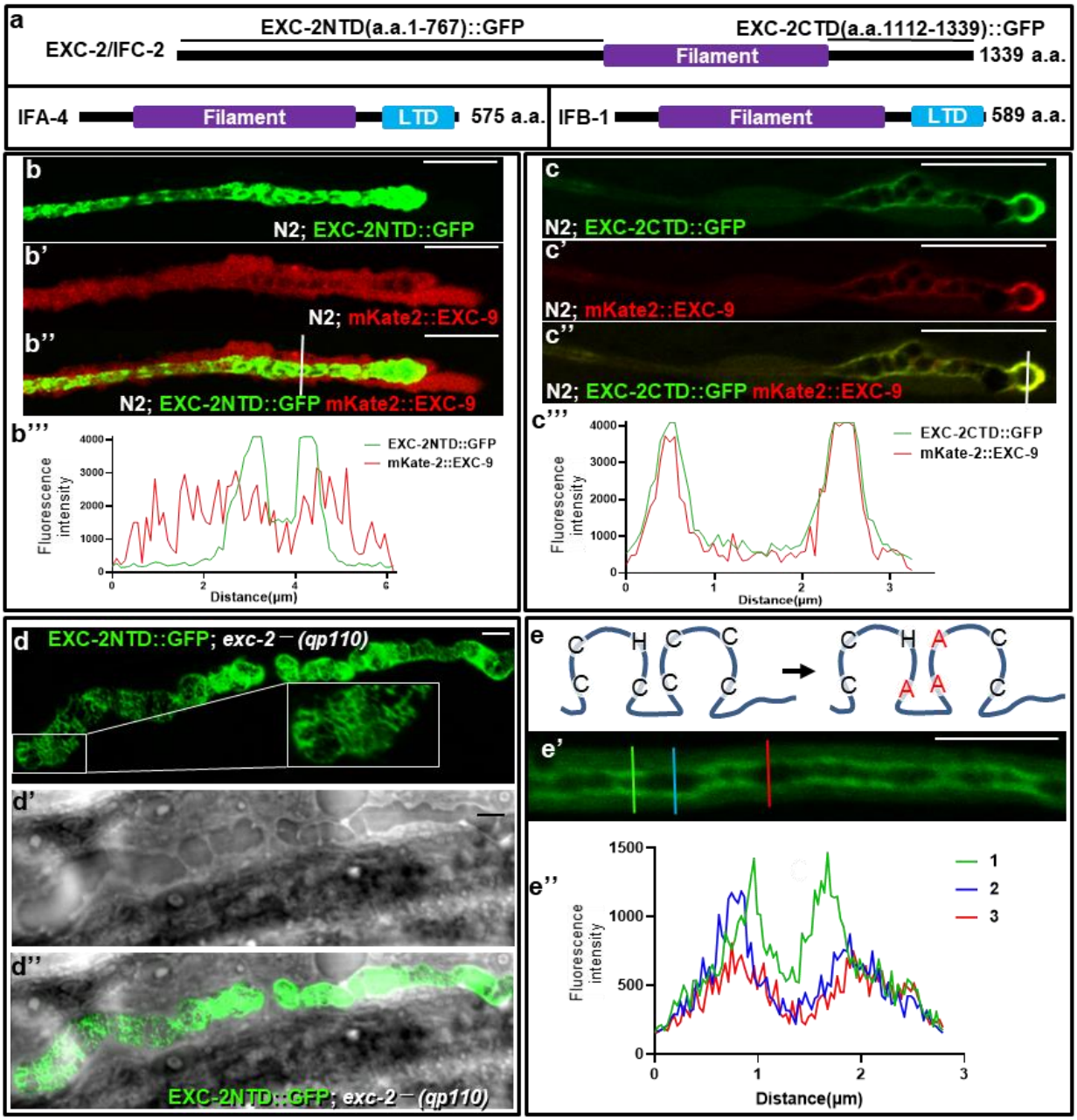


**Figure 3.2 EXC-2 C-terminal fragment is colocalized with EXC-9 to the canal apical membrane.**

**a.** Scale diagram of domains of intermediate filament expressed in the excretory cell, including EXC-2/IFC-2, IFB-1 and IFA-4. The lamin-like intermediate filament domain allows homo- and hetero-dimerization of the filaments.

**b.** Overexpression of EXC-2(1-767) (N-terminal half) in BK590 (EXC-9 modified via CRISPR/Cas9 insertion of mKate2) reduced binding of mKate::EXC-9 to the apical surface; b. Overexpressing EXC-2(1-767) fluorescence; b'. EXC-9 fluorescence; b''. Merge; b'''. Fluorescence intensity profiles of EXC-2(1-767) (green) and EXC-9 (red) along white line indicated in b''.

**c.** Overexpressing EXC-2 (1112-1339) in BK590 (mKate2::EXC-9) showed EXC-2 showed colocalization of both proteins to the growing tip of the luminal canal surface; c. EXC-2(1112-1339) (C-terminal portion) fluorescence; c'. EXC-9 fluorescence; c''. Merge; c'''. Fluorescence intensity profiles of EXC-2(1-767) (green) and EXC-9 (red) at the canal tip along the white line indicated in c''.

**d.** EXC-2(1-767) overexpressed in exc-2(qp110) homozygotes forms a wild-type meshwork comparable to that of wild-type animals at the canal apical surface; d. EXC-2 fluorescence; inset at 2x magnification; d'. DIC image showing cystic lumen; d''. Merge. e. Mutation of the LIM domain prevents EXC-9 localization to the apical surface;

**e.** Diagram of EXC-9 showing conserved cysteines and histidine in loops of LIM domain. Amino acids in red indicate replacement by alanine in mutant strain; e'. EXC-9 fluorescence in cysteine-substituted mutant is evenly expressed throughout the cytoplasm surrounding an enlarged lumen; e''. Fluorescence intensity profile along three lines in e'. All scale bars, 5 μm.

In the *exc-2*(*qp110*) null allele mutant background, EXC-2NTD::GFP was still localized at the apical surface (Fig. 3.2d), and its expression resembled pattern resembled the localization and meshwork pattern of wild-type EXC-2 (Al-Hashimi et al., 2018). This suggested that the N-terminus of EXC-2NTD is capable of binding either to the other intermediate filament proteins IFB-1 and IFA-4, or to other proteins anchored or bound to the luminal surface.

GFP attachment to either end of the small EXC-9 protein did not affect its expression at the apical surface of the excretory canals, although C-terminal GFP impaired EXC-9 function (Fig. 3.1.4d). We investigated the role of the LIM domain at the N-terminus of EXC-9 by using CRISPR/Cas9 to make endogenous mutations in key conserved cysteines (Fig. 3.2e). LIM domains are composed of two contiguous zinc fingers containing three conserved cysteine residues and one histidine in the first zinc finger and 4 conserved cysteines in the second zinc finger (Weiskirchen & Gunther, 2003). We used CRISPR/Cas9 to replace the last cysteine in the first zinc finger and first two cysteines in the second zinc finger with alanine (Fig. 3.2e). With these changes, about half of the animals (28 of 50) were mildly affected in regards to canal length, with canals reaching longer than half the length of the organism, while the other animals had full-length canals (81% of full-length average). In the cysteine-substituted mutant canals, apical retention of labeled EXC-9 was variably impaired, with some sections showing wild-type levels of EXC-9 at the apical surface as compared to the cytoplasm, while in others, almost no EXC-9 was retained at the apical surface. (Fig. 3.2e') Loss of apical EXC-9 was coincident with areas of wider lumen, possibly nascent cysts. These results suggest that LIM domain function plays a role in apical localization of EXC-9 to the canal apical surface.

### 3.3 SMA-1/spectrin is required for spacing of the EXC-2 meshwork

In addition to intermediate filaments, actin filaments are essential for maintaining canal diameter, anchored to the apical surface by β-heavy-spectrin SMA-1 and the ezrin-radixin-moesin homologue ERM-1 (Khan et al., 2019; Khan et al., 2013; Praitis et al., 2005). In *erm-1* knockdown animals, labeled IFB-1 showed the intermediate filament network to be greatly disrupted (Khan et al., 2019). We examined the other two canal intermediate filaments via separately crossing the fluorescent *mKate2*::*ifa-4* and *gfp*::*exc-2* strains into animals carrying a null mutation either in *sma-1* or *exc-4* (encoding a CLIC ion channel, as control with large cysts), both of which also severely disrupt canal morphology (Berry et al., 2003; Praitis et al., 2005). In the homozygous *sma-1*(*ru18*) mutant background, both mKate2::IFA-4 and GFP::EXC-2 fluorescence showed disruption to the spacing of filaments surrounding the apical surface (Fig. 3.3a,c). The "weave" of the intermediate filament meshwork is looser, allowing the appearance of large gaps of open membrane between intermediate filaments, as seen by the repetitive distance between peaks of fluorescence (Fig. 3.3a',c'). In contrast, in the *exc-4* background (Fig. 3.3b,d), the meshwork of both labeled filaments generally showed a tighter weave, with filaments aligned closely to each other, comparable to the meshwork of wild-type animals (Fig. 3.1.1a), even though *exc-4* animals exhibit very large canal cysts comparable in size to those of *sma-1* mutants (Buechner et al., 1999). Occasional filament breakdowns in very large cysts could be seen in *exc-4* mutant animals, but the background filament "weave" was generally as tight as in wild-type animals. The disruption of filament "weave" in *sma-1* mutants is similar to that caused by knock-down of ERM-1 (Khan et al., 2019). We conclude that both ERM-1 and SMA-1 are needed for proper layout of the intermediate filament network.

Examination of *sma-1* and *exc-4* mutants by means of electron microscopy (Fig. 3.3e-g) showed further differences between these animals. In the *exc-4*(*rh133*) mutant, the luminal surface

electron-dense terminal web is intact and associated tightly with the membrane at the luminal surface (Fig. 3.3e), as is seen in wild-type animals (Buechner et al., 1999). The membrane itself is in contact with long chains of small canalicular vesicles (Fig. 3.3e, marked by asterisks), rich in vacuolar ATPase and aquaporin, and which pump water into the canal lumen for expulsion from the animal (Sundaram & Buechner, 2016). In contrast, the *sma-1*(e30) mutant (Fig. 3.3f) exhibits an electron-dense terminal web layer that is no longer juxtaposed to the apical membrane. In addition, the terminal web is broken in places, with large gaps between electron-dense areas (arrowheads in Fig. 3.3f'). Although canalicular vesicles are numerous in this mutant, the canalicular membrane appears disorganized in areas where the terminal web is distant from the membrane. Finally, in the *exc-2*(*rh90*) mutant missing the largest intermediate filament protein, the terminal web was largely missing from the apical membrane, and very few canalicular vesicles were visible (Fig. 3.3g). These results confirm that intermediate filaments make up the terminal web of the excretory canal, similar to terminal webs in the gut (Coch & Leube, 2016) and that $\beta_H$-spectrin is required for proper arrangement of these intermediate filaments. In addition, the terminal web appears to be necessary for stabilization of the network of canalicular vesicles that are presumed to carry out osmoregulation of the animal in hypotonic environments.

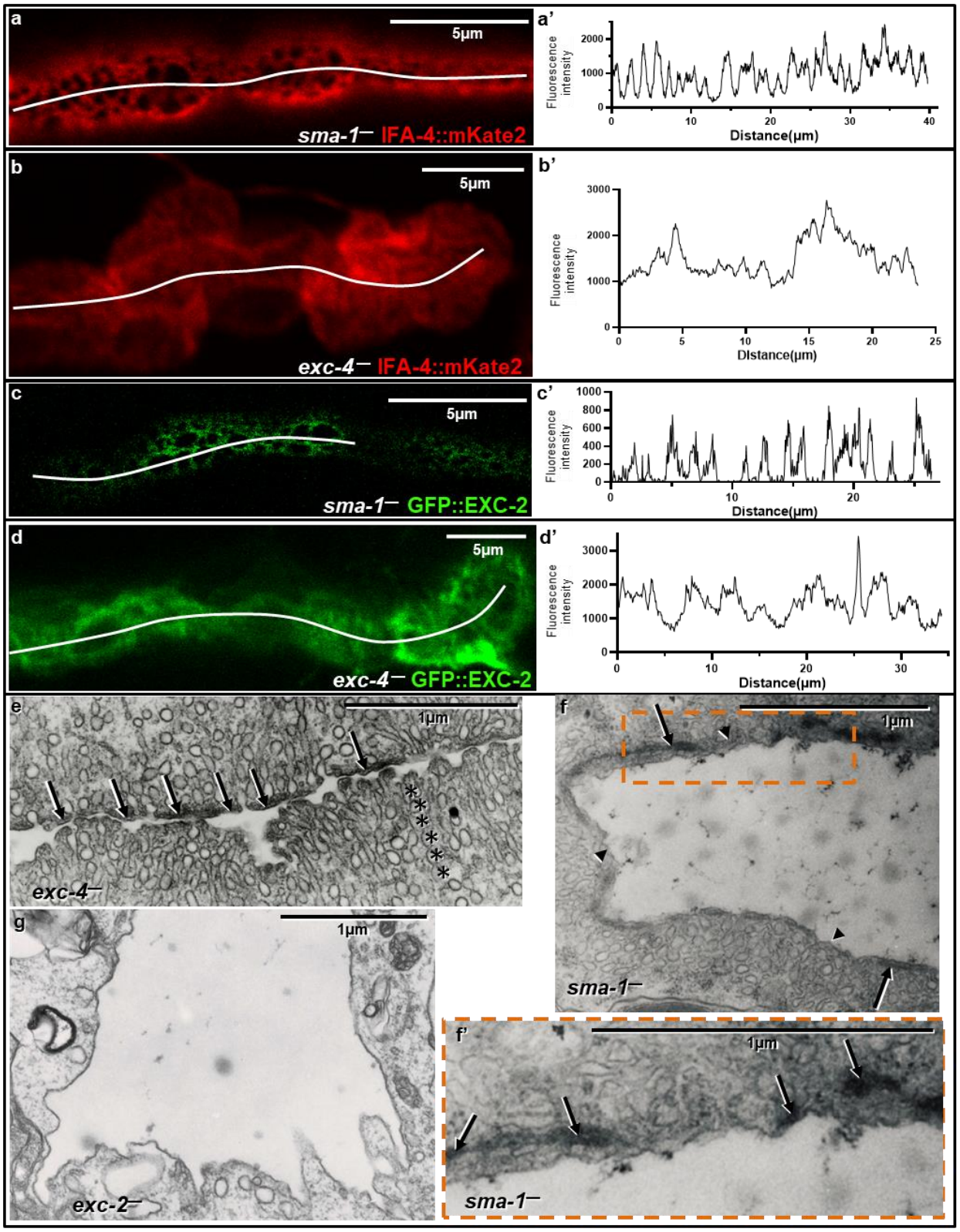


**Figure 3.3 SMA-1 is required for proper intermediate filament arrangement.**

**a-d**. Fluorescence of labeled IFA-4 or EXC-2 in homozygous *sma-1* or *exc-4* backgrounds; a'-d'. Fluorescence intensity profile along the white line in the corresponding micrograph.

**a.** IFA-4 fluorescence in *sma-1*(*ru18*) homozygous mutants.

**b.** IFA-4 fluorescence in *exc-4*(*rh133*) mutants.

**c.** EXC-2 fluorescence in *sma-1*(*ru18*) mutants.

**d.** EXC-2 fluorescence *exc-4*(*rh133*) mutants.

**e-g.** Transmission electron micrographs of homozgyous canal mutants;

**e**. *exc-4*(*rh133*) mutant; electron-dense intermediate-filament-rich terminal web (arrows) is closely opposed to apical membrane, and canalicular vesicles (asterisks) are connected to the lumen and to each other;

**f**. *sma-1*(*e30*) mutant shows frequent detachment of the terminal web (arrows) from the apical membrane, with visible gaps (arrowheads) between sections of terminal web; f'. Enlargement of boxed section of f; In spite of terminal web disruption, abundant canalicular membrane is visible, though the vesicles appear disrupted in areas where terminal web is separated from the membrane;

**g**. Large cyst of *exc-2*(*rh90*) mutant; terminal web is missing, as are the bulk of canalicular vesicles.

### 3.4 EXC-1 is also localized to the canal apical surface

EXC-9 binds to the N-terminal half of EXC-1, and acts genetically upstream of EXC-1 to mediate endosomal vesicle transport within the canals (Grussendorf et al., 2016). EXC-1 possesses two RAS-like GTPase domains and is the sole nematode homologue of mammalian IRG proteins (Fig. 3.4a) (Grussendorf et al., 2016). Since EXC-9 is largely collocated with EXC-2, we examined whether the EXC-9-binding partner EXC-1 is also retained near EXC-2 within the excretory cell. Through use of CRISPR/Cas9, GFP was inserted at the C-terminus of EXC-1. This labeled protein was found at the apical surface, and surprisingly, unlike EXC-9, little EXC-1 protein was apparent in the cytoplasm (Fig. 3.4b). In addition to the excretory canal cell, EXC-1 was expressed at lower levels in the amphid sheath cells. Localization of EXC-1 did not require activity of EXC-9, since in the deletion mutant *exc-9(qp130)*, EXC-1 fully retained its localization to the apical luminal membrane (Fig. 3.4c). Similarly, crossing labeled EXC-1 strain into a null *exc-2*(*qp110*) mutant strain caused no change to the apical localization of EXC-1 (Fig. 3.4d). EXC-1 appears to be anchored to the membrane independently of the EXC proteins that act genetically upstream of EXC-1.

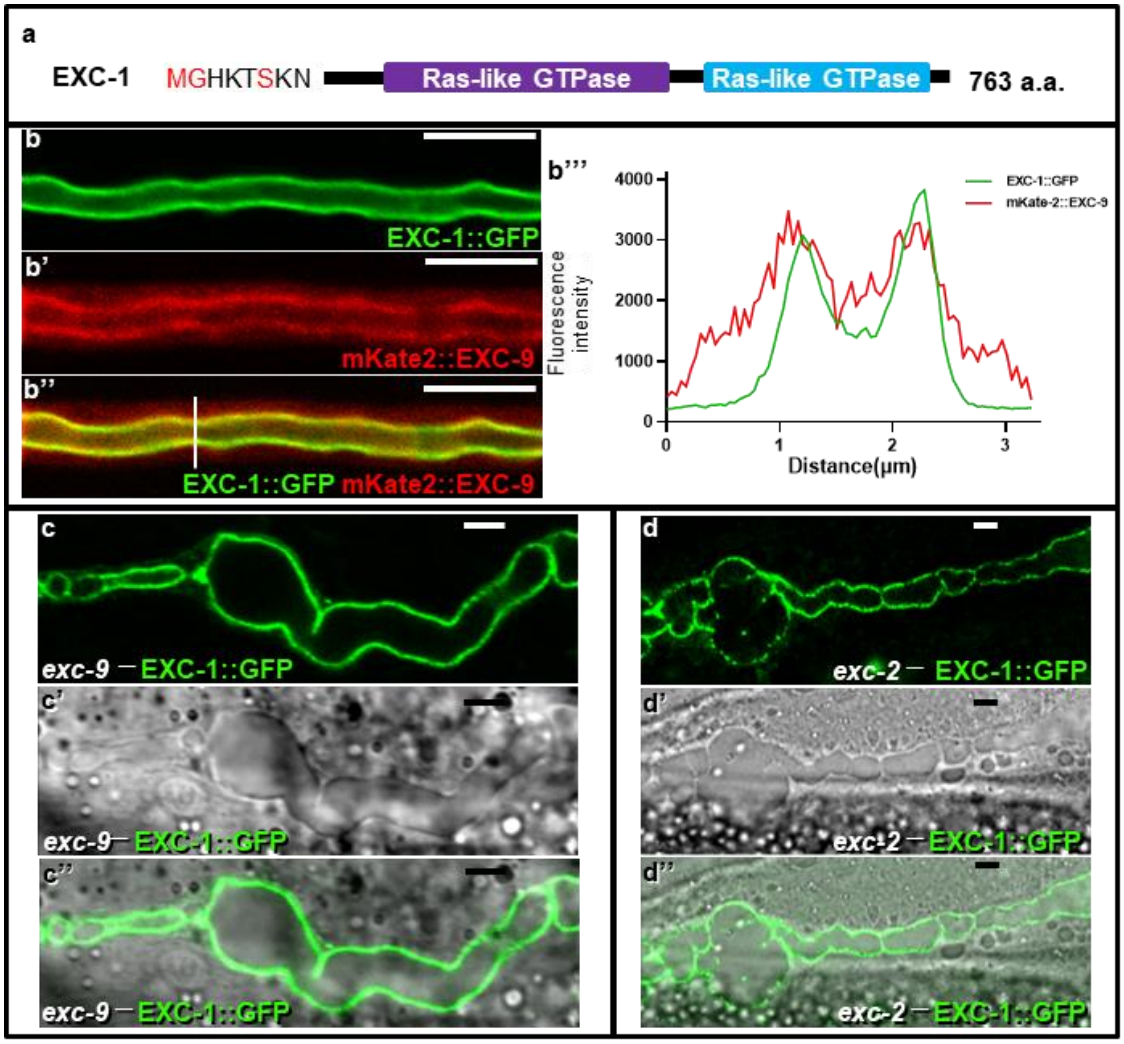


**Figure 3.4 EXC-1/IRG is localized exclusively at the apical surface of canals.**

**a.** Scale diagram of the GTPase domains within the EXC-1 protein.

**b-b''.** Collocation of EXC-1::GFP and mKate2::EXC-9 at the canal apical surface; b. EXC-1 fluorescence; b'. EXC-9 fluorescence; b''. Merge; b'''. Fluorescence intensity profiles of mKate2::EXC-9 (red) and EXC-1::GFP (green) along the white line of panel b''.

**c-c''.** EXC-1::GFP remains at the apical surface in a homozygous null *exc-9*(*qp130*) cystic mutant; c. EXC-1 fluorescence; c'. DIC image of fluid-filled cysts; c''. Merge.

**d.** EXC-1 is retained at the surface of canals in a homozygous *exc-2*(*qp110*) cystic mutant. d. EXC-1 fluorescence; d'. DIC image of fluid-filled cysts; d'''. Merge. All scale bars, 5 μm.

### 3.5 Apical actin filaments are bundled in *exc-1*, *exc-5*, and *exc-9* mutants

Previous data showed that EXC-9, EXC-1, and EXC-5 act in sequence to regulate endosomal vesicle transport in the excretory canals (Grussendorf et al., 2016; Mattingly & Buechner, 2011; Tong & Buechner, 2008). In order to investigate the potential cargo or cytoskeletal protein being regulated, we used a strain containing two integrated constructs that both use a canal-specific promoter to express either a cytoplasmic CFP or the actin dye LifeAct (Shaye & Greenwald, 2015). To better visualize the full length of actin filaments along the curved apical surface of the canals, a series of Z-axis pictures were taken and merged into a single micrograph (Fig. 3.5a). In the wild-type canal background (Fig. 3.5b), the apical membrane actin filaments a uniform field of short actin filaments throughout the length of the canal apical surface. This structure is maintained in the *sma-1* mutant (Fig. 3.5c), where the canal lumen is often enlarged to a similar degree throughout the canal without obvious septations (Buechner et al., 1999); this result suggests that the labeled actin filaments are anchored to the membrane by another means. In the *exc-9* mutant background, some aggregation of actin filaments into thick bundles (Fig. 3.5d, arrow) became evident in areas with larger septate cysts corresponding to septate cysts that thin the amount of cytoplasm present. This effect is progressively exacerbated in *exc-1* mutants (Fig. 3.5e) and most dramatically in the large cysts of *exc-5* mutants, where the actin filaments contain little actin except in thick bundles (Fig. 3.5f). In addition, in the *exc-5* mutant, these thick bundles are collocated with accumulations of cytoplasmic material around the swollen luminal cyst. We conclude that these three *exc* mutants therefore are needed to stabilize a uniform actin meshwork at the apical surface.

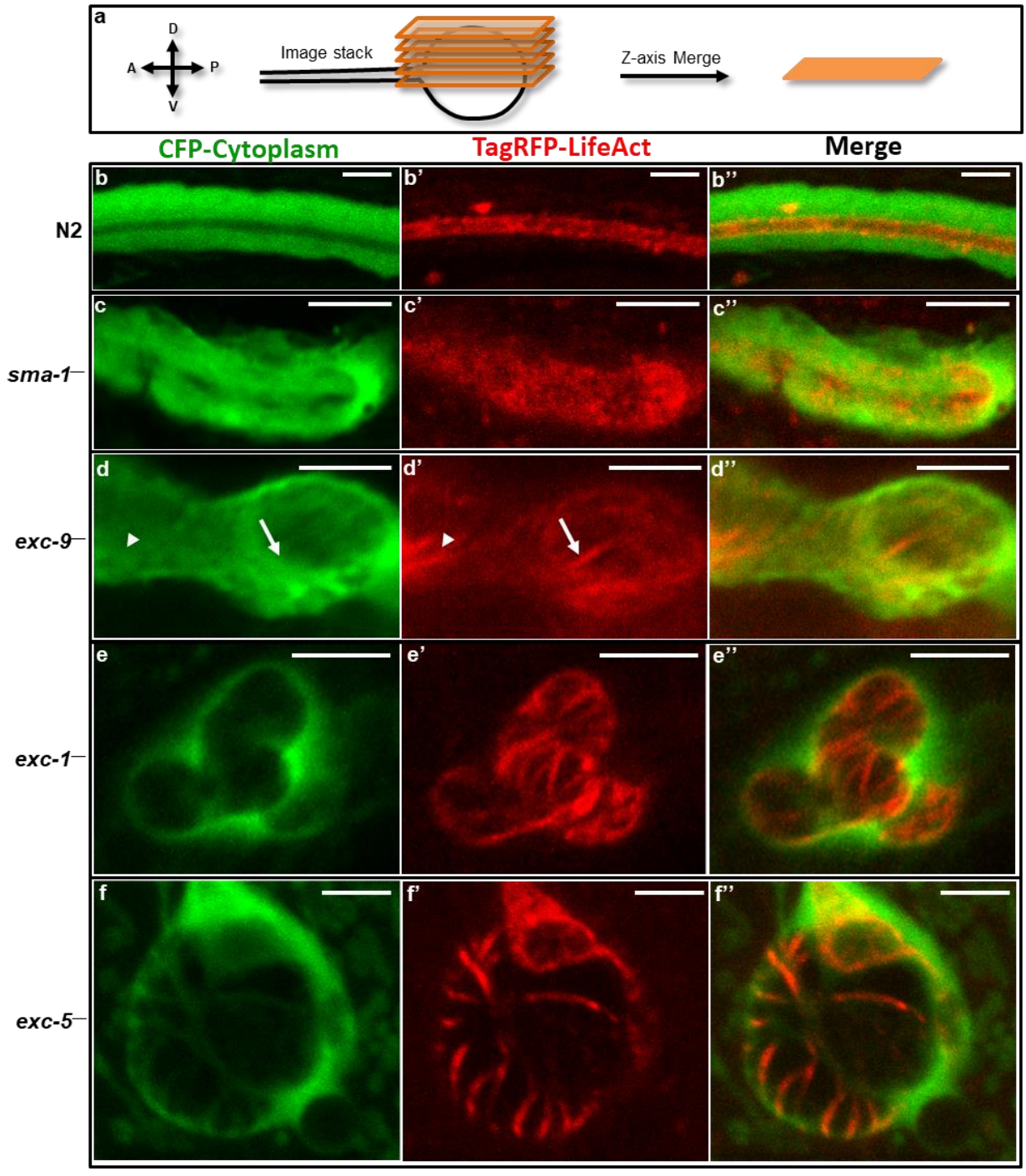


**Figure 3.5 Actin filament mesh exhibits increasingly severe bundling gaps in *exc-9*, *exc-1*, and *exc-5* mutants.**

**a.** Scheme of summation of fluorescence through z-stack serial pictures through half the depth (nearest to hypodermis and microscope objective) of canals and cysts to show filament morphology of Lifeact-labeled filaments at the canal apical surface.

**b-f.** All animals express cytoplasmic CFP under an integrated canal-specific promoter, and an overexpressing construct of fluorescent actin label (Lifeact) under the same promoter. Left column: cytoplasmic fluorescence; center column, actin filament mesh; right column, merge.

**b.** Wild-type background;

**c.** Homozygous *sma-1*(*ru18*) background;

**d.** Homozygous *exc-9*(*n2669*) background; arrows indicate a distinct thickly bundled actin filament, while the arrowhead indicates a less distinct actin bundle;

**e.** Homozygous *exc-1*(*rh26*) background;

**f.** Homozygous *exc-5*(*rh232*) background. All scale bars, 5 μm.

### 3.6 EXC-1 and EXC-9 promote RAB-mediated apical transport

In *exc-1*, *exc-5*, and *exc-9* mutants, endosomal expression of the basal trafficking marker RME-1 was significantly decreased within the cytoplasm of canal cysts, while that of other vesicular markers, especially early endosome antigen EEA-1, and (to a lesser extent) the apical trafficking marker RAB-11.1 were increased (Grussendorf et al., 2016; Mattingly & Buechner, 2011). In order to better understand the relationship of these EXC proteins on traffic movement within the excretory canal, we first examined competition between apical and basal traffic markers (Fig. 3.6a-c). A strain carrying a stable integrant of *mCherry::rme-1* driven by a canal-specific promoter (Mattingly & Buechner, 2011) exhibits punctate endosomes and strong cytoplasmic expression (Fig. 3.6a). We crossed this marker line to a strain harboring an integration of a construct that strongly expresses canal-specific *gfp::rab-11.1* (Fig. 3.6b). With the expression of *rab-11.1*, expression of mCherry::RME-1 in the canal was greatly reduced to near-background levels (Fig. 3.6c). We conclude that apical and basal transport within the excretory canal cell depends on the ratio of apical-directed and basal-directed transport machinery present.

Next, since expression of Rab proteins within the canal appears to affect transport ratios as in the intestine (Sato et al., 2014), and EXC-9, EXC-1, and EXC-5 proteins mediate trafficking to the apical surface, we examined whether overexpression of an apical-directed Rab protein could rescue mutation of the *exc-1*, *exc-5*, and *exc-9* genes (Fig. 3.6d,e). A construct overexpressing canal-specific *rab-8* was injected into *exc-1* (*rh26*), *exc-5* (*rh232*), and *exc-9* (*qp130*) mutants (Fig. 3.6d-f). Cyst formation in these mutants causes significant shortening of the canals, but in the presence of excess RAB-8, the canals of *exc-1* and *exc-9* mutants were significantly longer (Fig. 3.6d). Similarly, overexpression of any of these *exc* genes causes the canals to have a “convoluted” phenotype, where the basal surface is shortened, while normal-diameter luminal surface is still

extended and ends up coiled within the canal (Tong & Buechner, 2008) (Fig. 3.6e). Canal overexpression of *rab-8* also caused a significant increase in convoluted canals in *exc-1* and *exc-9* mutants, (though not as strong as overexpression of the *exc* proteins themselves (Grussendorf et al., 2016) (Fig. 3.6f). Surprisingly, overexpression of *rab-8* had no significant effect on the *exc-5* mutant, either in canal length or formation of cystic canals (Fig. 3.6d,f). These genetic epistasis experiments suggest that RAB-8 acts downstream of EXC-9 and EXC-1 in directing cargo to the apical surface.

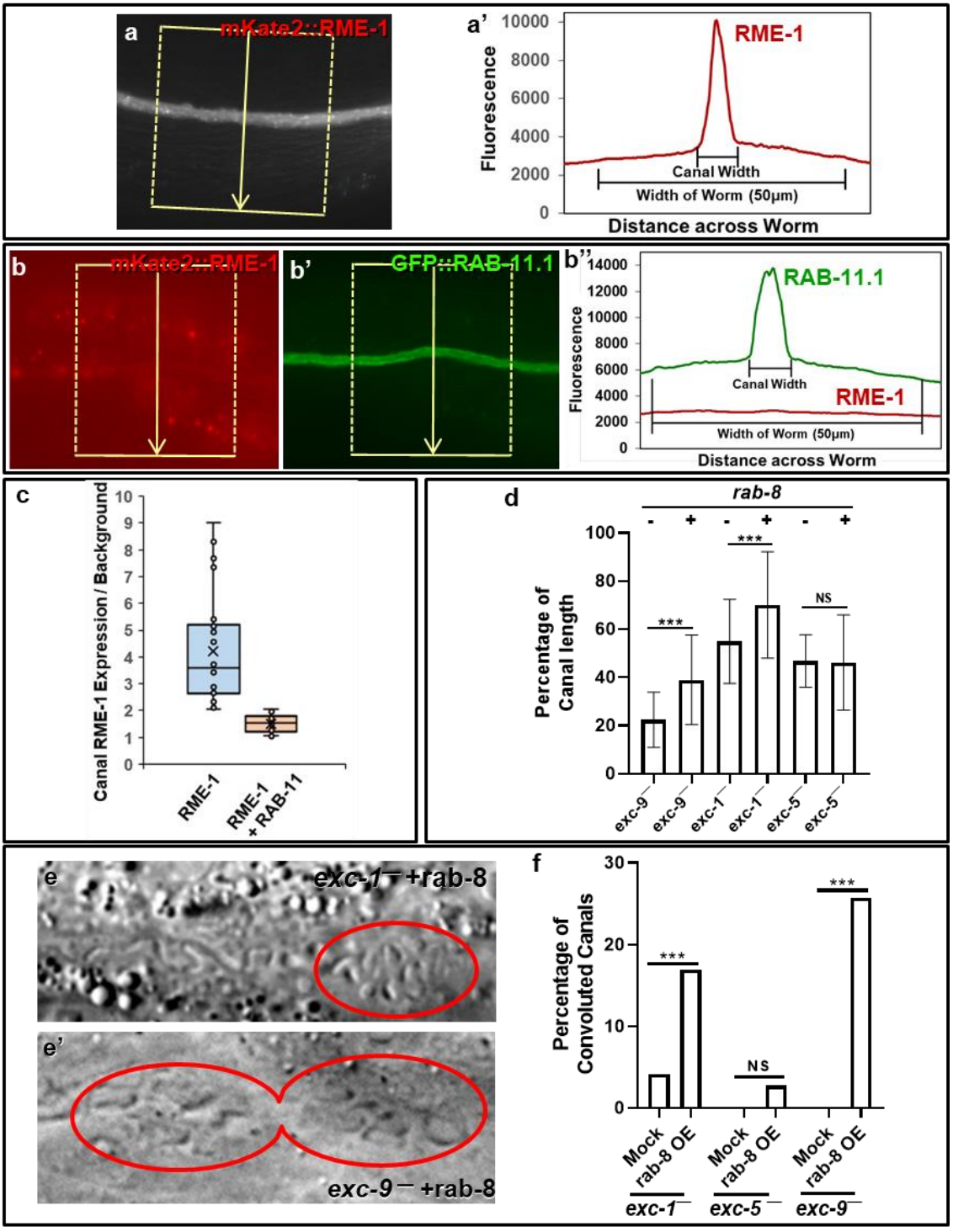


**Figure 3.6 EXC-1 and EXC-9 promote RAB-mediated apical transport.**

**a.** mCherry::RME-1 construct is overexpressed in the excretory canals; a. Fluorescence micrograph of section of excretory canal expressing *mCherry*::*rme-1* construct under a exc-9

promoter; endosomes are visible as bright puncta; a'. Measurement of fluorescence in boxed area of panel a, measured in direction of arrow along line in panel, with a width of 300 pixels (space between dotted lines).

**b.** Expression of GFP::RAB-11 in worms also expressing mCherry::RME-1. b. Fluorescence micrograph; b'. Fluorescence of mCherry::RME-1; area measured is shown in box; b''. Fluorescence intensity of GFP::RAB-11 and mCherry::RME-1.

**c.** Graph of average ratio of fluorescence of mCherry::RME-1 to autofluorescence within worm in area of canal; left column, average ratio for animals expressing fluorescent mCherrry::RME-1 alone; right column, for animals expressing GFP::RAB-11 in addition to mCherry::RME-1; n>25 animals for each column. X, average ratio; bar is median ratio; box, confidence limit.

**d.** Length of excretory canals of *exc* mutant animals, and same strain overexpressing *rab-8*; posterior canal lengths were measured.

**e.** Convoluted canal phenotype in *exc-1* and *exc-9* mutant animals with overexpression of RAB-8. e. *exc-1*$^{-/-}$; e'. *exc-9*$^{-/-}$. Circled areas show regions of normal-diameter lumen coiled within shortened, swollen cytoplasm.

**f.** Measurement of frequency of canals showing convoluted tubules trapped within shortened basal surface; a convolution is defined as the lumen crossing ditself at least once. Convolutions were counted in progeny of animals microinjected with buffer (Mock), and for animals overexpressing (OE) *rab-8*. $n \geq 35$ for all samples.

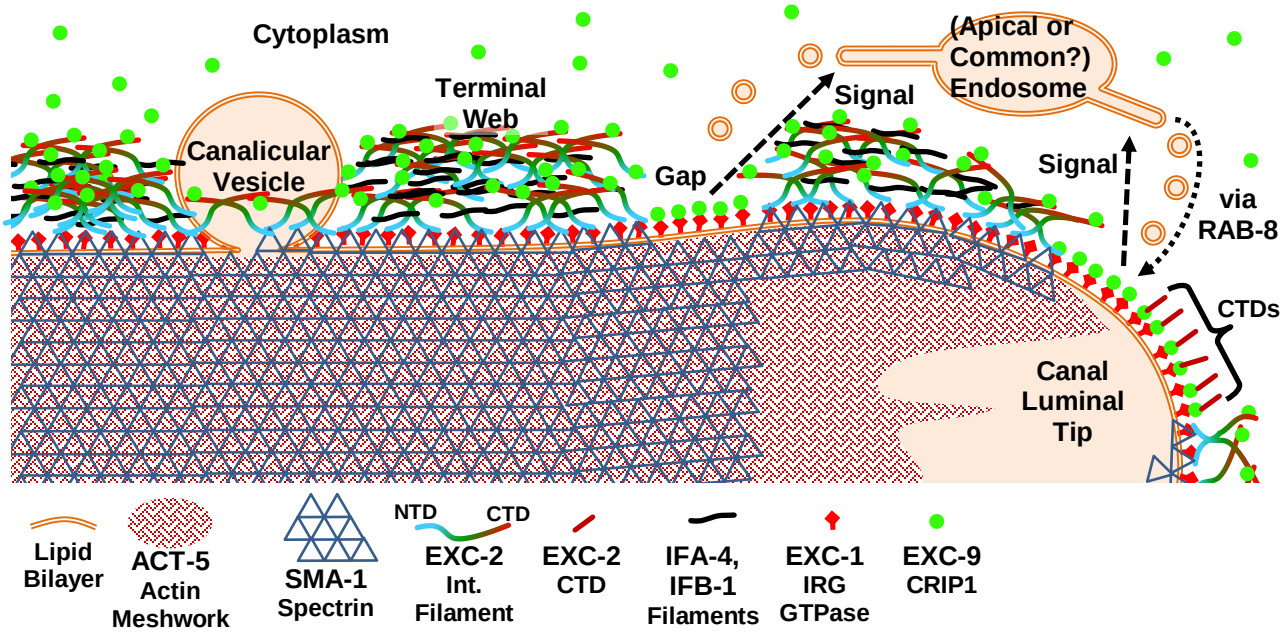


**Figure 3.7 Working model**

# Chapter 4. Discussion

## Cytoskeletal interactions

The cytoskeleton forms and reinforces the shape of cells. Projections of actin and microtubules underlie cell protrusions, while intermediate filaments act as ropes or stretchable bungee cords to allow limited stretch to plasma membrane and nuclei (Delacour, Salomon, Robine, & Louvard, 2016; Gerace & Burke, 1988; Gruenbaum & Foisner, 2015). Both of these elements are needed for formation of long hollow tubules, which must be guided to grow out along the length of the bodywall, but whose luminal diameter must be restrained as excess water is brought into the tubule to be expelled from the organism (Sundaram & Buechner, 2016; Sundaram & Cohen, 2017). The results in this paper show that EXC-1/IRG GTPase and EXC-9/CRIP1 are both held predominantly near the apical surface, either in the plasma membrane itself or together with the EXC-2/IFA-4/IFB-1 intermediate filaments of the terminal web surrounding the lumen. EXC-1 is located at the apical surface even in *exc-2* mutants where there is little or no terminal web (Fig. 3.4). Upon re-examining the amino acid sequence of EXC-1 with the help of predictive lipidation tools, we found that its N-terminus contains a co-translational myristoylation sequence MGHKTS (D. R. Johnson, Bhatnagar, Knoll, & Gordon, 1994; Udenwobele et al., 2017; Xie et al., 2016). Our attempts to engineer a CRISPR/Cas9-mediated insertion of GFP at the N-terminus of this protein were unsuccessful, which may indicate that this sequence is essential for organismal viability. Future biochemical studies of possible lipidation of this protein should be fruitful at further understanding its interactions with cytoskeletal elements.

EXC-9 was found predominantly coincident with the terminal web, though with a visible fraction in the cytoplasm (Fig. 3.1). This suggests that EXC-9 is either present in the cytoplasm

before being bound to the terminal web, or can be released from the terminal web. Impairment of the EXC-9 LIM domain (Fig. 3.2) reduced the ability of EXC-9 to bind to the terminal web, with regions of lower terminal web expression corresponding to formation of incipient cysts. This reinforces the idea that EXC-9 binding to the canal terminal web is essential for maintaining the narrow diameter of the excretory canals.

Overexpression of the EXC-2 (Intermediate filament) NTD largely prevented EXC-9 from binding to the terminal web, resulting in EXC-9 being essentially all cytoplasmic, while overexpression of the EXC-2 CTD lowered the amount of free EXC-9 visible in the cytoplasm, concentrating it at the terminal web towards the posterior end and especially at the canal tip (Fig. 3.2). The canal luminal surface extends the length of the animal, closely following the growing tip of the basal surface during embryogenesis and the first larval stage (Fujita et al., 2003). For overexpressed EXC-2 CTD to label only the canal luminal tip, CTD must accumulate there until a step requiring relatively equal proportions of NTD and CTD occurs, presumably terminal web formation.

Conversely, overexpressed EXC-2 NTD is bound along the entire canal length, but forms an uneven meshwork over the length of the canals, perhaps reflecting uneven levels of terminal web formed when balance of different domains of the intermediate filament proteins is upset.

There are eleven cytosolic intermediate filaments in *C. elegans* (Carberry et al., 2009; Dodemont, Riemer, Ledger, & Weber, 1994; Karabinos, Schmidt, Harborth, Schnabel, & Weber, 2001; Zuela & Gruenbaum, 2016). Several studies have focused on the intestinal terminal web, where intermediate filaments are also necessary to maintain narrow luminal diameter (Coch & Leube, 2016; Geisler et al., 2019; Khan et al., 2019; Khan et al., 2013). The *exc-2* gene is not expressed in the intestine (Al-Hashimi et al., 2018), and has multiple isoforms. The shortest

isoform, called isoform D, and also termed IFC-2 (Hüsken et al., 2008), is transcribed from a promoter present in an intron of EXC-2, resulting in a protein containing only the lamin-homology domain and CTD. A recent study of isoforms of proteins containing this common CTD of EXC-2 and IFC-2 (Geisler et al., 2020) found that only the longest isoforms (corresponding to EXC-2, and referred in that paper as IFC-2A/B) were expressed in the excretory canal cell, while IFC-2 (referred in that paper as IFC-2D/E) was expressed very strongly in the intestinal terminal web. We therefore conclude that the intracellular location and effects on canal length and cyst formation found when overexpressing the CTD of EXC-2 within the canals of wild-type animals reflects the function solely of this domain in full-length EXC-2 protein rather than interference with the shorter IFC-2 function.

**Implications: Modeling Tubule Growth**

Several alternative hypotheses can explain how these interactions form the terminal web and guide outgrowth of the canal lumen. One attractive hypothetical model is shown in Fig. 3.7. EXC-1/IRG is associated with the membrane along the entire length of the canal. At sites where EXC-1 is exposed to the cytoplasm, i.e. at the growing canal tip and at sites of membrane addition during growth (such as evenly spaced “beads” in the L1 stage (Kolotuev et al., 2013), soluble EXC-9/CRIP can bind to and activate EXC-1 (Grussendorf et al., 2016); as well as to bind to the CTD of EXC-2. EXC-1 then signals (via phosphorylation of as-yet unknown proteins) to direct movement of vesicles via RAB-8 to bring cargo (more lipid and cytoskeleton-related proteins), and/or via guanine exchange factor EXC-5/FGD to facilitate actin polymerization for vesicle delivery to that area of the tubules. Polymerization of cytoskeletal elements ACT-5/actin, SMA-1/spectrin, and the three intermediate filaments EXC-2, IFA-4, and IFB-1 follows.

Mutants in *sma-1* (encoding β-heavy spectrin) show disorganization of the terminal web (Fig. 3.3) (Buechner et al., 1999; Praitis et al., 2005), which indicates that this spectrin clearly has an organizing effect on the intermediate filament network, though *sma-1* mutation does not abrogate the terminal web's overall formation near the apical membrane. Significantly, *sma-1* mutants tend to exhibit very wide canals with few narrow septations, with numerous canaliculi attached to the apical membrane (Fig. 3.3f), unlike mutants of intermediate filament genes (Fig. 3.3)(Al-Hashimi et al., 2018; Khan et al., 2019; Kolotuev et al., 2013). The presence of intermediate filaments at the apical membrane therefore appears to be necessary for attachment of these canaliculi, as much as is the activity of the exocyst and STRIPAK complex (Armenti et al., 2014; Lant et al., 2015).

Loss of EXC-9, EXC-1, or EXC-5 function resulted in ACT-5 actin filaments appearing as thick cables restraining the lumen, which swells into cysts around those cables (Fig. 3.5). Surprisingly, *sma-1* mutants lacking $\beta_H$-spectrin still maintained a tightly-knit meshwork around the canal lumen, which suggests that, unlike the FERM-domain protein ERM-1 (Khan et al., 2019; Khan et al., 2013), this spectrin is not the most critical organizer of these actin filaments. This result was surprising, since SMA-1 regulates actomyosin cytoskeletal contractility in several *C. elegans* tissues (Wirshing & Cram, 2018). Disorganization of the terminal web could therefore be secondary to SMA-1's effects on cytoskeletal actin, or perhaps actomyosin contractility may not play a significant role in organizing the canal actin meshwork.

**Interactions with Rab Proteins**

EXC-9 acts genetically upstream of and binds to EXC-1, which itself acts upstream of EXC-5. Results here show that overexpressing RAB-8 partially rescues the *exc-9* and *exc-1* mutants, but not *exc-5* mutants (Fig. 3.6). While the result is consistent with RAB-8 acting

downstream of EXC-9 and EXC-1, the fact that rescue was much stronger if the EXC proteins themselves were overexpressed suggests that another protein may act downstream of EXC-9 and EXC-1. RAB-11.1 and RAB-8 both target vesicles to the apical membrane, so may be acting together downstream of EXC-1.

In addition, RAB-8 did not rescue the effects of *exc-5* mutation. This could indicate that RAB-8 acts upstream of EXC-5 (as in the model posited above), which is expressed at or near the canal apical surface (Mattingly & Buechner, 2011); or that RAB-8 stimulates a different guanine exchange factor while a different protein (perhaps again RAB-11) stimulates EXC-5. Further research on the function of various Rab proteins and guanine exchange factors at the canal apical surface should provide a fruitful avenue of study.

While the present results provide a plausible framework by which intermediate filaments can serve as luminal scaffold for proteins that regulate directed tubular growth, other models are equally plausible. Future studies examining the biochemistry of EXC-1 and EXC-9 activation during canal development will be invaluable in understanding tubular growth mediated by these two proteins and by intermediate filaments. Finally, the homology of EXC-9 to the CRIP and IRG family of proteins (including the autophagy regulator IRGM) suggests that study of the canal can provide models for greater understanding of regulation of these important mammalian proteins.

# Chapter 5. Second Project:

# RNA-Binding Proteins MSI-1 (Musashi) and EXC-7 (HuR) Regulate Serotonin-Mediated Behaviours in *C. elegans*

***This manuscript has been submitted and revised for publication***

## Abstract

The evolutionarily conserved RNA-binding proteins HuR and MSI are essential for multiple developmental processes and are upregulated in many cancer tissues. The *C. elegans* homologues EXC-7 (HuR) and MSI-1 (MSI1 and MSI2) have been implicated in tubulogenesis, neural development, and specific behaviours that include male tail-curling to maintain contact with the hermaphrodite during mating. This behaviour is mediated by serotonin signaling. Results here show that MSI-1 affects serotonergic signaling through stabilization of mRNA of the Gα protein GOA-1/GNAO1 in neurons, which in turn affects activity of the serotonin synthase TPH-1/tryptophan hydroxylase via the response element CRH-1/CREB. EXC-7 (HuR) is also involved in this regulatory pathway. These results indicate a novel pathway and role for these RNA-binding proteins in regulating neurotransmitter levels that could be conserved in other tissues where these RNA-binding proteins are present.

## 5.1 Material and Methods

### *C. elegans* strains

*C. elegans* strains were grown on a lawn of BK16 bacteria (a streptomycin-resistant derivative of OP50) on plates of Nematode Growth Medium (NGM) Agar at 20C according to standard techniques (Brenner, 1974). All mutants were crossed to *him-5*(*e1490*) to create strains with a high proportion of males (Hodgkin, Horvitz, & Brenner, 1979); this mutation is present in all strains used here (including wild-type) though is not listed in tables or figures. All strains used are listed in Table 4.

### DNA constructs and plasmids

*goa-1p::goa-1* was amplified from N2 wild-type genomic DNA using forward primer 5'-GTATTCAAAAGTTTCGCGCCAATGCG-3' (3136 bps upstream of ATG) and reverse primer 5'-GTACGGTAGTCCCATATGCAATTTCCC-3'. *tph-1p::tph-1* was amplified from N2 wild type genomic DNA using forward primer 5'-GCAATACTATTTTTCGGTGGTCTTCCC-3' (3139 bps upstream of ATG) and reverse primer 5'-CGTGTCACATCCTTTATGTGCGTTG-3'. pBK263 (*tph-1p::goa-1*) was derived from pCVO1. The *tph-1* promoter was amplified with forward primer 5'-cttggaaatgaaataagcttgcatgcGCAATACTATTTTTCGGTGGTCTTCC-3' (3139 bps upstream of ATG) and reverse primer 5'-CTTCCTGTGACATGGTACAACCCATatgattgaagagagcaatgctac-3'. The *goa-1* coding region insertion was amplified with forward primer 5'-GTAaccggtATGGGTTGTACCATGTCACAGG-3' and reverse primer 5'-CTAcggccgCAAATAAGATATCAATGAGTGGGTGCAGTC-3' and restriction enzyme AgeI (NEB Catalog #: R3552S) and EagI (NEB Catalog #: R3505S). Gibson assembly was carried out to assemble pBK263 by use of NEB NEBuilder High-Fidelity Master Mix (Catalog #:

M5520). pBK272 (*myo-3p::goa-1*) was derived from pCVO1. The *myo-3* promoter was amplified with forward primer 5'-cttggaaatgaaataagcttgcatgcCTGTTTGATGAAAACCAATGAAACAAGTG-3' (2525 bps upstream of ATG) and reverse primer 5'-cttcctgtgacatggtacaacccatTTCTAGATGGATCTAGTGGTCGTG-3'. The *goa-1* coding region insertion was amplified as previously described.

**Drug treatments**

Various concentrations of gossypol were added to nematodes as top-dressing on plates containing a lawn of BK16 bacteria on NGM medium plates. A single L4 hermaphrodite was placed on each plate for progeny F1 tests. Multiple L4 males were placed on each plate for P0 tests.

For treatment with serotonin, nematodes were soaked in various concentrations of serotonin in M9 buffer for 1 hour prior to testing for turning behavior.

**Male turning assay.**

The male turning assay developed in the Loer laboratory(Loer & Kenyon, 1993) was used: L4 males were picked and adapted to fresh 60mm plates for 24 hours, then scored via a double-blind assay. Individual adult males were placed on a 30mm plate with one drop of bacteria and 10-12 adult *unc-51* (paralyzed) young adult hermaphrodites. Each male was observed attempting to mate and 5 turns of the male backing along the hermaphrodite were scored. Each turn was categorized as either "good," "sloppy," or "missed". At least 34 males were tested for each genotype measured, with the exact numbers listed in Figshare. In some cases, the same numbers for controls are presented in multiple figures.

**Microscopy.**

Nematodes were examined via a Zeiss microscope equipped for both epifluorescence and DIC microscopy (Carl Zeiss, Thornwood, NY) and photographed by use of an Optronics MagnaFire Camera. Animals were placed on 3% agarose pads in M9 solution + 35mM $NaN_3$. Images of CP neurons of larger worms (Fig. 7B, C) required four photographs that were "stitched" together to provide a picture of the six CP neurons. Contrast on DIC images was uniformly enhanced over the entire image to increase clarity.

Subcellular location of fluorescent proteins at high resolution was examined through a FluoView FV1000 laser-scanning confocal microscope (Olympus, Tokyo, Japan). Lasers were set to 488 nm excitation and 520 nm emission (GFP), or 543 nm excitation and 572 nm emission (mKate2). All images were captured via FluoView software (Olympus) and collocation was analyzed by use of ImageJ software.

**Ribonucleoprotein-Immunoprecipitation, qPCR and western blot.**

The RNP-IP technique was adapted as previously described [24, 63]. Ribonucleoside Vanadyl Complex was from NEB (Catalog #: S1402S). Anti-FLAG® M2 Magnetic Beads were from Sigma-Aldrich (Catalog #: M8823). RNA was reverse-transcribed with random primers from Applied Biosystems (Catalog #: 4374966). qPCR was performed using the SYBR kit from Applied Biosystems (Cat #: A25742). Expression levels were normalized to the nematode housekeeping gene *tba-1* (encoding α-tubulin). Western blots were performed with Anti-Flag antibody DYKDDDDK Tag Monoclonal Antibody (FG4R) from Fisher Scientific (Catalog #: MA1-91878). Monoclonal Anti-α-Tubulin antibody produced in mouse was obtained from Sigma-Aldrich (Catalog #: T5168).

**Fluorescence Polarisation competition assay.**

Protocol is adapted from a previously published study [10]. Compounds at increasing doses were added to plate wells prior to the addition of pre-formed protein bound to the AU-RICH Element (ARE) of either Msi1 or c-Fos (as control). 10nM full-length HuR and 2 nM Msi1 or c-Fos ribonucleotide oligos were used. To form complexes using just the first two RNA-Recognition Motifs (RRM) of HuR, 50 nM HuR RRM1/2 and 2 nM c-Fos ribonucleotide oligos were used. Measurements were taken using a BioTek Synergy H4 hybrid plate reader (Biotek, Winooski, VT) after incubating for 2 hours at room temperature. IC50, the drug concentration causing 50% inhibition, was calculated by sigmoid fitting of the dose-response curve using GraphPad Prism 5.0. Percent inhibition was calculated by comparing to the DMSO (0% inhibition) and labeled free RNA only (100% inhibition) controls.

**Anti-serotonin staining and measurement.**

Anti-Serotonin staining protocol is adopted from the protocol of Loer *et al*(Loer & Kenyon, 1993). Anti-Serotonin antibody produced in rabbit was from Sigma-Aldrich (Catalog #: S5545). Secondary antibody Anti-Rabbit IgG (whole molecule)–TRITC antibody produced in goat from Sigma-Aldrich (Catalog #: T6778) was used. ImageJ was used to measure the brightness of serotonin in tissues in the red channel; some animals carried the *zdIS13*(*tph-1p*::*gfp*) construct, which allowed measurement of TPH-1 transcriptional expression levels in the green channel.

**Statistics**.

For male tail-turning assays, statistical differences between groups of animals were calculated via $\chi^2$ test of good, missed, and sloppy turns against the control results for N2 or *him-5*$^{-/-}$ animals. P-values of anti-serotonin staining and *tph-1::gfp* brightness are calculated by one-way ANOVA.

**Table 4 Strains used in this study.**

| Strain | Genotype | Source |
|---|---|---|
| **N2** | Wild-type | CGC |
| **DR466** | *him-5(e1490)* | CGC |
| **NJ683** | *exc-7(rh252)* | Buechner lab |
| **BK560** | *exc-7(rh252); him-5(e1490);* | This study |
| **BK562** | *exc-7(rh252); him-5(e1490); zdis13* | This study |
| **HS144** | *msi-1(os1); him-5(e1490)* | CGC |
| **BK561** | *msi-1::gfp::3xflag(qp120)* | This study |
| **BK563** | *msi-1::gfp::3xflag(qp120); him-5(e1490)* | This study |
| **BK564** | *msi-1(os1); him-5(e1490); zdis13* | This study |
| **BK565** | *exc-7(rh252); msi-1(os1); him-5(e1490)* | This study |
| **PS998** | *goa-1(sy192); him-5(e1490)* | CGC |
| **BK566** | *goa-1(sy192); him-5(e1490); zdis13* | This study |
| **BK567** | *goa-1::mKate2::3xmyc(qp121)* | This study |
| **BK568** | *goa-1::mKate2::3xmyc(qp121); him-5(e1490)* | This study |
| **BK569** | *goa-1::mKate2::3xmyc(qp121); him-5(e1490); zdis13* | This study |
| **BK570** | *msi-1(os1); goa-1(sy192); him-5(e1490);* | This study |
| **CB55** | *unc-2(e55)* | CGC |
| **BK571** | *unc-2(e55); him-5(e1490);* | This study |
| **BK572** | *unc-2(e55); him-5; zdis13* | This study |

| | | |
|---|---|---|
| **BK573** | *goa-1(sy192); unc-2(e55); him-5(e1490);* | This study |
| **YT17** | *crh-1(tz2)* | CGC |
| **BK574** | *crh-1(tz2); him-5(e1490);* | This study |
| **BK575** | *crh-1(tz2); him-5(e1490); zdis13* | This study |
| **BK576** | *goa-1(sy192); crh-1(tz2); him-5(e1490);* | This study |
| **BK577** | *unc-2(e55); crh-1(tz2); him-5(e1490);* | This study |
| **MT15434** | *tph-1(mg280)* | CGC |
| **BK578** | *tph-1(mg280); him-5(e1490);* | This study |
| **BK579** | *tph-1(mg280); him-5(e1490); zdis13* | This study |
| **BK580** | *goa-1(sy192); tph-1(mg280); him-5(e1490);* | This study |
| **BK581** | *crh-1(tz2); tph-1(mg280); him-5(e1490);* | This study |
| **BK582** | *unc-2(e55); tph-1(mg280); him-5(e1490);* | This study |
| **CB369** | *unc-51(e369)* | CGC |
| **BK583** | *gfp::3xflag::exc-9(qp124)* | This study |

## 5.2 Introduction

RNA-binding proteins (RBP) play vital roles in the translational regulation of gene expression, mRNA distribution, stability, and degradation(Holt & Bullock, 2009; Martin & Ephrussi, 2009). The Hu/ELAV and Musashi families of RNA-binding proteins have been particularly well studied. The ELAV family (from *Drosophila* Embryonic Lethal Abnormal Vision(Yao, Samson, Reeves, & White, 1993)) has four members in humans: HuB, HuC, HuD, and HuR (Good, 1995); and one nematode homologue, EXC-7(Buechner et al., 1999; Fujita et al., 2003). These proteins are critical for neural development, and affect stability and splicing of thousands of different mRNAs by binding to 3' UTRs (untranslated regions) of regulated mRNAs. In mammals, HuR is highly expressed in multiple human cancers(Barbisan et al., 2009; Heinonen et al., 2007). Several small-molecule compounds disrupt HuR-mRNA interactions and slow growth of cancerous tissues(Wu et al., 2015). HuR increases stability of many mRNAs, including mRNAs encoding the Musashi RNA-binding proteins(Vo et al., 2012). Similarly, in *C. elegans*, EXC-7 regulates stability of multiple mRNAs, for example that of *sma-1* (encoding the cytoskeletal protein $\beta_H$-spectrin) required for long tubule integrity(Buechner et al., 1999; Fujita et al., 2003), and also regulates mRNA splicing (Norris et al., 2014) and synaptic transmission(Loria, Duke, Rand, & Hobert, 2003).

The Musashi family was also initially identified in *Drosophila*, where it is required for sensory bristle and neural development(M. Nakamura, Okano, Blendy, & Montell, 1994). In mammals, MSI1 is predominantly expressed in neural precursor cells and multipotent CNS stem cells(Nagata et al., 1999), while a second homologue, MSI2, is involved in the proliferation and maintenance of CNS stem cell populations (Sakakibara et al., 2002). MSI1 is up-regulated in a variety of human cancers, and negatively regulates Notch and Wnt pathway signaling via binding

to Numb and APC, respectively (Imai et al., 2001; Spears & Neufeld, 2011). Knockdown of MSI1 function by means of siRNA(Sureban et al., 2008), miRNA(A. R. Smith et al., 2015), or small-molecule inhibitors results in inhibition of tumor progression(Lan et al., 2015; Lan et al., 2018). In the nematode *C. elegans*, the sole family member MSI-1 is required for a specific step of male mating behaviour and also acts via the Arp2/3 complex to mediate loss of memory(Hadziselimovic et al., 2014; Yoda, Sawa, & Okano, 2000).

The ability of male *C. elegans* to mate efficiently requires tail flexures mediated by signaling by the neurotransmitter serotonin(Loer & Kenyon, 1993; Mendel et al., 1995), a step defective in *msi-1* mutants. Serotonin is a neurotransmitter involved in many *C. elegans* behaviours, including locomotion(Horvitz, Chalfie, Trent, Sulston, & Evans, 1982; Sawin, Ranganathan, & Horvitz, 2000), defecation(Weinshenker, Garriga, & Thomas, 1995), pharyngeal pumping(Avery & Horvitz, 1989; Niacaris & Avery, 2003; Rogers, Franks, Walker, Burke, & Holden-Dye, 2001; Segalat, Elkes, & Kaplan, 1995), egg-laying(Trent, Tsung, & Horvitz, 1983; Waggoner, Zhou, Schafer, & Schafer, 1998; Weinshenker et al., 1995), and male tail flexure during mating (Loer & Kenyon, 1993; Mendel et al., 1995).

Since both serotonin and MSI-1 are required for male tail flexure, we have examined possible interactions between these two components. Findings here indicate that the human MSI1 inhibitor (-)-gossypol causes *C. elegans* male tail-turning defects, and this phenotype appears to be mediated by MSI-1. MSI-1 binds to and stabilizes mRNA encoding the G-protein alpha subunit GOA-1, which in turn alters expression of *tph-1* through *crh-1*/CREB. TPH-1 encodes the enzyme tryptophan hydroxylase that carries out the rate-limiting step of serotonin synthesis. In addition, EXC-7/HuR regulates serotonin level. By use of anti-serotonin staining, we found that mutants in either *exc-7*, *msi-1*, *goa-1*, *crh-1*, or *tph-1* show strong decreases in

serotonin level in neurons responsible for male tail flexure. These results demonstrate that a key EXC-7/MSI-1/GOA-1/Serotonin pathway is responsible for this mating behaviour in *C. elegans*. We believe that *C. elegans* provides a useful model for understanding the interactions of these essential RNA-binding proteins in the regulation of neuronal signal transduction.

### 5.3 Gossypol inhibits *C. elegans* MSI-1 interactions with mRNA

Once attracted to a hermaphrodite, the *C. elegans* male places its genital gubernaculum onto the hermaphrodite, and maintains contact while moving backward until sensory receptors in the tail locate the vulva near the center of the animal (Barr & Garcia, 2006; Emmons, 2005). If the male reaches the end of the hermaphrodite before locating the vulva, the male tightly flexes its tail, maintaining contact, and curls around the hermaphrodite to move backward along the other side of the animal. Several passes may be required before the vulva is located (Barr & Garcia, 2006). The turns must be precise for the male tail to remain in contact, as the hermaphrodite may be moving during this process, so strong stimulation and flexure of the male diagonal muscles of the tail is necessary. The male's ability to maintain tail contact with the hermaphrodite is defined as a "successful turn" (Fig. 1A). When the male's tail completely falls off the hermaphrodite, the turn is defined as "missed" (Fig. 1B). An intermediate "sloppy turn" occurs when the tail loses contact briefly, but the male then reestablishes placement on the hermaphrodite (Fig. 1C)(Loer & Kenyon, 1993).

The small molecule (-)-gossypol disrupts the interaction between mammalian Musashi1 and its target mRNAs(Lan et al., 2015). To test whether this compound has the same effect on *C. elegans* MSI-1, we allowed *C. elegans* wild-type L4 hermaphrodites to feed and lay eggs in the presence of 0-20 μM (-)-gossypol, and scored the ability of F1 progeny males grown in this environment to turn during mating (Fig. 1D) (n.b.: We used a *him-5*(*e1450)* strain as wild-type; all strains in this study were crossed to this background to increase the frequency of males). At higher (-)-gossypol concentrations, the frequency of turning defects increased from less than 10% to approximately 50% (Fig. 1D), similar to the rate of misturning of *msi-1* mutants. Treatment of *msi-1*(*os1*) mutants with (-)-gossypol showed no significant increase in the

frequency of poor turns, consistent with (-)-gossypol action on *C. elegans* MSI-1 being a major mechanism of action of the drug for this behaviour. These results indicate that (-)-gossypol induces the male turning defect and that (-)-gossypol likely functions by way of MSI-1. The effective concentration of (-)-gossypol on male turning (≥10 μm for strongest effect) is also similar to that needed to affect human cell growth rates [21], which suggests that the drug gets into the nematode by a means other than crossing the relatively impermeable cuticle(Cox, Kusch, DeNevi, & Edgar, 1981).

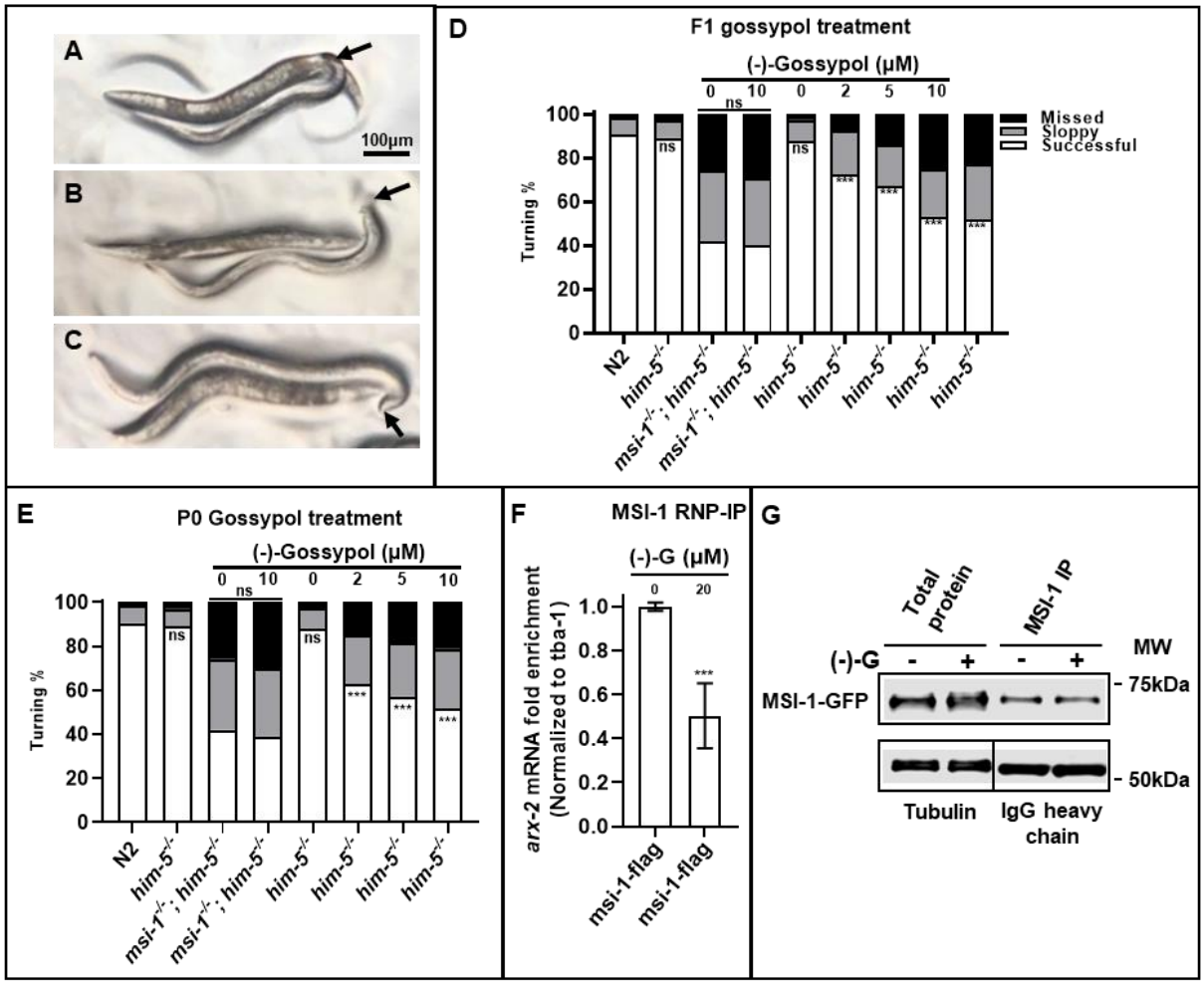


**Figure 1. Human RNA-binding Musashi-1 inhibitor (-)-gossypol causes a *C. elegans* male mating defect.**

**(A-C)** Micrographs of male (smaller animal) backing up in attempting to find vulva on hermaphrodite (larger animal); arrows indicate gubernaculum on back end of male. Scale bar, 100 μm.

**(A)** A "successful" turn, with male tail (arrow) maintaining contact while turning sharply to reverse direction of movement along the hermaphrodite.

**(B)** A "missed" turn; the tail has fallen off the end of the hermaphrodite, and does not regain contact.

**(C)** A "sloppy" turn; the male tail has slipped off the hermaphrodite, but through strong flexure, the male regains contact.

**(D-E)** Gossypol feeding assays. The concentration of (-)-gossypol applied to each group is indicated at the top of the panel. Black bars represent percentage of missed turns, grey bars represent sloppy turns, and white bars represent successful turns. Numbers for N2 and *him-5*$^{-/-}$ control groups are re-used in multiple figures. NS, no significant difference (from *him-5*$^{-/-}$ unless bar is shown to indicate comparison); ***, $P<0.001$.

**(D)** F1 assay: Cultures of worms growing on a bacterial lawn were treated with the indicated concentrations of (-)-gossypol for 48-72 hr, and mating behaviour of male progeny was measured. Total number of turns examined for each group is greater than 141.

**(E)** P0 assay: L4 worms were treated with (-)-gossypol for 24 hr and the mating behaviour of treated male animals was then tested. Total number of turns examined for each group is greater than 169. (Numbers for N2, *him-5*$^{-/-}$, and untreated *msi-1*$^{-/-}$;*him-5*$^{-/-}$ controls same as in Fig. 1D).

**(F)** Quantitative PCR to compare the amount of *arx-2* mRNA (control) bound by MSI-1 in the absence or presence of (-)-gossypol. *tba-1* (Tubulin) was used as housekeeping control.

**(G)** Western blot of RNP-IP of total protein and MSI-1::Flag. Lysate and immune-precipitated Flag-tagged protein from treated and untreated groups were loaded. Blotted for MSI-1::Flag and tubulin (housekeeping control).

As the effect described above could have resulted from defects in egg formation or early embryogenesis as well as direct effects on male behaviour, we reduced exposure time of animals to the drug by placing L4 males on plates containing varying amounts of (-)-gossypol, and measuring mating behaviour after just 24 hr (Fig. 1E). Again, application of (-)-gossypol substantially increased frequency of poor turns in wild-type males in a dosage-dependent manner, but had no effect on *msi-1* mutants. The rapid effect on turning is suggestive of action on a signaling pathway.

We next examined MSI-1 function. CRISPR/Cas-9 plasmids optimized for use in *C. elegans* were utilized to integrate *gfp* and 3 copies of *flag* DNA sequences at the 3' end of the *msi-1* coding region [39]. Mating ability of male animals of this strain (BK561) is not significantly different than that of the parental *him-5* strain. (91.8% successful, 5.5% sloppy and 2.7% missed).

This *msi-1*::*gfp*::3x*flag* strain allowed determination of whether (-)-gossypol directly blocks MSI-1 binding to mRNA as it does in mammals. We performed ribonucleoprotein-immunoprecipitation (RNP-IP) with anti-Flag antibody in the presence or absence of (-)-gossypol, and measured via qRT-PCR the amount of target mRNAs bound. MSI-1 was previously reported to bind to the 3'UTR of *arx-2* mRNA(Dickinson et al., 2015), so this gene was used as a positive control for mRNA binding by MSI-1. We found that application of 20 μM (-)-gossypol lowered the amount of bound *arx-2* mRNA by 50% as compared to the amount bound in untreated controls (Fig. 1F). A western blot (Fig. 1G) confirmed that (-)-gossypol binds directly to MSI-1, and we conclude that this interaction disrupts the interaction between MSI-1 and downstream target mRNAs such as *arx-2*.

**5.4 Gossypol may enter through the male tail to affect turning behavior**

The nematode cuticle restricts entry of many drugs, while (-)-gossypol acts on male tail turning at similar concentrations to its action on mammalian cells(Wu et al., 2015). We therefore hypothesized that (-)-gossypol entered via an opening allowing internal access to neurons that mediate tail turning. In a recent drug screen via fluorescent polarisation assay of approximately 2000 compounds(Wu et al., 2015), (-)-gossypol strongly inhibited binding ability of human HuR to AU-Rich Elements (ARE) of the msi-1 3'UTR, causing 50% inhibition at ~1 μM. The closely related molecule MP-Gr had little effect (Fig. 2A).

EXC-7 is the nematode orthologue of human HuR. Mutants in this gene exhibit distinctive defects in embryonic development and extension of the excretory canal cell(Fujita et al., 2003). The canals of wild-type animals have a narrow tubular shape and extend to the posterior end of the worm body, while mutants develop shortened canals with irregular tubules containing small fluid-filled cysts (Fig. 2B-C). Feeding (-)-gossypol to wild-type worms (Fig. 2D), the protocol used to impair male tail-turning, showed no effects on canal morphology. Injection of (-)-gossypol, however, into the gonad of *exc-7* young adult hermaphrodites caused strong effects on the canals of the progeny (Fig. 2E), and the effects were dosage-dependent (Fig. 2F, G). The effects were not exacerbated by injecting (-)-gossypol into *exc-7* null mutant progeny, consistent with (-)-gossypol exerting its effects through inhibition of EXC-7 function. These results indicate that (-)-gossypol does not pass through the cuticle nor diffuse through the nematode body to the canals, and by implication, to the tissues involved in tail turning.

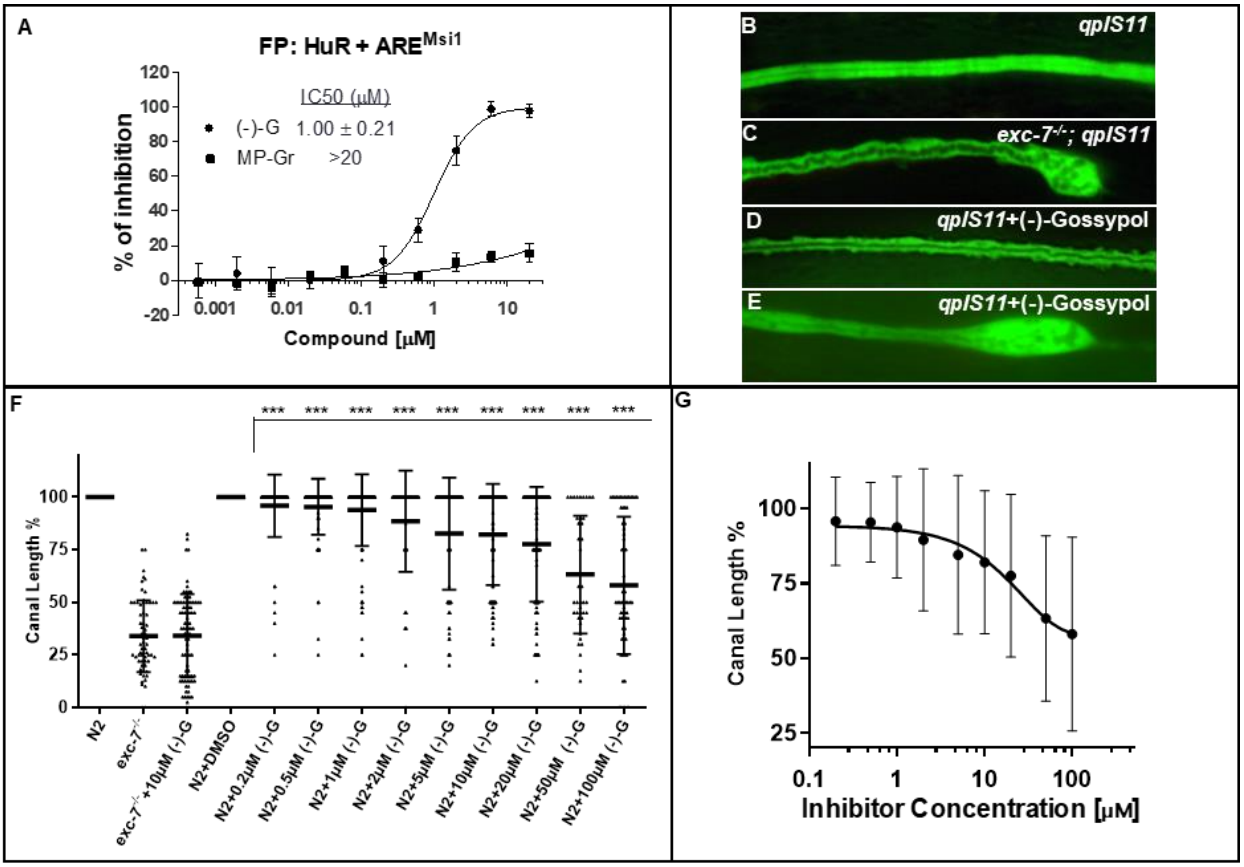


**Figure 2. Gossypol does not diffuse into the worm to inhibit *C. elegans* EXC-7/HuR.**

**(A).** Dose-response curves of (-)-gossypol and its negative analogue MP-Gr disrupting HuR-ARE$^{Msi1}$ binding in fluorescence polarisation assay using 5 nM HuR and 2 nM fluorescein-labeled ARE$^{Msi1}$. Result is presented as average of three independent experiments.

**(B)** *qpIs11* marker in wild-type animal background. Excretory canal shows normal elongation and morphology.

**(C).** *exc-7*$^{-/-}$ mutant canal expressing *qpIs11*.

**(D).** (-)-Gossypol administered by feeding does not affect excretory canal morphology.

**(E).** (-)-Gossypol injected into parental ovary caused excretory canal morphology defects.

**(F).** N2 injected with (-)-gossypol at concentrations comparable to those affecting male tail-turning behaviour. Bars represents average canal length, triangles represent each canal measured. ***, $P<0.001$.

**(G).** Logarithmic graph to summarize the trend of (-)-gossypol effects on excretory canal length

**5.5 MSI-1 binds *goa-1* mRNA to regulate male turning behaviour**

Male turning behaviour is mediated by serotonin signaling(Loer & Kenyon, 1993; Mendel et al., 1995). To study whether MSI-1 regulates this signaling, we performed an abbreviated screen of potential targets of MSI-1 binding to genes known to contribute to *C. elegans* male-turning behaviour (Fig. 3). Potential hits were identified via RNP-IP using anti-FLAG antibody to detect binding by MSI-1::GFP::3xFLAG. As negative control, GFP::3xFLAG was inserted (via CRISPR/Cas9 technology) into a protein that does not bind RNA, EXC-9 (Tong & Buechner, 2008) (Fig. 3A). As *Flag* inserted at the endogenous *msi-1* locus was used instead of a construct overexpressing MSI-1::FLAG, we measured binding to *arx-2* mRNA as positive binding control for pulldown by MSI-1::FLAG. We found that *cat-1* mRNA and *goa-1* mRNA were pulled down even more strongly than was *arx-2* mRNA by MSI-1::FLAG (Fig. 3B).

The *cat-1* gene encodes an orthologue of human SLC18A1 and SLC198A2 (solute carrier family 18 members A1 and A2) and is predicted to have monoamine transmembrane transporter activity. The *goa-1* gene encodes an orthologue of the mammalian heterotrimeric G-protein alpha subunit Go (GNAO1). A previous transcriptome-wide RNA-binding analysis (via CLIP-seq) for both endogenous and induced Msi1 in the intestinal epithelium identified mRNAs of GNAO1 and both SLC18A1 and SLC18A2 as likely targets of MSI1(Li et al., 2015). In nematodes, *goa-1* mutants exhibited more severe male turning defects than those of *cat-1* mutants (Loer & Kenyon, 1993; Mendel et al., 1995). We performed RNP-IP of MSI-1 in the presence or absence of (-)-gossypol, and utilized qPCR to measure binding to *goa-1* mRNA (Fig. 3C). In the treated group, the amount of *goa-1* mRNA bound was about 60% of that in the untreated control group, which confirmed that (-)-gossypol binding of MSI-1 affects the ability of this protein to bind to *goa-1* mRNA.

To see whether GOA-1 interaction with MSI-1 regulates serotonergic male turning behaviour, we created a line overexpressing a stable multi-copy array of *goa-1* genomic DNA driven by its native promoter (Fig. 3D). Overexpression of *goa-1* caused some embryonic lethality (data not shown), but in surviving animals, *goa-1* expression substantially restored the turning ability of *goa-1(sy192)* mutant males (control) and also rescued the male turning defects of *msi-1* mutants (Fig. 3D). A *msi-1*; *goa-1* double homozygote shows no significant difference in rate of turning defects from those of *goa-1* homozygotes alone (P=0.2), consistent with these genes acting in a common pathway.

The *goa-1* gene is expressed in many tissues, including the male-specific diagonal muscles and neurons. As noted above, *msi-1* is expressed in many neurons. In order to determine whether GOA-1 is needed within the muscles or neural tissues to mediate male turning, we stably overexpressed genomic *goa-1* driven either by the *tph-1* promoter (expressing in the serotonergic neurons required for male turning) or by the *myo-3* promoter (expressing in body wall muscles, including the diagonal muscles). Neuronal *goa-1* rescued male turning behaviour in *goa-1* mutants, while *goa-1* expressed in muscles failed to rescue (Fig. 3D). These results indicate that *goa-1* functions in serotonergic neurons to promote male turning ability.

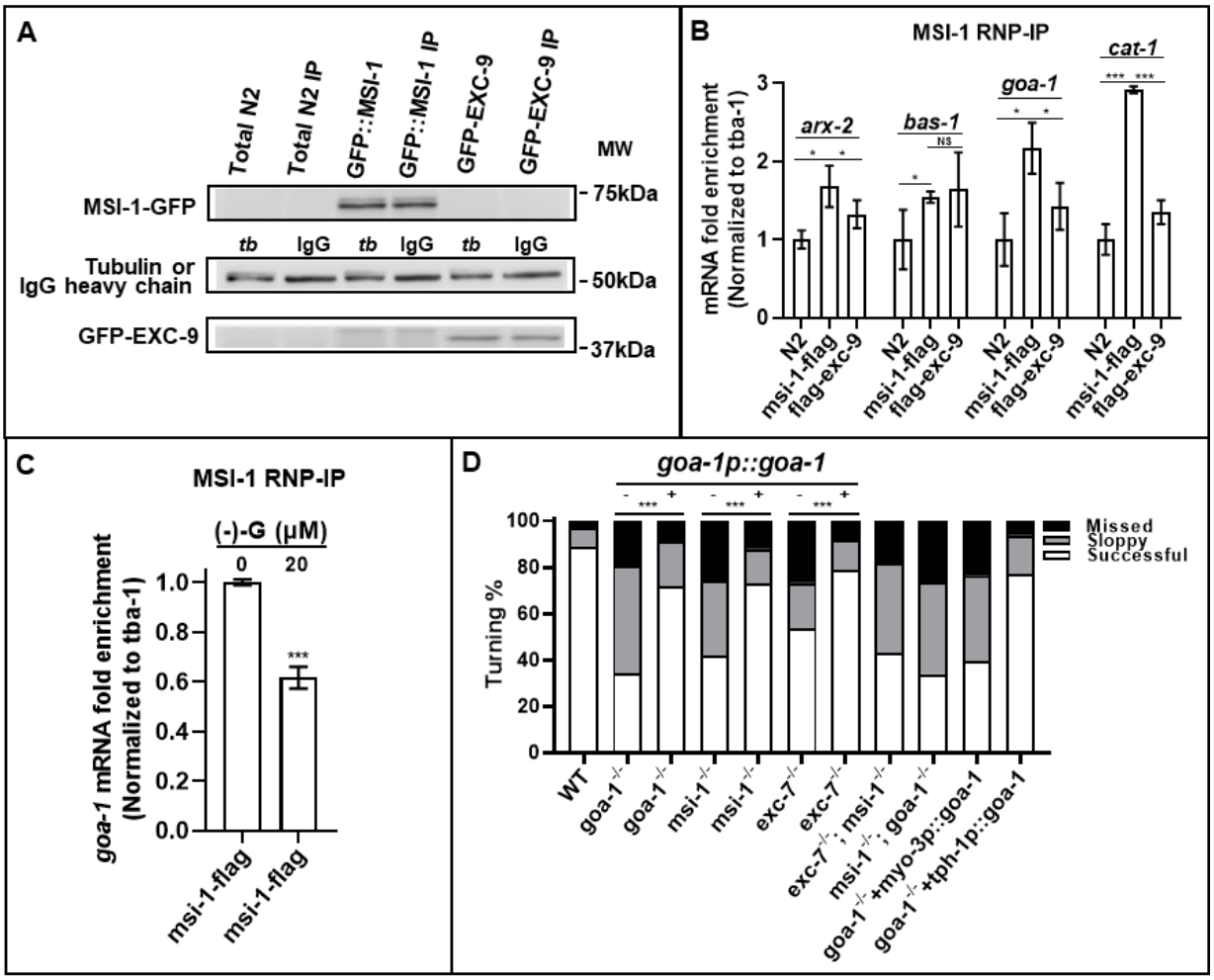


**Figure 3. MSI-1 binds and stabilizes *goa-1* mRNA to regulate male turning behaviour.**

**(A)** Western blot of MSI-1::Flag RNP-IP. Lysate and immune-precipitated protein were loaded. Blotting MSI-1::Flag, tubulin or IgG (housekeeping controls) and Flag::EXC-9.

**(B)** Comparison of amounts of specific mRNAs pulled down by MSI-1::3xFLAG from wild-type (N2), MSI-1::GFP::FLAG, and GFP::FLAG::EXC-9-expressing nematode cultures. *arx-2* is used as positive control. Statistical analysis was done via One-way Anova test. *, 0.01<P<0.05; ***, P<0.001. *tba-1* (Tubulin) was used as housekeeping control.

**(C)** Quantitative PCR to compare the amount of *goa-1* mRNA bound by MSI-1 in absence or presence of (-)-gossypol. Statistical analysis was done via One-way Anova test. ***, P<0.001. *tba-1* (Tubulin) was used as housekeeping control.

**(D)** Male-turning test of mutant strains, and the same strains containing a stable extrachromosomal array of *goa-1p::goa-1*. Bars as in Fig. 1: black, missed turns; grey, sloppy turns; white, good turns. ***, P<0.001. N(number of total turns)>184. (Numbers for WT and untreated *msi-1*$^{-/-}$ controls same as in Fig. 1D).

**5.6 EXC-7 functions through MSI-1 to regulate male turning behaviour**

In human tissues, HuR binds to and stabilizes the 3'UTR of *Musashi1* mRNA(Vo et al., 2012). In order to determine whether nematode EXC-7 (HuR homologue) also binds to *msi-1* mRNA, we utilized CRISPR/Cas-9 to insert *gfp* and 3x*flag* at the 5' end of the *exc-7* coding region. RNP-IP was then performed to compare the level of *msi-1* mRNA bound by Flag-tagged EXC-7 versus controls (wild-type and Flag-tagged EXC-9) (Fig. 4A). EXC-7 has a stronger affinity to *msi-1* mRNA than did the controls (wild-type and Flag-tagged EXC-9) (Fig. 4A, Supp. Fig. 2). Consistent with these observations, *C. elegans exc-7* mutants also exhibited male turning defects (Fig. 3D) (46% missed and sloppy turns), though at a lower frequency than did *msi-1* mutants (58% missed and sloppy turns, P=0.008 for the difference). We crossed *exc-7* to *msi-1* mutants to generate *msi-1; exc-7* double homozygotes. These animals show turning defects (57% missed and sloppy turns) no higher than those of *msi-1* homozygotes (P=0.1), with no evidence of synthetic effects. Stable *goa-1p::goa-1* overexpression in *exc-7* mutants partially rescues the *exc-7* phenotype (21% missed and sloppy turns) (Fig. 3D). These results indicate that EXC-7 likely acts upstream of GOA-1 to regulate its synthesis or activity.

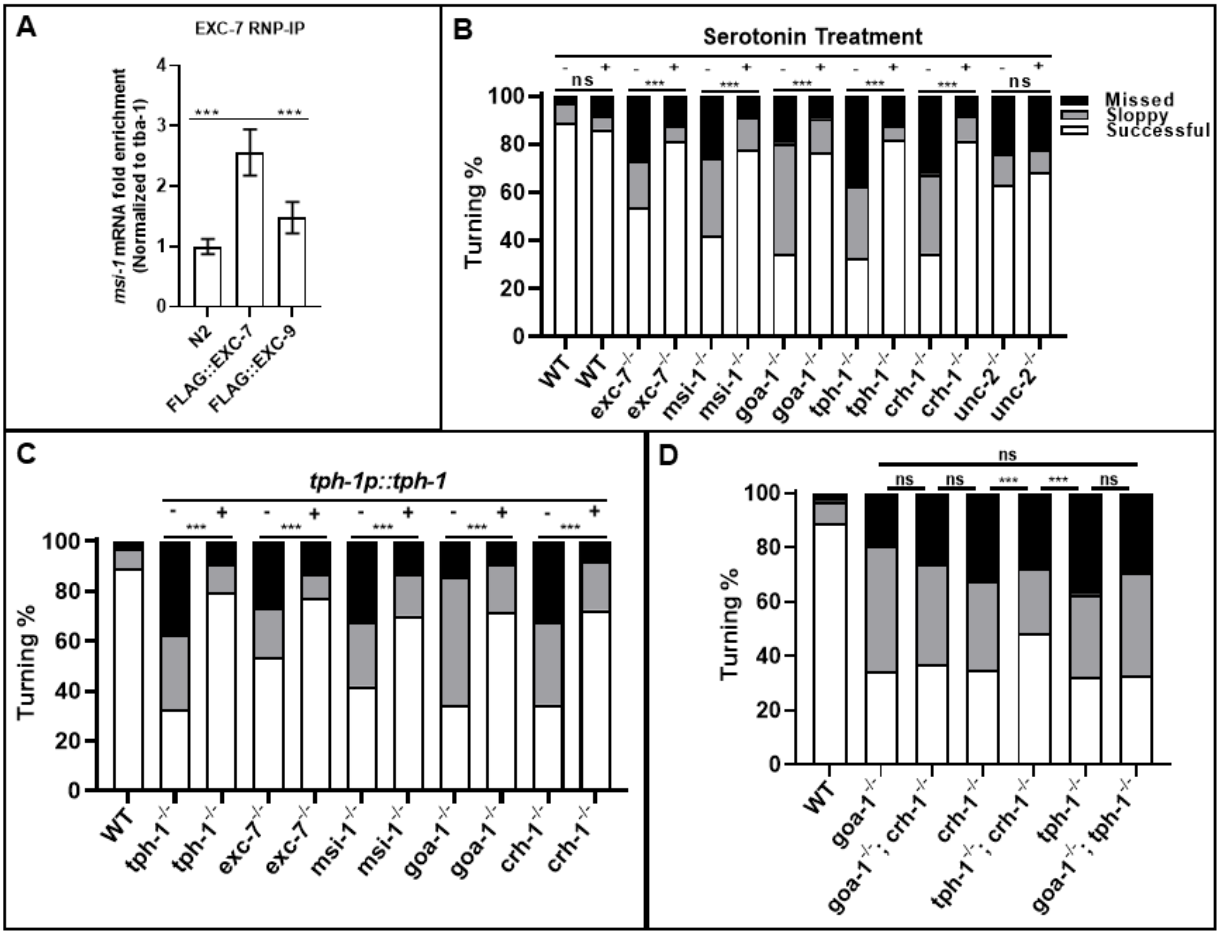


**Figure 4. EXC-7 and MSI-1 regulate serotonin synthesis.**

**(A)** RNP-IP of GFP::FLAG::EXC-7. Levels of MSI-1 mRNA pulled by N2, FLAG::EXC-7 and FLAG::EXC-9 were compared. ***, P<0.001. *tba-1* (Tubulin) was used as housekeeping control.

**(B)** 1mM exogenous serotonin is applied to various mutants, indicated on top. Black bars represent missed turns; grey bars sloppy turns, and white bars good turns (in all panels). N(number of total turns)>169.

**(C)** Male-turning test with extrachromosomal stable array of *tph-1p::tph-1*. N(number of total turns)>196.

**(D)** Male-turning test of doubly homozygous mutants of *goa-1*, *crh-1*, *tph-1*, and *unc-2*. Statistical analysis is calculated via $\chi^2$ test. ***, P<0.001. N(number of total turns)>124. (In all panels, numbers for untreated WT and mutant controls same as in Fig. 2D).

**5.7 EXC-7/HuR, MSI-1/MSI, and GOA-1/GNAO regulate serotonin synthesis**

Serotonin is a key regulator of male turning behaviour(Loer & Kenyon, 1993; Mendel et al., 1995). We tested whether *exc-7*, *msi-1*, and *goa-1* mutant behaviour were affected by exogenous serotonin. Mutants in these genes were soaked in buffer containing 1mM serotonin for 1 hour, and tested for male-turning ability. For *exc-7*, *msi-1*, and *goa-1*, male turning defects were significantly rescued by exogenous serotonin (Fig. 4B), consistent with the three proteins functioning together in a pathway to regulate serotonin synthesis or signaling.

GOA-1 affects transcription of the *tph-1* gene, which encodes tryptophan hydroxylase, the rate-limiting enzyme for serotonin biosynthesis, in both the HSN and NSM neurons in *C. elegans(Tanis, Moresco, Lindquist, & Koelle, 2008)*. Interestingly, GOA-1 activity inhibits *tph-1* transcription in HSN neurons, but promotes transcription in NSM neurons*(Tanis et al., 2008)*. We examined TPH-1 function in male turning. Mutants in *tph-1* showed strong male turning defects (68% missed plus sloppy turns, Fig. 4B), and 1mM serotonin rescued these defects (18% missed plus sloppy turns). We tested the ability of *tph-1* genomic DNA (*tph-1p::tph-1*) to restore wild-type behaviour to *exc-7*, *msi-1*, and *goa-1* mutants (Fig. 4C). Stable overexpression of *tph-1* genomic DNA rescued male turning ability to a similar level in each mutant (sum of missed plus sloppy turns: *exc-7*, 23%; *msi-1*, 30%; *goa-1*, 29%). We further confirmed a biological interaction between GOA-1 and TPH-1 by crossing the *goa-1* mutants to the *tph-1* mutants. The doubly homozygous mutant strain exhibited no significant difference in turning ability compared to either single mutant alone (Fig. 4D). These results suggest that TPH-1 acts downstream of EXC-7, MSI-1 and GOA-1, and that the activity of these proteins upregulates *tph-1* transcription.

Two major classes of protein are often involved downstream of G proteins in signaling: calcium channels and transcription factors(Berridge, Bootman, & Roderick, 2003). Mutants in *unc-2* (encoding a calcium channel α-subunit) and in *crh-1* (encoding a homologue of the cyclic AMP-response element-binding protein CREB) both affect serotonergic TPH-1 expression in other *C. elegans* neurons(Estevez, Roberts, & Strange, 2003; Zubenko, Jones, Estevez, Hughes, & Estevez, 2009). Here, mutants in either gene showed male mating defects (Fig. 4B). The defects in *crh-1* mutants (65% missed plus sloppy turns) were comparable to those in the *tph-1* mutant, while *unc-2* mutants were significantly less impaired (37% missed plus sloppy turns). Defective turning in *crh-1* mutants can be rescued by soaking the animals in 1mM serotonin (Fig. 4B) or by overexpression of *tph-1p::tph-1* (Fig. 4C). Mutants in *unc-2*, however, could not be rescued by exogenous serotonin (Fig. 4B). This result indicates that *unc-2* mutants, although exhibiting male turning defects, do not appear to act in the *goa-1*/*tph-1*/serotonin signaling pathway. We then crossed *crh-1*, *goa-1*, and *tph-1* mutants to each other (Fig. 4D). Double mutants that included the *goa-1* mutation were as strongly affected as was the single *goa-1* mutant strain alone, consistent with GOA-1 acting together with CRH-1 and TPH-1. Finally, the *tph-1; crh-1* double homozygotes exhibited more successful turns than either mutant alone. This data suggests that GOA-1 signals to CRH-1, which signals to TPH-1 to synthesize serotonin, although there may be more complicated regulatory mechanisms involved in the interactions of TPH-1 and CRH-1.

Although these results suggest that G-protein signaling affects serotonin synthesis to exert direct effects on neural function, it was also possible that the genes are involved in development of the male tail. We crossed these mutants to a strain carrying the construct *zdIs13*(*tph-1p*::*gfp*), which marks serotonergic neurons and examined the adult male tails (Clark & Chiu, 2003) (Fig.

5). For each of the single homozygotes mentioned (*exc-7*, *msi-1*, *goa-1*, *crh-1*, *tph-1*), the tails appeared to develop normally during the L4 larval stage, and the serotonergic neurons in the 1st, 3rd and 9th sensory rays on each side of the male tail showed normal expression from the *tph-1* promoter(Yang et al., 2007), so that male tail formation in these mutants appears to be normal.

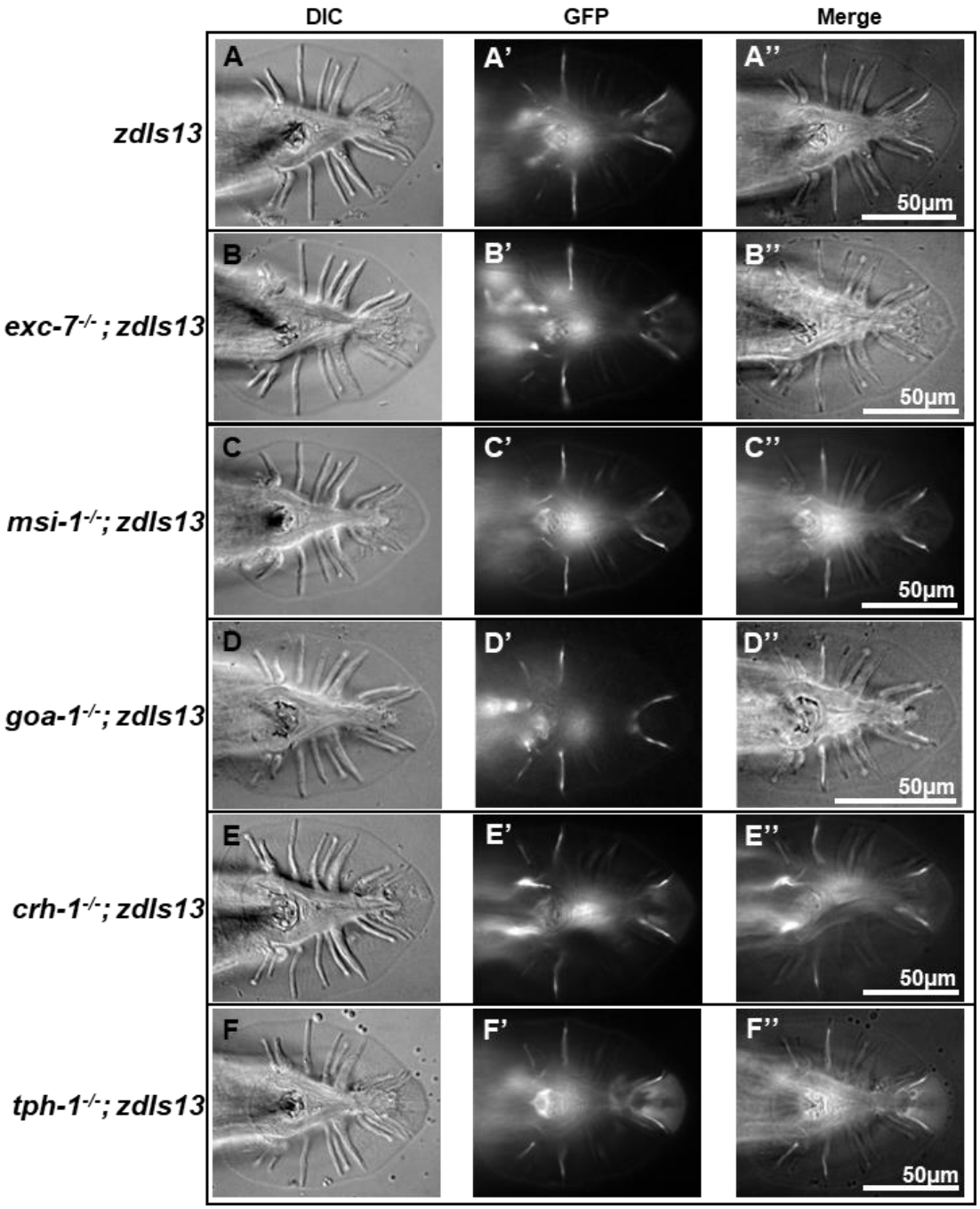


**Figure 5. Male mutant tails show wild-type morphology.**

DIC/fluorescence/merge micrographs of tail morphology of young adult males of indicated genotype. Fluorescence is *zdIS13* (*tph-1p::gfp*). **(A)** wild type; **(B)** *exc-7*$^{-/-}$; **(C)** *msi-1*$^{-/-}$; (**D**) *goa-1*$^{-/-}$; (**E**) *crh-1*$^{-/-}$; (**F**) *tph-1*$^{-/-}$.

**5.8 Serotonin levels vary in the various mutants.**

In addition to the serotonergic neurons R1B, R3B, and R9B inside male tail rays 1,3, and 9, respectively, there are many other serotonin immuno-reactive neurons, including NSM (neurosecretory motor neuron), RIH (unpaired interneuron), ADF (amphid sensory neurons), AIM (interneuron), HSN (Hermaphrodite-Specific Neurons), RIH (unpaired interneuron), ADF (amphid sensory neurons), AIM (interneuron), RPAG (Right preanal ganglion neuron) in all animals, plus VC4 and VC5 motor neurons in hermaphrodites, and in males the bilaterally symmetric CP neurons 1-6(Segalat et al., 1995). All of these neurons show expression by the transcriptional reporter *zdIs13* used above(Clark & Chiu, 2003), and GFP fluorescence was used to estimate relative levels of transcription of *tph-1* in the different male-specific neurons within wild type and the various mutant backgrounds tested in this study (Fig. 6B-H, complete results in Supp. Fig. 1A). Expression was highest in the CP5 and CP6 neurons, and decreased significantly in the more anterior CP neurons (Fig. 6B, 6H). Expression was also seen in ray neurons 3 and 9, and less strongly in ray neuron 1 (Fig. 6H). Expression in the mutant backgrounds was roughly proportional to the measured defects in male tail turning: Homozygous mutants in *exc-7* and in *msi-1* showed measurably less expression from the *tph-1* promoter, while *goa-1* mutants showed even more strongly decreased expression (Fig. 6C-6G). These results were reinforced by experiments measuring serotonin levels directly through immuno-staining with anti-serotonin antibody (Fig. 6I-6Q, complete results in Supp. Fig. 1B). Serotonin levels were highest within the CP5 and CP6 neurons, and lowered in ray neurons (Note: As permeabilisation of the animal to allow antibody entry required collagenase treatment, which degrades the male tail fan, the level of ray serotonin staining was measured only in ray

neuron 1) (Fig. 6Q). In mutants, serotonin levels were decreased significantly in mutants affecting the RNA-binding proteins EXC-7 and MSI-1, while mutation in *goa-1* or *crh-1* were much more strongly affected (Fig. 6J-N, 6P). As expected, mutation of the serotonin synthase gene *tph-1* abolished serotonin staining (Fig. 6O-P). In the mutants, serotonin levels in mutants were more strongly affected than were levels of expression from the *tph-1* promoter; the magnitude of this effect may reflect use of an overexpression construct for measuring *tph-1* transcription. These results indicate that EXC-7, MSI-1, GOA-1, and CRH-1 promote serotonin synthesis, and that this regulation is partially achieved at the transcriptional level.

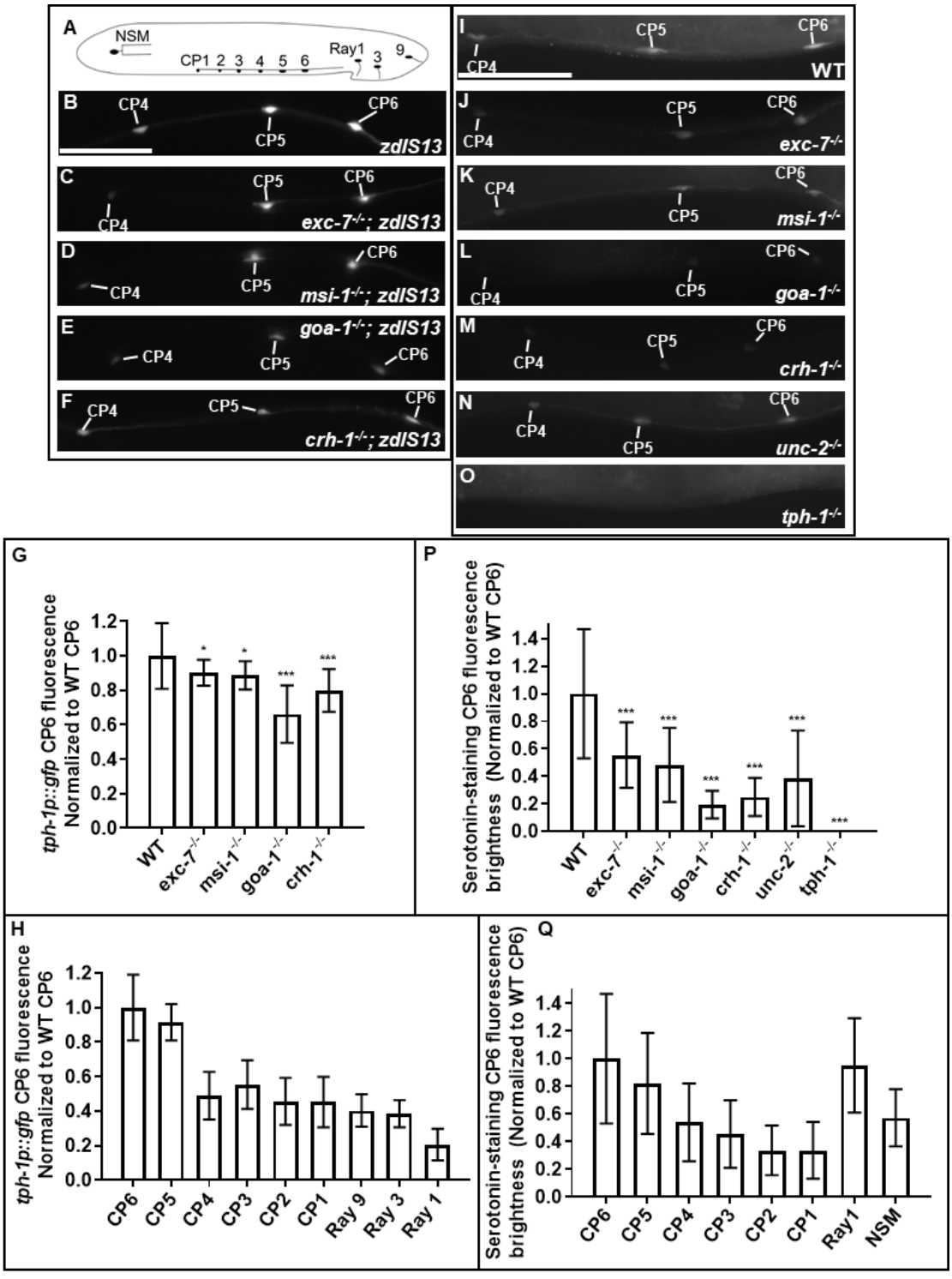


**Figure 6. Variation of endogenous serotonin levels in mutants.**

**(A)** Diagram of serotonergic neurons compared in this study. All strains shown are *in him-5*

mutant background.

**(B-F)** *tph-1* transcriptional reporter overexpression construct (*zdIS13*) expressed in strains of: **(B)** wild type; **(C)** *exc-7*$^{-/-}$; **(D)** *msi-1*$^{-/-}$; **(E)** *goa-1*$^{-/-}$; **(F)** *crh-1*$^{-/-}$.

**(G)** Average expression of *tph-1* transcriptional reporter across male-specific neuronal CP6 cell bodies in wild-type and homozygous mutants of the indicated genes.

**(H)** Relative fluorescence intensity of *tph-1* transcriptional reporter in neuronal cell bodies in wild-type animals.

**(I-O)** Anti-serotonin staining of young adult males of genotype:

**(I)** wild-type; **(J)** *exc-7*$^{-/-}$; **(K)** *msi-1*$^{-/-}$; **(L)** *goa-1*$^{-/-}$; **(M)** *crh-1*$^{-/-}$; **(N)** *unc-2*$^{-/-}$; **(O)** *tph-1*$^{-/-}$.

**(P)** Relative average fluorescence intensity of neuronal cell CP6 bodies labeled via anti-serotonin staining for the tested strains.

**(Q)** Relative fluorescence intensity in cells stained for serotonin in wild-type animals. *, $0.01<P<0.05$; ***, $P<0.001$.

**5.9 EXC-7, MSI-1, and GOA-1 are expressed in serotonergic neurons**

In order to confirm that EXC-7, MSI-1, and GOA-1 regulate serotonin synthesis, we examined the cellular location of these proteins (Fig. 7). Previous research found that MSI-1 is expressed in the male-specific CP neurons(Yoda et al., 2000). We observed the *msi-1::gfp*::*3xFlag* strain in which endogenous MSI-1 is fluorescently labeled, and confirmed that this protein is expressed in the cytoplasm of CP neurons and additionally in all nine of the male rays, as well as in the nerve ring, various head neurons, and male ray neurons (Fig. 7A,E). A line stably overexpressing *mCherry* driven by the *exc-7* promoter showed expression in the same CP neurons (CP1-CP6) as for *tph-1* expression, and in all nine male tail rays (Fig. 7B, 7B'). Another strain carrying *gfp* inserted into the endogenous locus of *exc-7* showed expression in all rays of the male tail and many other cell bodies of the male tail (Fig. 7F). Finally, we sought GOA-1 location through insertion (via CRISPR/Cas9) of a fluorescent marker into the endogenous gene. Insertion of *mKate* could not be made at the 5' end of the coding region, as it interfered with tethering of the protein to membrane, but the construct used, with insertion at the 3' end of the coding region, rendered GOA-1 nonfunctional, as locomotion and animal shape resembled that of *goa-1* mutants. The expression pattern in the ventral cord and nerve rings, however, matches the location of this protein (Fig. 7C)(Sarov et al., 2012). In this strain, *goa-1* was not expressed in the CP neural cell bodies, as no obvious collocation pattern with *zdIS13* (*tph-1p::gfp*) was identified (Fig. 7D-D''). Expression of *goa-1* was strong in all male rays, however (Fig. 7G). We conclude that EXC-7, MSI-1, and GOA-1 mediate serotonin synthesis in the male tail rays, and that EXC-7 and MSI-1 potentially affect serotonin synthesis in the CP neurons.

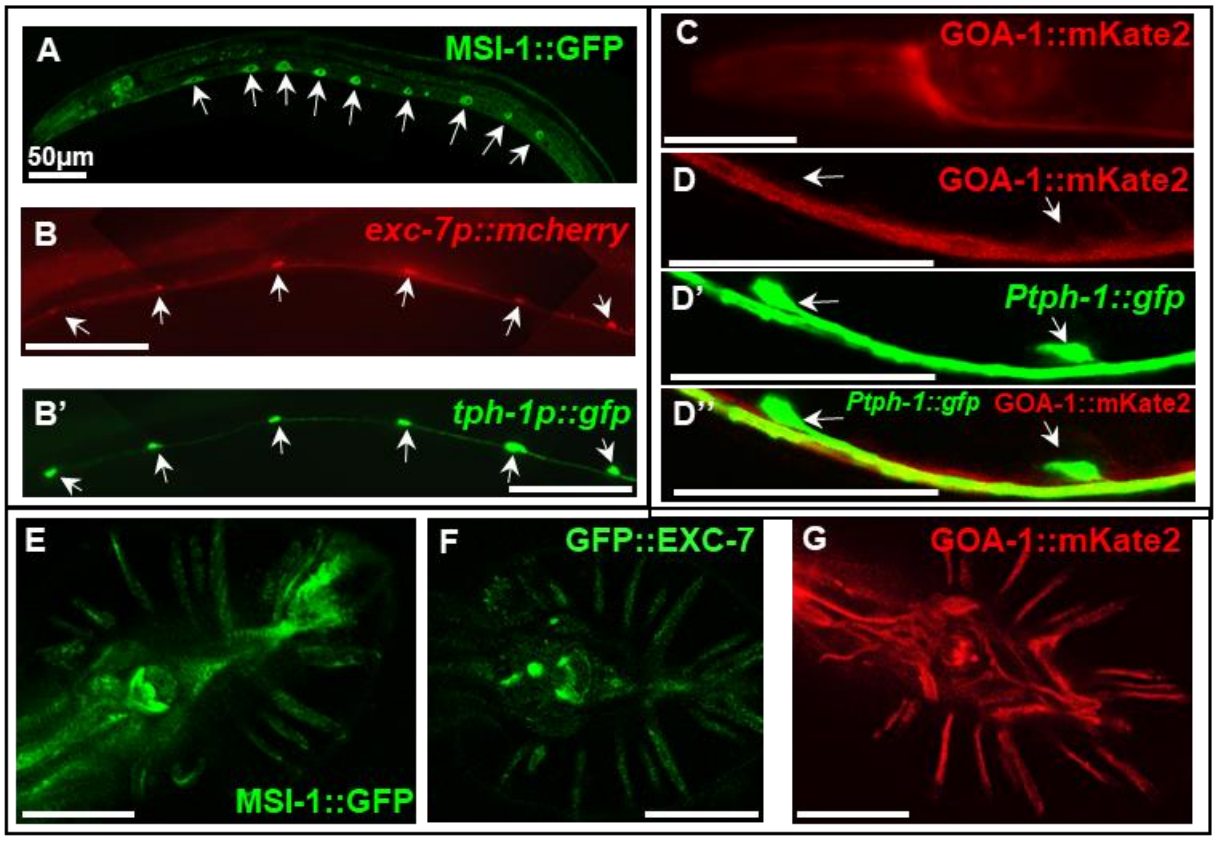


**Figure 7. EXC-7, MSI-1, and GOA-1 are expressed in serotonergic neurons.**

**(A)** MSI-1::GFP expression in cells of a young adult animal, including CP neurons (arrows).

**(B-B')** Co-expression in neuronal cell bodies and processes of CP neurons in a young adult male carrying both: **(B)** *exc-7p::mcherry* overexpression, and **(B')** *tph-1p::gfp (zdIs13)* stable array.

**(C)** GOA-1::mKate2 expression in nerve ring and ventral nerve cord.

**(D)** GOA-1::mKate2 and cytoplasmic GFP expression in male CP neurons. **(D')** *tph-1p::gfp (zdIs13)* expression in cytoplasm of CP5 and CP6 neurons. **(D'')** Merge.

**(E)** MSI::GFP expression in male tail.

**(F)** *exc-7p*::*gfp*::*exc-7* expression in male tail.

**(G)** GOA-1::mKate2 expression in male tail.

**5.10 Mutants exhibit CP neuron outgrowth defects**

Serotonergic marker *zdIS13* expression of GFP became visible within the CP1-CP6 neurons at the L4 larval stage, with strong expression evident in the cell body and weaker expression in axons extending posteriorward along the ventral nerve cord (Fig. 8A). Previous ablation studies found that as few as two functional CP neurons were sufficient to provide wild-type male turning ability(Loer & Kenyon, 1993). We examined axonal outgrowth of these mutants in strains carrying the *zdIs13* construct that strongly expressed GFP from the *tph-1* promoter. (Fig. 8B-E). Defects observed included: a CP neuron either missing, or not expressing GFP (Fig. 8B); some axonal outgrowths anteriorward instead of or in addition to posteriorward growth (Fig. 8C-D); and posterior axons not having fasciculated to the other CP axons (Fig. 8E). Surprisingly, a low level (2%) of otherwise wild-type animals carrying the *zdIs13* construct showed some CP axonal defects (Fig. 8F). The frequency of defects was exacerbated, to 5%, in animals carrying homozygous defects in *exc-7* or in *tph-1*, and strongly increased in animals with defects in *msi-1*, *goa-1*, or *crh-1* (7-17%). Growth of animals in plates containing 100μM (-)-gossypol also caused defects in the CP neurons (10%) (Fig. 8F). In all of these cases, the frequency of axonal outgrowth defects is too small to be the source of male turning defects in the serotonergic mutant animals, especially considering that ablation of as many of 4 CP neurons still allows normal turning [25]. We conclude that genes responsible for serotonin synthesis affect CP neuron development, but other potential pathways are also involved that contribute to CP neural outgrowth.

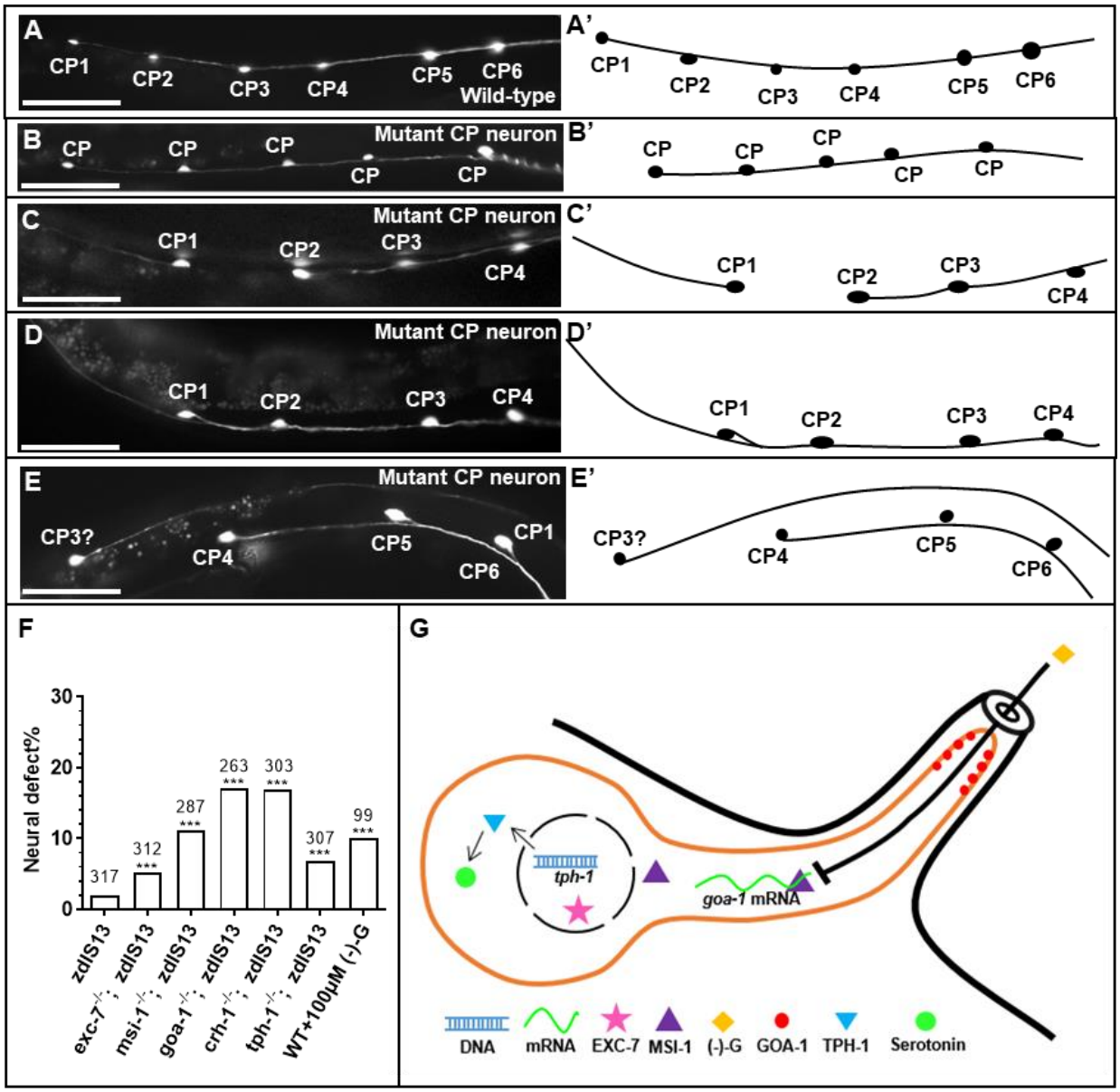


**Figure 8. CP neurons exhibit various defects in mutants.**

**(A-E).** Left-hand panels show fluorescence micrographs of CP neurons labeled in strain carrying *zdIs13* (*tphp::gfp*) marker construct. Right-hand panels provide diagram of CP neurons 1-6 and axons as seen in left-hand panels.

**(A)** Wild-type neuronal pattern; axon of each neuron grows to the posterior (right).

**(B)** Animal with fewer labeled CP neurons (Missing or non-GFP-expressing CP).

**(C)** Animal with CP1 axon growing anteriorward instead of posteriorward.

**(D)** At least one CP neuron appears to send an axon both anteriorward and posteriorward.

**(E)** The process from the presumed CP3 neuron did not join cord of other CP neurons.

**(F)** Graph showing frequency of animals exhibiting abnormal CP neuron morphology.

**(G)** Model of MSI-1 and EXC-7 influence on signal transduction machinery, and inhibition of synthesis by (-)-gossypol.

**5.11 Discussion**

The results of this study delineate a novel and likely conserved pathway by which RNA-binding proteins mediate synthesis and signaling of the neurotransmitter serotonin. We found that (-)-gossypol, inhibitor of human Musashi, also binds to *C. elegans* MSI-1 to inhibit its binding to mRNA. In *C. elegans*, MSI-1 bound to *goa-1* mRNA to mediate male turning behaviour; this binding could be interrupted by (-)-gossypol to cause defects in male turning. Mutations in *exc-7*, encoding the homologue of human HuR RNA-binding protein, also exhibited defects in male turning, as did homozygous mutations in the *goa-1* gene, encoding the α subunit of the Go heterotrimeric G-protein signal transduction complex. Stable expression of *goa-1*, in contrast, rescued the turning defects in both homozygous *msi-1* and homozygous *exc-7* mutants.

Two other genes, *crh-1* and *tph-1*, acted downstream of *goa-1*; both encode proteins that regulate production of serotonin(Estevez et al., 2003; Tanis et al., 2008; Zubenko et al., 2009): CRH-1 is the homologue of cyclic AMP-response element-binding protein CREB, while TPH-1 tryptophan hydroxylase enzyme conducts the rate-limiting step in serotonin synthesis(Sze, Victor, Loer, Shi, & Ruvkun, 2000). Mutations in these genes also caused male turning defects. All of these mutants showed reduced levels of serotonin in male ray and CP neurons, and application of serotonin to affected animals rescued mutants in all of the genes studied.

A previous study found that mutants in *cat-4(Yoda et al., 2000)*, which synthesizes GTP cyclohydrolase 1, a cofactor for serotonin synthesis, exhibited strong male mating defects, and that these defects were exacerbated in a *cat-4*; *msi-1* doubly mutant strain (decreasing from 10% to 4% male mating efficiency). While this could indicate that MSI-1 therefore acts on a pathway separate from serotonergic signaling, we note that *cat-4*(*e1141*) allele has a missense mutation, and others found residual staining male tail curling in this mutant(Loer & Kenyon, 1993). MSI-1

stabilizes mRNAs, so that even in null *msi-1* mutants, there should be some mRNA made. It is therefore possible that the combined loss of both proteins could cause a stronger loss of serotonin.

Mating behaviour of nematode males is stimulated by the neurons in the rays of the male tail, which have small openings to allow the ray neurons to detect the hermaphrodite by means of chemotactic and thigmotactic signaling(Barr & Garcia, 2006; Emmons, 2005). As treating males for a relatively short time in (-)-gossypol at concentrations in the same range as for human cells in culture strongly affected turning ability, while not interfering with EXC-7-mediated internal cell structure, we infer that the male ray openings are the most likely entry site for (-)-gossypol to affect male turning, and that the ray neurons are the most likely site of action of the pathway described above.

A model to summarize serotonin regulation at male tail rays is presented in Fig. 8G. In wild-type animals, MSI-1 binds to *goa-1* mRNA to promote its translation. GOA-1 upregulates *tph-1* transcription to facilitate serotonin synthesis through CRH-1. EXC-7 is also involved in this pathway to upregulate *tph-1* expression. The inhibitor (-)-gossypol passes through the ray opening to gain access to the neuron and interfere with MSI-1 function, leading to decreases in the amount of *goa-1* mRNA and concomitant decrease in serotonin synthesis.

Male ray neurons synapse with the male-specific CP neurons(Jarrell et al., 2012). The CP neurons are not well-studied, but appear to innervate the diagonal muscles needed for male tail flexure(C. D. Johnson, Reinitz, Sithigorngul, & Stretton, 1996). Interestingly, while *exc-7*, *msi-1*, *goa-1*, and *tph-1* were found to be expressed in Rays 1, 3, and 9, the GOA-1 protein did not appear to be expressed within the CP neurons (although we could not exclude the possibility that

GOA-1 is found solely at synapses to ray neurons). This reinforces our conclusion that the ray neurons are a major site of (-)-gossypol action on serotonin synthesis.

All of the proteins in the pathway have been well conserved from nematodes to humans, and several are involved in human diseases. In particular, the human homologues of nematode EXC-7 (HuR), MSI-1 (MSI1 and MSI2) and GOA-1 (GNAO1) have been implicated both in disorders that affect serotonin signaling and human cancer development. Up-regulation of MSI and Hu proteins is seen in multiple tumor tissues. siRNA-mediated knockdown of these genes slows tumor cell growth, as does treatment with (-)-gossypol or other inhibitors of these RNA-binding proteins (Lan et al., 2015; Lan et al., 2018; A. R. Smith et al., 2015; Sureban et al., 2008; Wu et al., 2015).

Mutations in GNAO1 have been linked to various human diseases, including breast carcinoma(Garcia-Marcos, Ghosh, & Farquhar, 2011), lung adenocarcinoma(Valdmanis et al., 2013), as well as epileptic encephalopathy(K. Nakamura et al., 2013; Talvik et al., 2015), and movement disorder(Danti et al., 2017; Okumura et al., 2018; Saitsu et al., 2015). Levels of GNAO1 are also significantly decreased in individuals with schizophrenia(Vawter et al., 2004). Finally, GNAO1 is predominantly expressed in brain, pancreas, and the gastrointestinal tract, all tissues that produce serotonin.

A pathway regulating serotonin activity from RNA-binding proteins to G-protein signaling to serotonin synthesis appears to be conserved from nematodes to humans. (-)-Gossypol, which inhibits the action of these RNA-binding proteins in humans exerts a similar effect on a serotonergic pathway in humans. Unlike many drug effects on *C. elegans*, the impermeability of the cuticle does not appear to be a hindrance to the action of (-)-gossypol on male tail turning(Gravato-Nobre et al., 2005; Holden-Dye & Walker, 2007). Assays to gauge male

turning ability in *C. elegans* therefore presents a non-invasive, useful method for gauging the effectiveness of (-)-gossypol and other drugs on HuR and MSI function both to regulate serotonin levels, and possibly to affect growth rates of tumor cells.

# Chapter 6. Conclusion

In the course of my graduate study, I worked on two projects, including studying the function and interaction between several cytoskeletal proteins in excretory canal, and research on function of RNA binding protein regulating the synthesis of neurotransmitter serotonin.

EXC-9/CRIP1 function was defined as a binding partner and acted genetically upstream of EXC-1/IRG. In this study, I discover the localization of EXC-9 and genetically EXC-9's upstream protein EXC-2, which surprisingly restrains EXC-9 at apical surface, likely through EXC-2 C-terminus domain. I also find that EXC-9 LIM domain is responsible for its apical localization, since mutating conserved cysteine disrupts EXC-9's apical localization. Moreover, I showed that SMA-1, which encodes beta-h spectrin is required for intermediate filament proper arrangement at the luminal surface. Also, when EXC-2 is missing, the terminal web covering canal luminal surface is missing, which also causes the loss of canaliculi connecting to the apical surface. This strengthen the possibility of EXC-2/IFA-2 serving as a scaffold protein to anchor proteins facilitating the formation and maintenance of canaliculi and incoming vesicles. Next I found that EXC-1 was also apical localized and surprisingly this localization in independent of EXC-2 nor EXC-9. As we look deeper into the sequence of EXC-1, we noticed a potential N-myristoylation site at the beginning of EXC-1 sequencing. Combining the fact that EXC-1 has multiple GTPase domain, this unveiled the similarity between EXC-1 and G-proteins that EXC-1 probably serves as a membrane anchored protein to phosphorylate downstream proteins to trigger the vesicular trafficking. To follow this lead, I tried to explain previous finding that, in the absence of EXC-1, 5 or 9, RME-1, which later was revealed to be a basal trafficking marker(Shi et al., 2012), was massively down-regulated (Grussendorf et al., 2016; Mattingly & Buechner, 2011). By overexpressing both RME-1 and RAB-11.1, which has been shown to be an

apical trafficking marker(Winter et al., 2012), we noticed the overexpression of RAB-11.1 suppressed the expression of RME-1 to almost none. This offered the confidence to keep looking for apical trafficking related proteins and overexpressing apical exocytosis related RAB-8 did partially rescued *exc-1* and *exc-9* mutants, but failed to rescue *exc-5* mutants. This genetically indicates that EXC-9 and EXC-1 genetically acts upstream of RAB-8 to promote apical exocytosis.

There is still many question need to be addressed. How EXC-2 affect the canaliculi formation? Is EXC-9 involve in this process? RAL-1 has been shown to affect the amount of canaliculi and excocytosis, does EXC-2, 9 and 1 work in the same pathway with RAL-1? Does EXC-1 activate RAB-8 directly? What activates EXC-5? What does EXC-2 interact with? What's the function of EXC-2 N-terminus domain? Overall, EXC-2 is atypical intermediate filament that provides many possibility of working model. It has conserved filament domain and a huge N-terminus unknown domain but lacks lamin tail domain. This feature illustrate the uniqueness of EXC-2 as an intermediate filament.

In the second project, I found that EXC-7/HuR regulates MSI-1 mRNA, which regulates GOA-1/GNAO1 mRNA to promote serotonin synthesis to regulate male turning behavior. It's a novel finding that RNA-binding proteins regulate the synthesis of serotonin. Since HuR are widely expressed, especially in nervous system, this provides insight on potential new function of how HuR help regulate and maintain neurons. I also found that (-)-gossypol, inhibitor of human Musashi, also binds to *C. elegans* MSI-1 to inhibit its binding to mRNA. Mutations in exc-7, encoding the homologue of human HuR RNA-binding protein, also exhibited defects in male turning. This also provides new model for Musashi and HuR drug testing in the future.

## Reference


Al-Hashimi, H., Chiarelli, T., Lundquist, E. A., & Buechner, M. (2019). Novel exc Genes Involved in Formation of the Tubular Excretory Canals of Caenorhabditis elegans. *G3 (Bethesda), 9*(5), 1339-1353. doi:10.1534/g3.119.200626

Al-Hashimi, H., Hall, D. H., Ackley, B. D., Lundquist, E. A., & Buechner, M. (2018). Tubular Excretory Canal Structure Depends on Intermediate Filaments EXC-2 and IFA-4 in Caenorhabditis elegans. *Genetics, 210*(2), 637-652. doi:10.1534/genetics.118.301078

Armenti, S. T., Chan, E., & Nance, J. (2014). Polarized exocyst-mediated vesicle fusion directs intracellular lumenogenesis within the C. elegans excretory cell. *Dev Biol, 394*(1), 110-121. doi:10.1016/j.ydbio.2014.07.019

Armstrong, K. R., & Chamberlin, H. M. (2010). Coordinate regulation of gene expression in the C. elegans excretory cell by the POU domain protein CEH-6. *Mol Genet Genomics, 283*(1), 73-87. doi:10.1007/s00438-009-0497-8

Avery, L., & Horvitz, H. R. (1989). Pharyngeal pumping continues after laser killing of the pharyngeal nervous system of C. elegans. *Neuron, 3*(4), 473-485.

Barbisan, F., Mazzucchelli, R., Santinelli, A., Lopez-Beltran, A., Cheng, L., Scarpelli, M., . . . Montironi, R. (2009). Overexpression of ELAV-like Protein HuR is Associated with Increased COX-2 Expression in Atrophy, High-grade Prostatic Intraepithelial Neoplasia, and Incidental Prostate Cancer in Cystoprostatectomies. *European Urology, 56*(1), 105-112. doi:10.1016/j.eururo.2008.04.043

Barr, M. M., & Garcia, L. R. (2006). Male mating behavior. *WormBook*, 1-11. doi:10.1895/wormbook.1.78.1

Barry, D. M., Xu, K., Meadows, S. M., Zheng, Y., Norden, P. R., Davis, G. E., & Cleaver, O. (2015). Cdc42 is required for cytoskeletal support of endothelial cell adhesion during blood vessel formation in mice. *Development, 142*(17), 3058-3070. doi:10.1242/dev.125260

Baum, P. D., & Garriga, G. (1997). Neuronal migrations and axon fasciculation are disrupted in ina-1 integrin mutants. *Neuron, 19*(1), 51-62.

Bennett, V., & Healy, J. (2008). Organizing the fluid membrane bilayer: diseases linked to spectrin and ankyrin. *Trends Mol Med, 14*(1), 28-36. doi:10.1016/j.molmed.2007.11.005

Berridge, M. J., Bootman, M. D., & Roderick, H. L. (2003). Calcium signalling: dynamics, homeostasis and remodelling. *Nat Rev Mol Cell Biol, 4*(7), 517-529. doi:10.1038/nrm1155

Berry, K. L., Bulow, H. E., Hall, D. H., & Hobert, O. (2003). A C. elegans CLIC-like protein required for intracellular tube formation and maintenance. *Science, 302*(5653), 2134-2137.

Brenner, S. (1974). The genetics of Caenorhabditis elegans. *Genetics, 77*(1), 71-94.

Buechner, M., Hall, D. H., Bhatt, H., & Hedgecock, E. M. (1999). Cystic Canal Mutants in *Caenorhabditis elegans* Are Defective in the Apical Membrane Domain of the Renal (Excretory) Cell. *Dev Biol, 214*, 227-241. Retrieved from C:\Stuff\PDFs\Mine\DevBiolv214pp227-241.pdf.

Carberry, K., Wiesenfahrt, T., Windoffer, R., Bossinger, O., & Leube, R. E. (2009). Intermediate filaments in Caenorhabditis elegans. *Cell Motil Cytoskeleton*. doi:10.1002/cm.20372

Chiou, J. G., Balasubramanian, M. K., & Lew, D. J. (2017). Cell Polarity in Yeast. *Annu Rev Cell Dev Biol, 33*, 77-101. doi:10.1146/annurev-cellbio-100616-060856

Clark, S. G., & Chiu, C. (2003). <em>C. elegans</em> ZAG-1, a Zn-finger-homeodomain protein, regulates axonal development and neuronal differentiation. *Development, 130*(16), 3781. doi:10.1242/dev.00571

Coch, R. A., & Leube, R. E. (2016). Intermediate Filaments and Polarization in the Intestinal Epithelium. *Cells, 5*(3). doi:10.3390/cells5030032

Cousins, R. J., & Lanningham-Foster, L. (2000). Regulation of cysteine-rich intestinal protein, a zinc finger protein, by mediators of the immune response. *J Infect Dis, 182 Suppl 1*, S81-84.

Cox, G. N., Kusch, M., DeNevi, K., & Edgar, R. S. (1981). Temporal regulation of cuticle synthesis during development of Caenorhabditis elegans. *Dev Biol, 84*(2), 277-285. doi:10.1016/0012-1606(81)90395-x

Danti, F. R., Galosi, S., Romani, M., Montomoli, M., Carss, K. J., Raymond, F. L., . . . Guerrini, R. (2017). GNAO1 encephalopathy: Broadening the phenotype and evaluating treatment and outcome. *Neurology. Genetics, 3*(2), e143-e143. doi:10.1212/NXG.0000000000000143

Davis, B. A., Blanchard, R. K., Lanningham-Foster, L., & Cousins, R. J. (1998). Structural characterization of the rat cysteine-rich intestinal protein gene and overexpression of this LIM-only protein in transgenic mice. *DNA Cell Biol, 17*(12), 1057-1064.

Delacour, D., Salomon, J., Robine, S., & Louvard, D. (2016). Plasticity of the brush border - the yin and yang of intestinal homeostasis. *Nat Rev Gastroenterol Hepatol, 13*(3), 161-174. doi:10.1038/nrgastro.2016.5

Delague, V., Jacquier, A., Hamadouche, T., Poitelon, Y., Baudot, C., Boccaccio, I., . . . Levy, N. (2007). Mutations in FGD4 encoding the Rho GDP/GTP exchange factor FRABIN cause autosomal recessive Charcot-Marie-Tooth type 4H. *Am J Hum Genet, 81*(1), 1-16.

Dickinson, D. J., Pani, A. M., Heppert, J. K., Higgins, C. D., & Goldstein, B. (2015). Streamlined Genome Engineering with a Self-Excising Drug Selection Cassette. *Genetics, 200*(4), 1035. doi:10.1534/genetics.115.178335

Dodemont, H., Riemer, D., Ledger, N., & Weber, K. (1994). Eight genes and alternative RNA processing pathways generate an unexpectedly large diversity of cytoplasmic intermediate filament proteins in the nematode Caenorhabditis elegans. *EMBO J, 13*(11), 2625-2638.

Emmons, S. W. (2005). Male development. *WormBook*. doi:10.1895/wormbook.1.33.1

Estevez, A. Y., Roberts, R. K., & Strange, K. (2003). Identification of store-independent and store-operated Ca2+ conductances in Caenorhabditis elegans intestinal epithelial cells. *J Gen Physiol, 122*(2), 207-223. doi:10.1085/jgp.200308804

Falin, R. A., Morrison, R., Ham, A. J., & Strange, K. (2009). Identification of regulatory phosphorylation sites in a cell volume- and Ste20 kinase-dependent ClC anion channel. *J Gen Physiol, 133*(1), 29-42. doi:10.1085/jgp.200810080

Fujita, M., Hawkinson, D., King, K. V., Hall, D. H., Sakamoto, H., & Buechner, M. (2003). The role of the ELAV homologue EXC-7 in the development of the Caenorhabditis elegans excretory canals. *Dev Biol, 256*(2), 290-301.

Gao, J., Estrada, L., Cho, S., Ellis, R. E., & Gorski, J. L. (2001). The Caenorhabditis elegans homolog of FGD1, the human Cdc42 GEF gene responsible for faciogenital dysplasia, is critical for excretory cell morphogenesis. *Hum Mol Genet, 10*(26), 3049-3062.

Garcia-Marcos, M., Ghosh, P., & Farquhar, M. G. (2011). Molecular basis of a novel oncogenic mutation in GNAO1. *Oncogene, 30*, 2691. doi:10.1038/onc.2010.645

Geisler, F., Coch, R., Richardson, C., Goldberg, M., Bevilacqua, C., Prevedel, R., & Leube, R. E. (2019). *Intestinal intermediate filament polypeptides in C. elegans: Common and isotype-specific contributions to intestinal ultrastructure and function*.

Geisler, F., Coch, R. A., Richardson, C., Goldberg, M., Bevilacqua, C., Prevedel, R., & Leube, R.

E. (2020). Intestinal intermediate filament polypeptides in C. elegans: Common and isotype-specific contributions to intestinal ultrastructure and function. *Sci Rep, 10*(1), 3142. doi:10.1038/s41598-020-59791-w

Gerace, L., & Burke, B. (1988). Functional organization of the nuclear envelope. *Annu Rev Cell Biol, 4*, 335-374. doi:10.1146/annurev.cb.04.110188.002003

Gettner, S. N., Kenyon, C., & Reichardt, L. F. (1995). Characterization of β*pat-3* heterodimers, a family of essential integrin receptors in *C. elegans*. *The Journal of Cell Biology, 129*, 1127-1141.

Good, P. J. (1995). A conserved family of elav-like genes in vertebrates. *Proceedings of the National Academy of Sciences, 92*(10), 4557-4561. doi:10.1073/pnas.92.10.4557

Gravato-Nobre, M. J., Nicholas, H. R., Nijland, R., O'Rourke, D., Whittington, D. E., Yook, K. J., & Hodgkin, J. (2005). Multiple genes affect sensitivity of Caenorhabditis elegans to the bacterial pathogen Microbacterium nematophilum. *Genetics, 171*(3), 1033-1045. doi:10.1534/genetics.105.045716

Gruenbaum, Y., & Foisner, R. (2015). Lamins: Nuclear Intermediate Filament Proteins with Fundamental Functions in Nuclear Mechanics and Genome Regulation. *Annual Review of Biochemistry, 84*(1), 131-164. doi:10.1146/annurev-biochem-060614-034115

Grussendorf, K. A., Trezza, C. J., Salem, A. T., Al-Hashimi, H., Mattingly, B. C., Kampmeyer, D. E., . . . Buechner, M. (2016). Facilitation of Endosomal Recycling by an IRG Protein Homolog Maintains Apical Tubule Structure in Caenorhabditis elegans. *Genetics, 203*(4), 1789-1806. doi:10.1534/genetics.116.192559

Hadziselimovic, N., Vukojevic, V., Peter, F., Milnik, A., Fastenrath, M., Fenyves, Bank G., . . . Stetak, A. (2014). Forgetting Is Regulated via Musashi-Mediated Translational Control of the Arp2/3 Complex. *Cell, 156*(6), 1153-1166. doi:10.1016/j.cell.2014.01.054

Hahn-Windgassen, A., & Van Gilst, M. R. (2009). The Caenorhabditis elegans HNF4alpha Homolog, NHR-31, mediates excretory tube growth and function through coordinate regulation of the vacuolar ATPase. *PLoS Genet, 5*(7), e1000553. doi:10.1371/journal.pgen.1000553

Hakanen, J., Ruiz-Reig, N., & Tissir, F. (2019). Linking Cell Polarity to Cortical Development and Malformations. *Frontiers in Cellular Neuroscience, 13*(244). doi:10.3389/fncel.2019.00244

Hall, D. H. (1995). Electron Microscopy and Three-Dimensional Image Reconstruction. In H. F. Epstein & D. C. Shakes (Eds.), *Caenorhabditis elegans: Modern Biological Analysis of an Organism* (Vol. 48, pp. 451-482). San Diego: Academic Press.

Hedgecock, E. M., Culotti, J. G., Hall, D. H., & Stern, B. D. (1987). Genetics of cell and axon migrations in Caenorhabditis elegans. *Development, 100*, 365-382.

Heinonen, M., Fagerholm, R., Aaltonen, K., Kilpivaara, O., Aittomäki, K., Blomqvist, C., . . . Ristimäki, A. (2007). Prognostic Role of HuR in Hereditary Breast Cancer. *Clinical Cancer Research, 13*(23), 6959. doi:10.1158/1078-0432.CCR-07-1432

Herrmann, H., & Aebi, U. (2016). Intermediate Filaments: Structure and Assembly. *Cold Spring Harb Perspect Biol, 8*(11). doi:10.1101/cshperspect.a018242

Hodgkin, J., Horvitz, H. R., & Brenner, S. (1979). Nondisjunction mutants of the nematode *Caenorhabditis elegans*. *Genetics, 91*, 67-94.

Holden-Dye, L., & Walker, R. J. (2007). Anthelmintic drugs. *WormBook*, 1-13. doi:10.1895/wormbook.1.143.1

Holt, C. E., & Bullock, S. L. (2009). Subcellular mRNA Localization in Animal Cells and Why It

Matters. *Science, 326*(5957), 1212. doi:10.1126/science.1176488

Horvitz, H. R., Chalfie, M., Trent, C., Sulston, J. E., & Evans, P. D. (1982). Serotonin and octopamine in the nematode Caenorhabditis elegans. *Science, 216*(4549), 1012. doi:10.1126/science.6805073

Howard, J. C., Hunn, J. P., & Steinfeldt, T. (2011). The IRG protein-based resistance mechanism in mice and its relation to virulence in Toxoplasma gondii. *Curr Opin Microbiol, 14*(4), 414-421. doi:10.1016/j.mib.2011.07.002

Hüsken, K., Wiesenfahrt, T., Abraham, C., Windoffer, R., Bossinger, O., & Leube, R. E. (2008). Maintenance of the intestinal tube in Caenorhabditis elegans: the role of the intermediate filament protein IFC-2. *Differentiation, 76*(8), 881-896. doi:10.1111/j.1432-0436.2008.00264.x

Igual Gil, C., Jarius, M., von Kries, J. P., & Rohlfing, A. K. (2017). Neuronal Chemosensation and Osmotic Stress Response Converge in the Regulation of aqp-8 in C. elegans. *Front Physiol, 8*, 380. doi:10.3389/fphys.2017.00380

Imai, T., Tokunaga, A., Yoshida, T., Hashimoto, M., Mikoshiba, K., Weinmaster, G., . . . Okano, H. (2001). The Neural RNA-Binding Protein Musashi1 Translationally Regulates Mammalian <em>numb</em> Gene Expression by Interacting with Its mRNA. *Molecular and Cellular Biology, 21*(12), 3888. doi:10.1128/MCB.21.12.3888-3900.2001

Jarrell, T. A., Wang, Y., Bloniarz, A. E., Brittin, C. A., Xu, M., Thomson, J. N., . . . Emmons, S. W. (2012). The connectome of a decision-making neural network. *Science, 337*(6093), 437-444. doi:10.1126/science.1221762

Johnson, C. D., Reinitz, C. A., Sithigorngul, P., & Stretton, A. O. (1996). Neuronal localization of serotonin in the nematode Ascaris suum. *J Comp Neurol, 367*(3), 352-360. doi:10.1002/(sici)1096-9861(19960408)367:3<352::Aid-cne3>3.0.Co;2-4

Johnson, D. R., Bhatnagar, R. S., Knoll, L. J., & Gordon, J. I. (1994). Genetic and biochemical studies of protein N-myristoylation. *Annu Rev Biochem, 63*, 869-914. doi:10.1146/annurev.bi.63.070194.004253

Karabinos, A., Schmidt, H., Harborth, J., Schnabel, R., & Weber, K. (2001). Essential roles for four cytoplasmic intermediate filament proteins in Caenorhabditis elegans development. *Proc Natl Acad Sci U S A, 98*(14), 7863-7868. doi:10.1073/pnas.121169998

Khan, L. A., Jafari, G., Zhang, N., Membreno, E., Yan, S., Zhang, H., & Gobel, V. (2019). A tensile trilayered cytoskeletal endotube drives capillary-like lumenogenesis. *J Cell Biol, 218*(7), 2403-2424. doi:10.1083/jcb.201811175

Khan, L. A., Zhang, H., Abraham, N., Sun, L., Fleming, J. T., Buechner, M., . . . Gobel, V. (2013). Intracellular lumen extension requires ERM-1-dependent apical membrane expansion and AQP-8-mediated flux. *Nat Cell Biol, 15*(2), 143-156. doi:10.1038/ncb2656

Kiral, F. R., Kohrs, F. E., Jin, E. J., & Hiesinger, P. R. (2018). Rab GTPases and Membrane Trafficking in Neurodegeneration. *Curr Biol, 28*(8), R471-r486. doi:10.1016/j.cub.2018.02.010

Knust, E., & Bossinger, O. (2002). Composition and formation of intercellular junctions in epithelial cells. *Science, 298*(5600), 1955-1959. doi:10.1126/science.1072161

Kolotuev, I., Hyenne, V., Schwab, Y., Rodriguez, D., & Labouesse, M. (2013). A pathway for unicellular tube extension depending on the lymphatic vessel determinant Prox1 and on osmoregulation. *Nat Cell Biol, 15*(2), 157-168. doi:10.1038/ncb2662

Kumar, S., Jain, A., Farzam, F., Jia, J., Gu, Y., Choi, S. W., . . . Deretic, V. (2018). Mechanism of Stx17 recruitment to autophagosomes via IRGM and mammalian Atg8 proteins. *J Cell Biol*.

doi:10.1083/jcb.201708039

Labouesse, M., Hartwieg, E., & Horvitz, H. R. (1996). The *Caenorhabditis elegans* LIN-26 protein is required to specify and/or maintain all non-neuronal ectodermal cell fates. *Development, 122*, 2579-2588.

Lan, L., Appelman, C., Smith, A. R., Yu, J., Larsen, S., Marquez, R. T., . . . Xu, L. (2015). Natural product (−)-gossypol inhibits colon cancer cell growth by targeting RNA-binding protein Musashi-1. *Molecular Oncology, 9*(7), 1406-1420. doi:10.1016/j.molonc.2015.03.014

Lan, L., Liu, H., Smith, A. R., Appelman, C., Yu, J., Larsen, S., . . . Xu, L. (2018). Natural product derivative Gossypolone inhibits Musashi family of RNA-binding proteins. *BMC Cancer, 18*(1), 809. doi:10.1186/s12885-018-4704-z

Lant, B., Yu, B., Goudreault, M., Holmyard, D., Knight, J. D., Xu, P., . . . Derry, W. B. (2015). CCM-3/STRIPAK promotes seamless tube extension through endocytic recycling. *Nat Commun, 6*, 6449. doi:10.1038/ncomms7449

Li, N., Yousefi, M., Nakauka-Ddamba, A., Li, F., Vandivier, L., Parada, K., . . . Lengner, C. J. (2015). The Msi Family of RNA-Binding Proteins Function Redundantly as Intestinal Oncoproteins. *Cell Rep, 13*(11), 2440-2455. doi:10.1016/j.celrep.2015.11.022

Loer, C. M., & Kenyon, C. J. (1993). Serotonin-deficient mutants and male mating behavior in the nematode Caenorhabditis elegans. *The Journal of Neuroscience, 13*(12), 5407. doi:10.1523/JNEUROSCI.13-12-05407.1993

Loria, P. M., Duke, A., Rand, J. B., & Hobert, O. (2003). Two neuronal, nuclear-localized RNA binding proteins involved in synaptic transmission. *Curr Biol, 13*(15), 1317-1323.

Mack, N. A., & Georgiou, M. (2014). The interdependence of the Rho GTPases and apicobasal cell polarity. *Small GTPases, 5*(2), 10. doi:10.4161/21541248.2014.973768

MacQueen, A. J., Baggett, J. J., Perumov, N., Bauer, R. A., Januszewski, T., Schriefer, L., & Waddle, J. A. (2005). ACT-5 is an essential Caenorhabditis elegans actin required for intestinal microvilli formation. *Mol Biol Cell, 16*(7), 3247-3259. doi:10.1091/mbc.E04-12-1061

Mah, A. K., Armstrong, K. R., Chew, D. S., Chu, J. S., Tu, D. K., Johnsen, R. C., . . . Baillie, D. L. (2007). Transcriptional regulation of AQP-8, a Caenorhabditis elegans aquaporin exclusively expressed in the excretory system, by the POU homeobox transcription factor CEH-6. *The Journal of biological chemistry, 282*(38), 28074-28086. doi:10.1074/jbc.M703305200

Mancuso, V. P., Parry, J. M., Storer, L., Poggioli, C., Nguyen, K. C., Hall, D. H., & Sundaram, M. V. (2012). Extracellular leucine-rich repeat proteins are required to organize the apical extracellular matrix and maintain epithelial junction integrity in C. elegans. *Development, 139*(5), 979-990. doi:10.1242/dev.075135

Martin, K. C., & Ephrussi, A. (2009). mRNA Localization: Gene Expression in the Spatial Dimension. *Cell, 136*(4), 719-730. doi: 10.1016/j.cell.2009.01.044

Mattingly, B. C., & Buechner, M. (2011). The FGD homologue EXC-5 regulates apical trafficking in C. elegans tubules. *Dev Biol, 359*(1), 59-72. doi:10.1016/j.ydbio.2011.08.011

Mendel, J. E., Korswagen, H. C., Liu, K. S., Hajdu-Cronin, Y. M., Simon, M. I., Plasterk, R. H., & Sternberg, P. W. (1995). Participation of the protein Go in multiple aspects of behavior in C. elegans. *Science, 267*(5204), 1652. doi:10.1126/science.7886455

Nagata, T., Kanno, R., Kurihara, Y., Uesugi, S., Imai, T., Sakakibara, S.-i., . . . Katahira, M. (1999). Structure, backbone dynamics and interactions with RNA of the C-terminal RNA-binding domain of a mouse neural RNA-binding protein, Musashi111Edited by P. E. Wright. *J Mol*

*Biol, 287*(2), 315-330. doi: 10.1006/jmbi.1999.2596

Nakamura, K., Kodera, H., Akita, T., Shiina, M., Kato, M., Hoshino, H., . . . Saitsu, H. (2013). De Novo Mutations in GNAO1, Encoding a Gαo Subunit of Heterotrimeric G Proteins, Cause Epileptic Encephalopathy. *The American Journal of Human Genetics, 93*(3), 496-505. doi: 10.1016/j.ajhg.2013.07.014

Nakamura, M., Okano, H., Blendy, J. A., & Montell, C. (1994). Musashi, a neural RNA-binding protein required for drosophila adult external sensory organ development. *Neuron, 13*(1), 67-81. doi: 10.1016/0896-6273(94)90460-X

Neefjes, J., & van der Kant, R. (2014). Stuck in traffic: an emerging theme in diseases of the nervous system. *Trends Neurosci, 37*(2), 66-76. doi:10.1016/j.tins.2013.11.006

Nelson, F. K., Albert, P. S., & Riddle, D. S. (1983). Fine structure of the *Caenorhabditis elegans* secretory-excretory system. *Journal of Ultrastructural Research, 82*, 156-171.

Nelson, F. K., & Riddle, D. L. (1984). Functional study of the *Caenorhabditis elegans* secretory-excretory system using laser microsurgery. *Journal of Experimental Zoology, 231*, 45-56.

Nemetschke, L., & Knust, E. (2016). Drosophila Crumbs prevents ectopic Notch activation in developing wings by inhibiting ligand-independent endocytosis. *Development, 143*(23), 4543-4553. doi:10.1242/dev.141762

Niacaris, T., & Avery, L. (2003). Serotonin regulates repolarization of the <em>C. elegans</em> pharyngeal muscle. *Journal of Experimental Biology, 206*(2), 223. doi:10.1242/jeb.00101

Norris, A. D., Gao, S., Norris, M. L., Ray, D., Ramani, A. K., Fraser, A. G., . . . Calarco, J. A. (2014). A pair of RNA-binding proteins controls networks of splicing events contributing to specialization of neural cell types. *Mol Cell, 54*(6), 946-959. doi:10.1016/j.molcel.2014.05.004

Oka, T., & Futai, M. (2000). Requirement of V-ATPase for ovulation and embryogenesis in Caenorhabditis elegans. *The Journal of biological chemistry, 275*(38), 29556-29561. doi:10.1074/jbc.M002756200

Okumura, A., Maruyama, K., Shibata, M., Kurahashi, H., Ishii, A., Numoto, S., . . . Kojima, S. (2018). A patient with a GNAO1 mutation with decreased spontaneous movements, hypotonia, and dystonic features. *Brain and Development, 40*(10), 926-930. doi:10.1016/j.braindev.2018.06.005

Patel, N., Thierry-Mieg, D., & Mancillas, J. R. (1993). Cloning by insertional mutagenesis of a cDNA encoding Caenorhabditis elegans kinesin heavy chain. *Proc Natl Acad Sci U S A, 90*(19), 9181-9185.

Pilla-Moffett, D., Barber, M. F., Taylor, G. A., & Coers, J. (2016). Interferon-inducible GTPases in host resistance, inflammation and disease. *J Mol Biol*. doi:10.1016/j.jmb.2016.04.032

Pires, H. R., & Boxem, M. (2018). Mapping the Polarity Interactome. *J Mol Biol, 430*(19), 3521-3544. doi:10.1016/j.jmb.2017.12.017

Praitis, V., Ciccone, E., & Austin, J. (2005). SMA-1 spectrin has essential roles in epithelial cell sheet morphogenesis in C. elegans. *Dev Biol, 283*(1), 157-170.

Rogers, C. M., Franks, C. J., Walker, R. J., Burke, J. F., & Holden-Dye, L. (2001). Regulation of the pharynx of Caenorhabditis elegans by 5-HT, octopamine, and FMRFamide-like neuropeptides. *Journal of Neurobiology, 49*(3), 235-244. doi:10.1002/neu.1078

Román-Fernández, Á., Roignot, J., Sandilands, E., Nacke, M., Mansour, M. A., McGarry, L., . . . Bryant, D. M. (2018). The phospholipid PI(3,4)P2 is an apical identity determinant. *Nat Commun, 9*(1), 5041. doi:10.1038/s41467-018-07464-8

Saitsu, H., Fukai, R., Ben-Zeev, B., Sakai, Y., Mimaki, M., Okamoto, N., . . . Matsumoto, N. (2015). Phenotypic spectrum of GNAO1 variants: epileptic encephalopathy to involuntary movements with severe developmental delay. *European Journal Of Human Genetics, 24*, 129. doi:10.1038/ejhg.2015.92

Sakakibara, S.-i., Nakamura, Y., Yoshida, T., Shibata, S., Koike, M., Takano, H., . . . Okano, H. (2002). RNA-binding protein Musashi family: Roles for CNS stem cells and a subpopulation of ependymal cells revealed by targeted disruption and antisense ablation. *Proceedings of the National Academy of Sciences, 99*(23), 15194. doi:10.1073/pnas.232087499

Sarov, M., Murray, J. I., Schanze, K., Pozniakovski, A., Niu, W., Angermann, K., . . . Hyman, A. A. (2012). A genome-scale resource for in vivo tag-based protein function exploration in C. elegans. *Cell, 150*(4), 855-866. doi:10.1016/j.cell.2012.08.001

Sato, K., Norris, A., Sato, M., & Grant, B. D. (2014). C. elegans as a model for membrane traffic. *WormBook*, 1-47. doi:10.1895/wormbook.1.77.2

Sawin, E. R., Ranganathan, R., & Horvitz, H. R. (2000). *C. elegans* Locomotory Rate Is Modulated by the Environment through a Dopaminergic Pathway and by Experience through a Serotonergic Pathway. *Neuron, 26*(3), 619-631. doi:10.1016/S0896-6273(00)81199-X

Segalat, L., Elkes, D. A., & Kaplan, J. M. (1995). Modulation of serotonin-controlled behaviors by Go in Caenorhabditis elegans. *Science, 267*(5204), 1648. doi:10.1126/science.7886454

Shaye, D. D., & Greenwald, I. (2015). The Disease-Associated Formin INF2/EXC-6 Organizes Lumen and Cell Outgrowth during Tubulogenesis by Regulating F-Actin and Microtubule Cytoskeletons. *Dev Cell, 32*(6), 743-755. doi:10.1016/j.devcel.2015.01.009

Shi, A., Liu, O., Koenig, S., Banerjee, R., Chen, C. C.-H., Eimer, S., & Grant, B. D. (2012). RAB-10-GTPase–mediated regulation of endosomal phosphatidylinositol-4,5-bisphosphate. *Proceedings of the National Academy of Sciences, 109*(35), E2306. doi:10.1073/pnas.1205278109

Sigurbjörnsdóttir, S., Mathew, R., & Leptin, M. (2014). Molecular mechanisms of de novo lumen formation. *Nature Reviews Molecular Cell Biology, 15*(10), 665-676. doi:10.1038/nrm3871

Smith, A. R., Marquez, R. T., Tsao, W. C., Pathak, S., Roy, A., Ping, J., . . . Xu, L. (2015). Tumor suppressive microRNA-137 negatively regulates Musashi-1 and colorectal cancer progression. *Oncotarget, 6*(14), 12558-12573. doi:10.18632/oncotarget.3726

Smith, M. A., Blankman, E., Gardel, M. L., Luettjohann, L., Waterman, C. M., & Beckerle, M. C. (2010). A zyxin-mediated mechanism for actin stress fiber maintenance and repair. *Dev Cell, 19*(3), 365-376. doi:10.1016/j.devcel.2010.08.008

Spears, E., & Neufeld, K. L. (2011). Novel Double-negative Feedback Loop between Adenomatous Polyposis Coli and Musashi1 in Colon Epithelia. *Journal of Biological Chemistry, 286*(7), 4946-4950.

Stendel, C., Roos, A., Deconinck, T., Pereira, J., Castagner, F., Niemann, A., . . . Senderek, J. (2007). Peripheral nerve demyelination caused by a mutant Rho GTPase guanine nucleotide exchange factor, frabin/FGD4. *Am J Hum Genet, 81*(1), 158-164. doi:10.1086/518770

Sundaram, M. V., & Buechner, M. (2016). The Caenorhabditis elegans Excretory System: A Model for Tubulogenesis, Cell Fate Specification, and Plasticity. *Genetics, 203*(1), 35-63. doi:10.1534/genetics.116.189357

Sundaram, M. V., & Cohen, J. D. (2017). Time to make the doughnuts: Building and shaping seamless tubes. *Semin Cell Dev Biol, 67*, 123-131. doi:10.1016/j.semcdb.2016.05.006

Sureban, S. M., May, R., George, R. J., Dieckgraefe, B. K., McLeod, H. L., Ramalingam, S., . . . Houchen, C. W. (2008). Knockdown of RNA Binding Protein Musashi-1 Leads to Tumor Regression In Vivo. *Gastroenterology, 134*(5), 1448-1458.e1442. doi:10.1053/j.gastro.2008.02.057

Sze, J. Y., Victor, M., Loer, C., Shi, Y., & Ruvkun, G. (2000). Food and metabolic signalling defects in a Caenorhabditis elegans serotonin-synthesis mutant. *Nature, 403*(6769), 560-564. doi:10.1038/35000609

Talvik, I., Møller, R. S., Vaher, M., Vaher, U., Larsen, L. H., Dahl, H. A., . . . Talvik, T. (2015). Clinical Phenotype of De Novo GNAO1 Mutation: Case Report and Review of Literature. *Child neurology open, 2*(2), 2329048X15583717-12329048X15583717. doi:10.1177/2329048X15583717

Tanis, J. E., Moresco, J. J., Lindquist, R. A., & Koelle, M. R. (2008). Regulation of serotonin biosynthesis by the G proteins Galphao and Galphaq controls serotonin signaling in Caenorhabditis elegans. *Genetics, 178*(1), 157-169. doi:10.1534/genetics.107.079780

Tong, X., & Buechner, M. (2008). CRIP homologues maintain apical cytoskeleton to regulate tubule size in C. elegans. *Dev Biol, 317*(1), 225-233.

Trent, C., Tsung, N., & Horvitz, H. R. (1983). Egg-Laying Defective Mutants of the Nematode *Caenorhabditis elegans*. *Genetics, 104*(4), 619.

Udenwobele, D. I., Su, R. C., Good, S. V., Ball, T. B., Varma Shrivastav, S., & Shrivastav, A. (2017). Myristoylation: An Important Protein Modification in the Immune Response. *Front Immunol, 8*, 751. doi:10.3389/fimmu.2017.00751

Valdmanis, P. N., Roy-Chaudhuri, B., Kim, H. K., Sayles, L. C., Zheng, Y., Chuang, C. H., . . . Kay, M. A. (2013). Upregulation of the microRNA cluster at the Dlk1-Dio3 locus in lung adenocarcinoma. *Oncogene, 34*, 94. doi:10.1038/onc.2013.523

Vawter, M. P., Ferran, E., Galke, B., Cooper, K., Bunney, W. E., & Byerley, W. (2004). Microarray screening of lymphocyte gene expression differences in a multiplex schizophrenia pedigree. *Schizophrenia Research, 67*(1), 41-52. doi:10.1016/S0920-9964(03)00151-8

Vo, D. T., Abdelmohsen, K., Martindale, J. L., Qiao, M., Tominaga, K., Burton, T. L., . . . Penalva, L. O. F. (2012). The Oncogenic RNA-Binding Protein Musashi1 Is Regulated by HuR via mRNA Translation and Stability in Glioblastoma Cells. *Molecular Cancer Research, 10*(1), 143. doi:10.1158/1541-7786.MCR-11-0208

Waggoner, L. E., Zhou, G. T., Schafer, R. W., & Schafer, W. R. (1998). Control of Alternative Behavioral States by Serotonin in Caenorhabditis elegans. *Neuron, 21*(1), 203-214. doi:10.1016/S0896-6273(00)80527-9

Weinshenker, D., Garriga, G., & Thomas, J. H. (1995). Genetic and pharmacological analysis of neurotransmitters controlling egg laying in C. elegans. *The Journal of Neuroscience, 15*(10), 6975. doi:10.1523/JNEUROSCI.15-10-06975.1995

Weiskirchen, R., & Gunther, K. (2003). The CRP/MLP/TLP family of LIM domain proteins: acting by connecting. *Bioessays, 25*(2), 152-162. doi:10.1002/bies.10226

Winter, J. F., Höpfner, S., Korn, K., Farnung, B. O., Bradshaw, C. R., Marsico, G., . . . Zerial, M. (2012). Caenorhabditis elegans screen reveals role of PAR-5 in RAB-11-recycling endosome positioning and apicobasal cell polarity. *Nat Cell Biol, 14*(7), 666-676. doi:10.1038/ncb2508

Wirshing, A. C. E., & Cram, E. J. (2018). Spectrin regulates cell contractility through production and maintenance of actin bundles in the Caenorhabditis elegans spermatheca. *Mol Biol Cell, 29*(20), 2433-2449. doi:10.1091/mbc.E18-06-0347

Woo, W. M., Goncharov, A., Jin, Y., & Chisholm, A. D. (2004). Intermediate filaments are required for C. elegans epidermal elongation. *Dev Biol, 267*(1), 216-229. doi:10.1016/j.ydbio.2003.11.007

Wood, W. B. (1988). Introduction to *C. elegans* Biology. In W. B. Wood (Ed.), *The Nematode Caenorhabditis elegans* (Vol. 17, pp. 1-16). Cold Spring Harbor, NY: Cold Spring Harbor Press.

Wu, X., Lan, L., Wilson, D. M., Marquez, R. T., Tsao, W. C., Gao, P., . . . Xu, L. (2015). Identification and validation of novel small molecule disruptors of HuR-mRNA interaction. *ACS Chem Biol, 10*(6), 1476-1484. doi:10.1021/cb500851u

Xie, Y., Zheng, Y., Li, H., Luo, X., He, Z., Cao, S., . . . Ren, J. (2016). GPS-Lipid: a robust tool for the prediction of multiple lipid modification sites. *Sci Rep, 6*, 28249. doi:10.1038/srep28249

Yang, Y., Sun, Y., Luo, X., Zhang, Y., Chen, Y., Tian, E., . . . Zhang, H. (2007). Polycomb-like genes are necessary for specification of dopaminergic and serotonergic neurons in Caenorhabditis elegans. *Proc Natl Acad Sci U S A, 104*(3), 852-857. doi:10.1073/pnas.0610261104

Yao, K.-M., Samson, M.-L., Reeves, R., & White, K. (1993). Gene elav of Drosophila melanogaster: A prototype for neuronal-specific RNA binding protein gene family that is conserved in flies and humans. *Journal of Neurobiology, 24*(6), 723-739. doi:10.1002/neu.480240604

Yoda, A., Sawa, H., & Okano, H. (2000). MSI-1, a neural RNA-binding protein, is involved in male mating behaviour in Caenorhabditis elegans. *Genes to Cells, 5*(11), 885-895. doi:10.1046/j.1365-2443.2000.00378.x

Zhang, X., & Gao, N. (2016). RAB and RHO GTPases regulate intestinal crypt cell homeostasis and enterocyte function. *Small GTPases, 7*(2), 59-64. doi:10.1080/21541248.2016.1159274

Zubenko, G. S., Jones, M. L., Estevez, A. O., Hughes, H. B., 3rd, & Estevez, M. (2009). Identification of a CREB-dependent serotonergic pathway and neuronal circuit regulating foraging behavior in Caenorhabditis elegans: a useful model for mental disorders and their treatments? *Am J Med Genet B Neuropsychiatr Genet, 150b*(1), 12-23. doi:10.1002/ajmg.b.30891

Zuela, N., & Gruenbaum, Y. (2016). Intermediate Filaments in Caenorhabditis elegans. *Methods Enzymol, 568*, 661-679. doi:10.1016/bs.mie.2015.09.020